GENETIC POPULATION STRUCTURE, PATTERNS OF GENETIC VARIATION, AND PATTERNS OF PHENOTYPIC LEAF VARIATION AMONG PERIPHERAL AND CORE POPULATIONS OF THE MANGROVE SPECIES *AVICENNIA MARINA* (FORSK.) VIERH. (ACANTHACEAE) ON THE RED SEA, SAUDI ARABIA.

by

Faisal Khalid G Alharbi

BSc, King Saud University, 2005
MSc, King Saud University, 2010

A THESIS SUBMITTED IN PARTIAL FULFILLMENT OF
THE REQUIREMENTS FOR THE DEGREE OF
DOCTOR OF PHILOSOPHY

in

THE FACULTY OF GRADUATE AND POSTDOCTORAL STUDIES

(Forestry)

THE UNIVERSITY OF BRITISH COLUMBIA
(Vancouver)

December 2018

The following individuals certify that they have read, and recommend to the Faculty of Graduate and Postdoctoral Studies for acceptance, the dissertation entitled:

GENETIC POPULATION STRUCTURE, PATTERNS OF GENETIC VARIATION, AND PATTERNS OF PHENOTYPIC LEAF VARIATION AMONG PERIPHERAL AND CORE POPULATIONS OF THE MANGROVE SPECIES AVICENNIA MARINA (FORSK.) VIERH. (ACANTHACEAE) ON THE RED SEA, SAUDI ARABIA.

submitted by Faisal Khalid G Alharbi in partial fulfillment of the requirements for

the degree of DOCTOR OF PHILOSOPHY

in THE FACULTY OF GRADUATE AND POSTDOCTORAL STUDIES (Forestry)

Examining Committee:

Dr. Yousry El-Kassaby
Co-supervisor

Dr. Quentin Cronk
Co-supervisor

Dr. Richard Hamelin
Supervisory Committee Member

Dr. Bruce C. Larson
University Examiner

Dr. Chris P. Chanway
University Examiner

Additional Supervisory Committee Members:

Supervisory Committee Member

Supervisory Committee Member

Abstract

This study utilized both of leaf dimension measurements (leaf area, length, maximal width, and the ratio of length: width) and 12 microsatellite loci screened across 315 samples of the entomophilous mangrove species *Avicennia marina* (Forsk.) Vierh. The samples collected from 9 sites along the Saudi Arabian Red Sea coastline with an estimated sampling range of 1,345 kilometres. The study objectives were to examine the genetic diversity, population structure, and the field observed phenotypic leaf variation, and to inspect the influence of the distribution limit on the genetic compositions and the phenotypic leaf traits variation. The 12 loci detected a total of 89 alleles with an average allelic diversity of 7.42. Observed heterozygosity (H_o) was close to expected heterozygosities (H_e) for most sites, and the average (H_o) was 0.298. The levels of inbreeding ranged from negative 0.044 to positive 0.126, with an average inbreeding coefficient of 0.012. The component of variation among populations were (25%, 34%) ($p < 0.001$), corresponding to the estimates of both F_{ST} and R_{ST} (0.25 and 0.34, respectively). The isolation by distance model (IBD) reflected the distribution of genetic variation with the existence of transitional zones and one distinct population at the farthest northerly edge of the geographic distribution. Significant differences in the various leaf characters occurred among the sites, which were explained by latitudes and inter-site distances. There was an obvious influence of the distribution limit mainly from Annual Sea Surface Temperature (SSTAnn) and Sea Surface Salinity in Winter (SW) on both of the genetic and morphological variations that manifested in a northwards declining trend for most gene diversity statistics and effective population size (*Ne*) mean values, and a northwards increasing tendency of leaf traits mean values and lower phenotypic variation. The morphological differentiation did not increase or decrease strictly based on the genetic differentiation among sites. However, the significant negative correlation between the mean values of leaf length and inbreeding coefficients suggested the occurrence of inbreeding depression in one site. Overall, the insights from this study imply the suitability of a geographically broad-scale conservative approach (100 km) to sourcing plant material for mangrove restoration projects.

Lay Summary

Avicennia marina (Forsk.) Vierh. is the most wide-ranging of all mangrove species, ranging in latitude from 25°N to 38°S. Mangrove ecosystems have a vital importance in supporting a wide spectrum of biodiversity, maintaining coastline stability and water quality, and serving in carbon sequestration. Up to date, populations of *A. marina* on the Red Sea have rarely ever been genetically investigated for their variation and structure even though the documented status of their degradation anticipates the potential loss of regionally undocumented genetic diversity in mangrove ecosystems. This study is significant to addressing the inadequacies in present-day knowledge, representing one of the first population genetic studies in the farthest northwest edge of *A. marina* global distribution. It will also open avenues for the advancement of the conservation and sustainable management of mangrove ecosystems at local/regional levels on the Red Sea which is ultimately a protection of groups of globally endangered species.

Preface

This dissertation is an original, independent, and intellectual product of the author, F. Alharbi. None of the text of the dissertation is taken directly from previously published or collaborative articles. My supervisors and I participated in identifying and designing of the research program, and my supervisory committee and I conceptualized the research questions. The fieldwork, data collection, data analyses and interpretation were conducted by the author, F. Alharbi.

Table of Contents

List of Tables

List of Figures

Acknowledgements

I offer my enduring gratitude to the faculty, staff and my fellow students at the UBC, who have inspired me to continue my work in this field. I owe particular thanks to my program supervisors Dr. Yousry El-Kassaby and Dr. Quentin Cronk, and to my supervisory committee members, Dr. Richard Hamelin (UBC), Dr. Jaroslav Klápště (Scion, New Zealand), Dr. Charles Chen (Oklahoma State University). Moreover, I would like to thank my funding agency: Ministry of Education in Saudi Arabia. Special thanks are owed to my parents, whose have supported me throughout my years of education, both morally and financially.

Chapter 1: Introduction

1.1 Introduction

Mangrove plants comprise a heterogeneous group of independently derived lineages that are defined ecologically by their occurrence in tidal zones along shorelines and in estuaries of the tropical and subtropical coastlines of the world. Also, mangrove plants are defined physiologically by their ability to withstand high salt concentrations and low soil aeration. (Schwarzbach and Ricklefts 2001). Mangroves contain some 70 higher plant species in several taxonomic groups, including 40 species in South-East Asia, approximately 15 species in Africa, and 10 species in the Americas (Kitamura *et al*. 1997), and their distribution divided primarily into two global hemispheres, the Atlantic East Pacific (AEP), and the Indo-West Pacific (IWP). The total area of mangroves worldwide is estimated at about 182 000 km^2 (Dodd *et al*. 1998).

Mangrove ecosystems have a vital importance in supporting a wide spectrum of biodiversity, maintaining coastline stability and water quality, sustaining fisheries, presenting a forestry resource, and serving in carbon sequestration (Ong 1995; Saenger 2002; Glaser 2003; Lovelock *et al*. 2014). More specifically, mangroves nurture both marine and terrestrial food-webs (Milward 1982; Schodde *et al.* 1982; Robertson and Duke 1987; Sasekumar *et al.* 1992; Laegdsgaard and Johnson 1995; Nagelkerken *et al.* 2000; Wolff *et al.* 2000), and they physically reduce wave energy and sediment losses (Tomlinson 1986; Mazda *et al.* 1997; Saenger 2002). Mangroves also have been utilized for fishery production, salt production, honey/wax production, and food or animal fodder (Yap 2000; Saenger 2002). Mangroves accumulate larger carbon stocks within their sediments comparing to other forests which are extremely beneficial with the global warming phenomenon (Chmura *et al*. 2003; Mcleod *et al*. 2011; Lovelock *et al*. 2014). Unfortunately, mangroves are one of the world's most threatened ecosystems (Duke *et al*. 2007). At least 35% of the area of mangrove forests has been lost in the past two decades, more than losses of tropical rainforest or coral reefs (Valiela *et al*. 2001). Many studies have documented the degradation of mangroves through direct or indirect anthropogenic degradation such as overdevelopment, pollution and unsustainable use (Farnsworth and Ellison 1997; Blasco *et al.* 2001; Alongi 2002; Saenger 2002). Other studies have reported ambiguous ecological degradations (Dahdouh-Guebas *et al*. 2005); therefore, the sustainable management, conservation,

and reforestation of mangroves areas have become a priority in many countries (Barbier and Strand 1997; Lakshmi and Rajagopalan 2000; Kairo *et al*. 2001; Saenger 2002).

Mangrove forests in Saudi Arabia exist as fragmented and scattered stands with discontinuous distribution in the tidal areas of the Red Sea and the Arabian Gulf. Mainly, they consist of *Avicennia marina* (Forssk.) Vierh., but *Avicennia marina* is accompanied by a few examples of *Rhizophora mucronata* Lam. on the Red Sea (Saenger 1993). In addition to the importance of mangrove ecosystem functions on the Red Sea, the Red Sea is a globally significant semi-enclosed sea area in terms of its biodiversity, species endemism, significance for maritime culture, and its renewable resources (Gladstone *et al*. 1999). For example, the Farasan Islands on the Red Sea have been regarded as having a high conservation value because of the diversity of marine habitats of high importance for marine mammals, turtles, and seabirds (Child *et al*. 1990). Critical habitats within the islands include four major types of reefs, mangrove stands, seagrass beds with seven species of seagrass, and fish nurseries with 231 species. Sea mammals recorded in the coastal waters include the globally threatened dugong *Dugong dugon* Müller., three species of dolphin, *Stenella longirostris* Gray., *Tursiops truncatus* Montagu. and *Stenella attenuate* Gray., and two species of whale, humpback whale *Megaptera novaeangliae* Borowski. and minke whale *Balaenoptera acutorostrata* Lacépède. Animal species recorded in the coastal waters include the globally endangered green turtle *Chelonia mydas* L. and the critically endangered hawksbill turtle *Eretmochelys imbricata* L. Also, a record of more than 145 bird species have been observed in the Farasan Islands by which the Islands are listed as an Important Bird Area (Evans 1994). The pink-backed pelican *Pelicanus rufescens* Gmelin. with an internationally significant population and the osprey *Pandion haliaetus* L. are two of the most significant bird species. Finally, the area is home to the largest population of Idmi gazelle in Saudi Arabia.

Despite the ecological importance of mangrove forests on the Red Sea, they have been subjected to many kinds of disturbances that affected their growth and distribution. For instance, Badr *et al*. (2009) reported an increase in heavy metals concentrations in the mangroves environment on the Red Sea. Generally, the heavy metals pollution of mangroves is associated with the following causes: industrial effluents, agro-based industries (construction of shrimp ponds), agricultural runoff, sewage treatment plants leakages, leaching from domestic garbage dumps, urbanization (especially dams establishment), and chemical and oil spills on one of the world's heaviest marine traffic routes (Bodin *et al*. 2013). As a result, The Regional Organization

for the Conservation of the Environment of the Red Sea and Gulf of Aden (PERSGA) stated that mangroves on the Red Sea area are susceptible to degradation, and about 74% of the surveyed stands of mangroves are damaged and shrinking rapidly (PERSGA 2005; Kotb *et al*. 2008). The magnitude of the problem is fully recognized within the countries that have accesses to the Red Sea and the Arabian Gulf where conservation actions have been carried out on the ground. For example, some of these conservation actions include reports of mangroves' status, establishment of mangrove reserves, afforestation schemes, enrichment plantings, and ecological or physiological studies (Nawata 2013). However, the choice of mangrove reserves ignores the genetic background of mangroves, and the replantation across distant geographical locations uses genetically unknown source materials. This might be one of the major reasons for the low growth rate and survival of seedlings which reached 56.7% in some plantations in the Arabian Gulf (Tamaei 2013). Knowledge of the genetic structuring can be an important consideration for the conservation and sustainable management of mangroves; population genetics could provide basic information for both the development of efficient protection of genetic resources (*in-situ* population conservation), and the designing of strategies for conserving representative samples of their genetic diversity (*ex-situ* germplasm conservation), leading to maximization of the genetic diversity protection and afforestation (Schoen and Brown 1993). To date, the extent and patterns of genetic diversity in natural mangrove populations are largely unknown on the Red Sea. Moreover, the documented status of mangrove degradation anticipates the potential loss of undocumented genetic diversity in mangrove ecosystems. Therefore, this study is significant to addressing the inadequacies in present-day knowledge. It will also open avenues for the advancement of the conservation and sustainable management of mangrove ecosystems at local and regional levels.

1.2 Research objectives

1.2.1 Chapter 2: Genetic population structure in the mangrove species *Avicennia marina* (Forsk.) Vierh. (Acanthaceae) on the Red Sea, Saudi Arabia.

Utilizing microsatellite markers, the aims of this chapter were to examine the genetic variation in *A. marina* along the Saudi Arabian Red Sea coastline, to determine which model best described the distribution of genetic variation within and among populations, and to assess indirectly over what distance gene flow occurred with its transitions or barriers.

1.2.2 Chapter 3: Patterns of differential genetic variation among peripheral and core populations of the mangrove species *Avicennia marina* (Forsk.) Vierh. (Acanthaceae) on the Red Sea, Saudi Arabia.

The aims of this chapter were to test the hypothesis of lower genetic diversity and higher genetic structure towards the range edges of *A. marina* on the Red Sea, and to examine the influence of the distribution limit on the populations' genetic compositions.

1.2.3 Chapter 4: Phenotypic leaf variation in the mangrove species *Avicennia marina* (Forsk.) Vierh. (Acanthaceae) on the Red Sea, Saudi Arabia.

Utilizing measurements of leaf dimension (leaf area, length, maximal width, and the ratio of length: width), the aims of this chapter were to examine the field observed phenotypic leaf variation in *A. marina* along the Saudi Arabian Red Sea coastline, to determine which model best described the distribution of phenotypic leaf variation within and among populations (isolation by distance, discrete subpopulation), and to examine the influence of the distribution limit on the phenotypic leaf variation.

Chapter 2: Genetic population structure in the mangrove species *Avicennia marina* (Forsk.) Vierh. (Acanthaceae) on the Red Sea, Saudi Arabia.

2.1 Introduction

Avicennia marina (Forsk.) Vierh. is the most wide-ranging of all mangrove tree species because it has the largest longitudinal and latitudinal distribution, ranging in latitude from 25°N to 38°S. The distribution of *A. marina* is within the Indo-West Pacific, extending from the Red Sea to South Africa up to the West Pacific from Japan to New Zealand (Maguire *et al*. 2000 a). Furthermore, *A. marina* can grow and reproduce across a wide range of climatic, saline, and tidal conditions which would imply a large genetic variation. The same vast geographic range and a large number of propagules, which can float and disperse with ocean current, suggest also that this species exhibits long-distance gene flow. A possibility that populations throughout the range would be genetically undifferentiated (Duke *et al*. 1998; Maguire *et al*. 2000a).

Regarding the scale of spatial differentiation, most species display little genetic structuring over short distances, but some species show strong genetic structuring (Knowles *et al*. 1992; Shapcott 1995). Yet, the majority of forest trees show weak genetic structure (Leonardi & Menozzi 1996; Leonardi *et al*. 1996; Rossetto *et al*. 1999).

In the Indo-West Pacific study that used *A. marina* specimens from Australia, New Zealand, New Caledonia, Thailand, Malaysia, and South Africa, allozyme variation showed high levels of genetic diversity and low levels of inbreeding (Duke *et al*. 1998). Strong genetic structuring was observed with drastic changes in gene frequencies at the geographical margins of distributions. In spite of the indication of high degrees of outcrossing, gene flow among populations was relatively low (Nm < 1-2), except for geographically continuous populations. Likewise, field experiments on propagule dispersal showed limitations by ocean currents, the patchy presence of suitable environmental conditions, and the limited longevity of propagules during dispersal (Clarke 1992). The widespread mangrove species assumption of having high levels of long-distance dispersal was questioned.

Using three microsatellite loci, another study in the Indo-West Pacific investigated the genetic structure among *A. marina* specimens from Australia, New Zealand, New Caledonia, Papua New Guinea, Malaysia, Japan, India, United Arab Emirates, and South Africa. The genetic

structure was tested using three models: (i) a single panmictic model; (ii) the discrete subpopulation model; and (iii) the isolation by distance model. The results indicated the lack of gene flow between the populations that were about 500 kilometres apart supporting the model of genetically discrete subpopulations with an overall F_{ST} of 0.41 (p<0.001). There was no significant isolation by distance, and the overall gene diversity was 0.407 (Maguire *et al*. 2000a).

Ten sites along the eastern and western coasts of India revealed a high degree of divergence among populations of *A. marina*. The inter-population variations were 76.7% for random amplified polymorphic DNA (RAPD) and 66% for restriction fragment length polymorphism (RFLP), and one distinct entity was indicated (Parani *et al*. 1997). Nonetheless, the differences tended to be greater among populations than within populations, which Parani *et al* (1997) attributed to the diversity of environmental and physical conditions at different locations. These studies showed that populations of *A. marina* around the world were more distinct than previously realized. As the differences tended to be greater among populations than within populations, it seemed that the widespread distribution was combined with the local sorting of populations.

Studies of *A. marina* populations at different sampling scales have provided contrasting results on the spatial differentiation. For example, eleven sites with a distance along the water between the two most distant sites of 210 kilometres in the Northern Rivers of New South Wales, Australia were investigated using 8 microsatellite markers. The level of gene flow was high with an overall F_{ST} of 0.065 (p<0.001). This study suggested panmixia and complete genetic exchange over a distance of approximately 620 meters, and the expected maximum distance of gene flow was approximately 200 kilometres where differentiation may begin beyond it (Homer 2009). According to the study of Giang *et al* (2003), strong genetic structuring and reduced diversity revealed by both five microsatellite (SSR) loci (F_{ST} of 0.262) and amplified fragment length polymorphism (AFLP) (F_{ST} of 0.34) among six natural populations of *A. marina* located in coastal areas of Vietnam and separated by at least 100 kilometres. A smaller geographical scale with nine sites within 100 kilometres in three estuaries of Sydney, Australia, Melville and Burchett (2002) found that the genetic distance in *A. marina* was correlated with geographic distance using isozyme/allozyme analyses. Their findings supported the isolation by distance on a scale beyond 80 kilometres. By using three and five microsatellite loci in other studies in the coastal area of Iran with few sites separated by 60 - 120 kilometres, low level of genetic differentiation among

populations was detected, except for populations that had small sample sizes due to a high level of exploitation. Their findings supported an isolation by distance model (Kahrood *et al*. 2008; Zolgharnein *et al*. 2010).

Utilizing SSR markers, this study, the dissertation, examined the genetic variation in *A. marina* along the Saudi Arabian Red Sea coastline, and it determined which model best described the distribution of genetic variation within and among populations. That helped in assessing indirectly over what distance gene flow occurred and its transitions or barriers. Information concerning the distance at which populations begin to diverge or become genetically distinct helps in conservation and reforestation decisions (Allendorf and Luikart 2007).

2.2 Materials and methods

2.2.1. *A. marina* sample sites

The Red Sea is a narrow and relatively deep oceanic trough extending for over 1,900 km, between 13º and 28º N latitude. It is the world's northernmost tropical sea, with extensive shallow shelves that support complex coral reefs and associated ecosystems. The sampling sites are within the Saudi Arabian Red Sea coastline which extends from the border with Jordan in the northern Gulf of Aqaba (29°30' N) to the border with Yemen, south of the Farasan Islands (16°22' N), an approximate distance of 1,600 km, figure 2.1 (Bruckner *et al* 2012).

Given the huge area that this study covered, and an approximate of 1,345 km range of the sampling sites, the sampling strategy was justified by two steps. First, the whole coastline of the Red Sea was divided into three major sections; these were north, middle, and south sections where each section extended for about 450 km. In the second step three well-developed stands, separated by various distances 59-200 km, were chosen within each section, totalling 9 sampling sites included in this study in figure 2.1. The most distant sites were site 1 in the far north and site 9 in the far south, which were approximately 1,345 km apart, table 2.1. Within each of the nine sampling sites, transects parallel to the water's edge were established, then randomly selecting 35 adult trees of *A. marina*, which were spaced with a distance of 10-30 m from each other, in order to avoid sampling among related individuals and to maximize the inclusion of diverse genotypes. The total sample size was 315 individuals.

2.2.2. DNA extraction, microsatellite primers and genotyping

Leaf samples from 35 adult trees (5–6 leaves per tree) were collected and stored in bags with silica gel in each sampling site for the DNA isolation. The DNA was extracted and purified using a modified CTAB protocol (Doyle and Doyle 1990), following the method of Maguire *et al*. (1994) as it was recommended for plants belonging to the family Proteaceae and plants with high levels of secondary metabolites and polysaccharides. All the lab work was done in Source BioScience, Nottingham, UK.

Microsatellite primer sequences (16 pairs) published by Maguire *et al.* (2000b) and microsatellite primer sequences (3 pairs) published by Yoshimori *et al*. (2015) were synthesized for optimization and testing across all 315 *A. marina* individuals sampled. The final data set consisted of 12 microsatellite markers out of the total 19 markers tested as 7 microsatellite markers either failed to prime or showed strong evidence for null alleles. These 12 microsatellites consisted of 5 dinucleotide repeats, 4 trinucleotide repeats, and three compound repeats in table 2.2. Also, genotype frequencies were checked for the presence of null alleles, large allele drop out and stuttering using MICRO-CHECKER 2.2.3 (Van Oosterhout *et al*., 2004, 2006), and no loci showed evidence for a null allele.

Polymerase chain reaction (PCR) amplification conditions were: 1 reaction buffer (10 mM Tris– HCl, 50 mM KCl, pH 8.3, pH 8.3, Boehringer Mannheim), 1.5 mM MgCl2, 200 m each dNTP, 0.2 m each primer, 1 unit *Taq* polymerase (Boehringer Mannheim), and 10–50 ng genomic DNA, in a total volume of 25 L. Microsatellite amplification was carried out using the following cycling parameters: preheating for 3 min at 94°C, followed by 30 cycles of denaturing at 90°C for 30 s, annealing at primer-specific temperatures of 60°C to 55°C for 30s and extension for 1 min at 72°C. Reactions were completed by incubation at 72°C for 5 min and holding at 4°C.
PCR products were fluorescent-labelled with (FAM-6, VIC, and NED), then denatured for 3 min at 95°C, and separated by capillary electrophoresis on a 310 Genetic Analyser (PE Applied Biosystems). GeneScan™ and Genotyper ™ software (PE Applied Biosystems) was used for gel analysis.

2.2.3. Genetic Data Analyses

Gene diversity statistics were estimated using GenAlEx (Peakall and Smouse 2006) with 999 random permutations performed to determine significance for all statistics calculated. Genetic diversity statistics were calculated as follows: the total number of different alleles per locus (A), average allelic diversity (Ā), average number of different alleles per locus and per site (N_a), effective number of alleles (N_e=1/ pi^2) where *pi* is the frequency of the *i*th allele at a locus (Frankham *et al.* 2002), the expected heterozygosity or gene diversity (H_e = 1- pi^2), the observed heterozygosity (H_o)=(number of heterozygotes determined by direct count/ *N* = sample size), the

fixation index ($F = (H_e-H_o)/ H_e = 1- (H_o/ H_e)$), and the outcrossing rate = $(1 – F_{IS})/(1 + F_{IS})$ where inbreeding coefficient within individuals, $F_{IS} = (H_e- H_o)/ H_e$. (Weir 1996).

Hardy-Weinberg and linkage disequilibrium were assessed using the exact tests in the program Genepop, version 4.0 (Rousset 2007); significance levels for both were determined using the Markov chain method. For all Markov chain tests in Genepop, the parameters used were 1000 dememorization iterations and 100 or 200 batches of 1000 iterations per batch. Also, sequential Bonferroni adjustments for both were used to judge significance levels for all tests with an initial level of 0.05 (Rice 1989).

Using Genepop 4.0 (Rousset 2007) and/or GenAlEx 6.2 (Peakall and Smouse 2006), the degree of sites differentiation was estimated by testing F_{ST}, R_{ST}, allele frequency histograms, and isolation by distance (Mantel test, with significance determined through 999 random permutations) (Mantel 1967). For isolation by distance testing, the statistical relationships were estimated between geographic distances among sites and both of pairwise F_{ST} and Nei's genetic distances (Nei 1972). The calculation of Nei's genetic distances was performed using GenAlEx 6.2.

The F statistics F_{IS}, F_{IT} and F_{ST} were estimated using both the infinite alleles model (F_{ST}) and the stepwise mutation model (R_{ST}) of microsatellite evolution where F_{IS} and R_{IS} = the average inbreeding of individuals within subpopulations, F_{IT} and R_{IT} = the average inbreeding of individuals relative to the total population, and F_{ST} and R_{ST} = the average inbreeding of subpopulations relative to the total population. F_{ST} and R_{ST} were estimated as per Cockerham (1973) and Weir and Cockerham (1984). G_{ST} values, the multiallelic version of F_{ST} (Nei 1973), were computed using GenAlEx 6.2.

Percentages of molecular variance among sites, within sites, and within individuals were calculated with AMOVA (The Analysis of Molecular Variance) using GenAlEx 6.2 (Meirmans 2006). AMOVA procedure in GenAlEx 6.2 follows the method of Peakall *et al* (1995) that brings the estimates for F_{ST} in line with the Weir-Cockerham estimates. When performing AMOVA in GenAlEx, statistical testing by random permutation determines whether the observed value is significantly greater than that expected by chance at a 5% significance level.

Gene flow via the number of migrants (*Nm)* was evaluated via Genepop and GenAlEx using F_{ST} ($Nm = [(1/ F_{ST})-1]/4$), R_{ST}, and the private alleles' method (Barton and Slatkin 1986). The private alleles' method uses the conditional (within the sample) average frequency of rare

alleles as an estimator of the number of individuals exchanged between local populations in an island model, and its predictions are based on the assumption that the rare alleles found in samples have reached a "quasi-equilibrium" distribution.

For all sites, population structure was assessed by both indirect allele frequency methods, software Genepop and GenAlEx, and Bayesian multilocus genetic inference techniques, software BAPS (Corander *et al.* 2003; Corander *et al.* 2004) and *STRUCTURE* (Pritchard *et al.* 2000; Pritchard *et al.* 2007). Bayesian multilocus genetic inference techniques have greater computational power and more realistic modelling assumptions (Beaumont and Rannala 2004). Multilocus methods use genotype likelihoods to infer populations of origin of individuals or to estimate population substructure. They are claimed as having an advantage over previous methods that use statistics averaged over all loci or that require an input of known predefined populations (Luikhart and England 1999; Corander *et al.* 2003; Pearse and Crandall 2004; Latch *et al.* 2006).

Bayesian analysis of Population Structure (BAPS) 5 (Corander *et al.* 2003; Corander *et al.* 2004) was applied to the data set using both clustering of groups (samples sites) and clustering of individuals (315 individuals), and the significance in BAPS determined based on 50 simulations from posterior allele frequencies.

SRUCTURE 2.2 (Pritchard *et al.* 2000; Pritchard *et al.* 2007) was applied to the data set using the admixture model, and correlated allele frequencies (Falush *et al.* 2003; Pritchard *et al.* 2007). A burn-in length of 50,000 and twenty iterations (for K =1 to K=15 in three replicates) of 500,000 Markov chain Monte Carlo (MCMC) repetitions were parameters set for the data. Then the K method, which was used by Evanno *et al.* (2005), was applied to the output from *STRUCTURE.*

Even though Bayesian multilocus genetic inference techniques such as BAPS and *STRUCTURE* are ones of the most widely applied approaches for the inference of population structuring, they are model-based approaches, and they rely on explicit assumptions regarding population subdivision. For example, one assumption is the equal probabilities of migrations among all populations, and this assumption is often difficult to verify in nature. Therefore, model-free approaches were added and used for assessing population structure in this study.

Principal Coordinate Analysis (PCoA) is a multivariate technique that allows detecting and plotting of the major patterns within a multivariate data set. PCoA was conducted by GenAlEx

6.2 to visualize patterns of genetic differentiation on two different levels: individual level and site by site level. The procedure in GenAlEx 6.2 is based on an algorithm published by (Orloci 1978). PCoA aims to summarize the entire genetic variation among individuals that takes account of both variations: between groups (structured genetic variability) and within groups (random genetic variability). Hence, PCoA would not provide a clear picture of between-population variation. On the contrary, the Discriminant Analysis of Principal Components (DAPC) focuses on between-group variability, while almost neglecting within-group variation.

All sites were analyzed by DAPC using the adegenet package (Jombart 2008) for the R software (R Development Core Team 2015). The number of clusters was assessed using the function "find.clusters", which runs successive K means clustering with an increasing number of clusters (K). I assessed a wide range of possible clusters from K=1 to K=40. In this analysis, 50 principal components of PCA were retained in the preliminary variable transformation step, which accounted for most (approximately 95%) of the total genetic variability. Based on the associated Bayesian information criterion (BIC) of different runs, the ‘optimal' number of clusters was selected. Ideally, the value of BIC would decrease to the lowest value ‘optimal' then it would increase drastically creating an elbow shape in the curve of BIC values. In the case where the optimal number of clusters is ambiguous, the chosen number of clusters is the minimum number of clusters after which the BIC increases or decreases by a negligible amount. Also, the chosen number of clusters takes into account the question of “how many individuals from the sites would be identified and included in the inferred clusters?”

For all the analyses accomplished by PCoA, *STRUCTURE,* and DAPC, all the nine sites were submitted as a first step of the investigation. Based on the first step results, the most differentiated site was removed from the data set, and the remnant sites were reanalyzed.

2.3 Results

2.3.1 Genetic diversity

For the genetic diversity analyses, I used a final data set of 12 microsatellite loci screened across 315 *A. marina* individuals from 9 separate sites on the Red Sea. Table 2.2 summarized genetic diversity statistics for these 12 loci.

A total of 89 different alleles were the outcomes of the 315 *A. marina* individuals utilizing 12 microsatellite loci, resulting in an allelic diversity average ($\bar{A}$) of 7.42. The minimum alleles per locus were 2 alleles for locus M34, and the maximum alleles per locus were 19 alleles for locus M81. The average number of different alleles per site (N_a) ranged from 1.2 for locus M34 to 6.6 for locus M81 with an average of 3.2 alleles over all loci. The effective number of alleles (N_e) ranged from 1.009 for locus M34 to 3.406 for locus M81 with an average over all loci of 1.783.

Overall, the average of gene diversity (H_e) was 0.295 in table 2.2. Genetic diversity estimated from the 12 microsatellite loci varied greatly (examined by the expected heterozygosity - H_e), ranging from 0.009 for locus M98 to 0.666 for locus M81. The random union of gametes of Hardy-Weinberg Equilibrium (HWE) could not be rejected for all loci except locus M13; however, the patterns of unconformity to HWE in this locus showed up in only one site (site 8), whereas it was found to be in HWE in other sites. Although one significant linkage disequilibrium was detected between locus M13 and locus M49 in only one site (site 5), no statistically significant linkage disequilibrium was found to be consistent between any pair of microsatellite loci.

From a site perspective, genetic diversity summary statistics for sites were listed in table 2.3. The total number of different alleles per site for all loci ranged from 29 alleles (site 5) to 55 alleles (site 9). Also, the average number of different alleles per locus (N_a) ranged from 2.4 (site 5) to 4.6 (site 9) with an average of 3.2. The observed heterozygosity (H_o) ranged from 0.202 (site 2) to 0.404 (site 8) with an average of 0.298. In most sites, expected heterozygosities (H_e) were close to observed heterozygosities (H_o), and (H_e) ranged from 0.191 (site 2) to 0.401 (site 8) with an average of 0.295. This led to Fixation Indices very close to zero in most sites, as expected under random mating. The levels of inbreeding ranged from negative 0.044 (site 3) to positive 0.126 (site 7), with an average inbreeding coefficient of 0.012 (very low level of inbreeding). On the other hand, the outcrossing rate ranged from 0.77 (site 7) to 1.092 (site 3), with an average of 0.978

(high outcrossing). 31 alleles out of the 89 alleles were found to be site specific; the numbers of private alleles in each site ranged from 1 (site 2) to 10 (site 9), and the frequencies of these private alleles fluctuated between 0.014 and 0.171. Detailed of private alleles and their frequencies can be seen in table 2.4.

2.3.2 Partitioning genetic variation

The null hypotheses "allelic or genotypic distribution is identical across sites" were tested for each locus in each pair of sites first then over all sites. For all 9 sites, 36 site-pair comparisons for each one of the 12 loci were tested resulting in 432 comparisons for the allelic distribution and another 432 comparisons for the genotypic distribution. For both allelic and genotypic distributions, 64% of these comparisons (277 out 432) rejected the null hypotheses ($p < 0.05$) indicating heterogeneity between sites and signifying that panmixia did not occur across all the 9 sites. Over all sites, each locus had a computed unbiased estimate of *p-value*, and the null hypotheses at all loci were rejected ($p < 0.05$) except for locus M98.

The allelic compositions varied between sites, and figure 2.2 summarized the allelic patterns across sites. Generally, the degrees of similarity in allelic compositions between groups of sites suggest the effect of gene flow among these sites. Noticeably, sites 8 and 9 had higher values compared with the rest in their N_a, N_e, H_e, and private alleles. Some sites showed a level of similarity such as (site 1 and site 2), and (site 8 and site 9), but a fluctuation occurred between the remnants. The low frequencies of private alleles at some sites could easily be an effect of sampling, but sites 8 and sites 9 had higher values which could indicate genetic differences.

Table 2.5 presented the matrix of pairwise comparisons of site genetic differentiation calculated using the infinite alleles model (F_{ST}). All F_{ST} values were found to be significant at the 99% level, and F_{ST} values ranged from 0.031 (sites 8 and 9) to 0.31 (sites 2 and 7) with an overall F_{ST} of 0.246. Table 2.6 provided the matrix of pairwise comparisons of site genetic differentiation calculated using the stepwise mutation model (R_{ST}). All R_{ST} values were found to be significant at the 99% level, and R_{ST} values ranged from 0.0088 (sites 8 and 9) to 0.65 (sites 2 and 7) with an overall R_{ST} of 0.34. Even though most of F_{ST} and R_{ST} values showed overall similar patterns of genetic differentiation, pairwise comparisons values of F_{ST} were generally lower than R_{ST}, and R_{ST} revealed some of the non-captured differentiation by F_{ST}. For instance, site 5 and site 6 which were

geographically the closest sites in this study (59 km) had an F_{ST} value of 0.06 and R_{ST} of 0.26. Both of F_{ST} and R_{ST} indicated low levels of differentiation between sites 8-9. However, there were 20 site pairs in the range 0.05–0.15 (moderate genetic differentiation) for F_{ST}, and 15 site pairs out of these 20 pairs were above 0.151 for R_{ST} indicating more differentiation. G_{ST} values, the multiallelic version of F_{ST} (Nei 1973), were computed in table 2.7, but they did not provide an additional information about the genetic differentiation as they were similar to Fst values. In table 2.8, the overall values of F_{IS} and R_{IS} were 0.005 ($p = 0.366$) and 0.2 ($p < 0.001$), respectively. Only the significant value of R_{IS} indicated a low to moderate level of inbreeding. The overall values of F_{IT} and R_{IT} were 0.249 and 0.472, respectively.

The estimates of the number of migrants (*Nm*) varied depending on the levels of genetic differentiation in table 2.8. Over all sites and loci, the number of migrants was 0.76, 0.48, and 1.9 using F_{ST}, R_{ST}, and the private alleles' method, respectively (Barton & Slatkin 1986). These values of *Nm*, which represent a historical average of the number of migrants per generation, reflected an overall low level of gene flow.

Percentages of molecular variance among sites, within sites, and within individuals were calculated with AMOVA using both theoretical models, the infinite alleles model (F-statistics), and the stepwise mutation model (R-statistics) in table 2.9. The results from AMOVA showed that the variation among sites were (25%, 34%) ($p < 0.001$), within sites were (0%, 13%), and within individuals were (75%, 53%) ($p < 0.001$). This corresponded to the estimates of both F_{ST} and R_{ST} (0.246 and 0.339, respectively).

The correlations between geographic distances among sites and both of pairwise F_{ST} and Nei's genetic distances were tested by Mantel tests in figure 2.3-A and B. The independences between two variables were rejected for both correlations with F_{ST} and with Nei's distances, and significant positive correlations were found (*p*-value of 0.046 'borderline significant' and 0.02, respectively), and the (R^2) values were 0.12 and 0.123, respectively. The isolation by distance model could explain 12-12.3% of the population structure.

Principal Coordinates Analysis (PCoA) plot in figure 2.4-A, which visualized the pattern of differentiation at the individual level for all 315 individuals from all nine sites, showed that most differences in individual genotypes scattered close to each other except individuals from site 7. The first two axes of PCoA plot in figure 2.4-A accounted for 36.6% of the variation, and the second axe, which separated site 7 individuals, accounted for 17.2% of the variation. After

excluding site 7 individuals from the data set, the PCoA plot in figure 2.4-B separated individuals from site 2 and site 1 by the first axe which accounted for 21.4% of the variation.

PCoA plot in figure 2.5-A, which visualized the pattern of differentiation at the site by site level for all nine sites using pairwise F_{ST} values, showed that the significant (25%) among population differentiation was mostly due to site 2, 1, and 7, and the remnants were relatively closely placed. The first axe of PCoA plot in figure 2.5-A, which separated site 2 and site 1, accounted for 42.1% of the variation, while the second axe, which separated site 7, accounted for 30.4%. After excluding site 7 from the dataset, PCoA plot in figure 2.5-B distinguished site 2 and site 1 by the first axe which accounted for 54.2% of the variation, and the plot separated site 4 by the second axe which accounted for 14% of the variation.

The first two axes of both PCoA plots at the individual level in the figure 2.4-A and B accounted for 36.63% and 29.9% of the variation, respectively, but the first two axes of both PCoA plots at the site by site level in the figure 2.5-A and B accounted for 72.5% and 68.2% of the variation, respectively.

BAPS clustering analysis was applied in two ways: clustering of groups (sites) and clustering of individual genotypes in figure 2.6 and figure 2.7. BAPS clustering of groups in figure 2.6 resulted in the partitioning of the 9 sites into 7 clusters with a probability of 0.85 and log (marginal likelihood) of -5196.62 supporting this estimate of clustering. Bayesian goodness of fit measure for the optimal partition of genetic mixture estimates depends on the highest values of Log (marginal likelihood) of different runs (Corander and Marttinen 2006). The clusters were (site 1 and 2), (site 8 and 9), site 3, site 4, site 5, site 6, and site 7. BAPS clustering of individual genotypes in figure 2.7 resulted in a total of 12 clusters, which appeared as a highly mixed clustering with no obvious groupings except for slight differentiation of (sites 1 and 2).

Assessing all nine sites by the methods in Pritchard *et al.* (2007) and Pritchard *et al.* (2000), the maximum posterior probability for the number of populations (K) in *STRUCTURE* was at K =14 with relatively high standard deviation in figure 2.8-A, but all the means probability values stabilized around the same range for K = 7 to K = 14 with clear and alarming standard deviations for some values. Also, the ad hoc statistic K reported by Evanno *et al.* (2005) was applied to the data resulting in K = 3 in figure 2.8-B. After excluding site 7 from the data, the maximum posterior probability for the number of populations (K) in *STRUCTURE* was at K = 7 in figure 2.8-C. The *ad hoc* statistic K resulted in K = 2 in figure 2.8-D.

Comparing the two figures 2.8-A and 2.8-C, K = 7 was chosen as the best estimate of the number of populations (K), and I visualized the *STRUCTURE* plots of genetic mixture differentiation for the number of populations K = 7, 3, and 2 in figure 2.9. When all nine sites were included, the *STRUCTURE* plots for K = 7 and 3 were visualized in figures 2.9-A and 2.9-B. After the exclusion of site 7, the *Structure* plots for K = 7 and 2 were visualized in figures 2.9-C and 2.9-D.

Two main points could be observed from all the *STRUCTURE* plots in figure 2.9, site 1 and site 2 were almost one cluster with gene diversity H_e range of 0.22-0.25, and site 3 was a transitional area with mixed clusters. The plots in figures 2.9-A and 2.9-B represented site 7 as a cluster with a H_e range of 0.28-0.29. Both plots in figures 2.9-B and 2.9-D showed sites 4, 5, 6, 8, and 9 as nearly one cluster with a H_e range of 0.36-0.37.

Two data sets were used to assess the number of clusters by plotting BIC values of different K values for DAPC: the first data set had all nine sites in figure 2.10-A, and the second one was without site 7 in figure 2.10-B. There were no obvious 'optimal' numbers of clusters (true K), and a wide range of cluster numbers could summarize the data, so the question in this case would be: "how many clusters would be useful to describe the data?". The chosen numbers of clusters were 7 in figure 2.10-A, and 6 in figure 2.10-B. The numbers of clusters 7 and 6 were the minimum number of clusters after which the BIC increased or decreased by a negligible amount, and they retained the highest numbers of individuals from the sites in the inferred clusters.

Figure 2.11 and figure 2.12 provided a visual assessment of between-group structures using DAPC scatterplots and group membership's plots (*STRUCTURE*-like plots). Figure 2.11 reflected the case with all nine sites included (K = 7), while site 7 was excluded in figure 2.12 (K = 6).

Numbers of observations were identified in the figure 2.11 and figure 2.12. First, site 1 and site 2 were one cluster, and the clusters of (sites 1 and 2), site 3, site 4, and site 7 were relatively more clear-cut genetic clusters, while the clusters that included sites 5, 6, 8, and 9 were more loose clusters reflecting higher admixture possibilities. Second, the cluster of (sites 1 and 2) and the cluster of site 7 were genetically the farthest clusters, while the clusters that comprised sites 5, 6, 8, and 9 were genetically the closest clusters. Third, the cluster of site 3 and the cluster of site 4 took intermediate positions in the global picture of clusters. More specifically, the cluster of site 3 was closer to the cluster of (sites 1 and 2), but the cluster of site 4 was closer to the clusters that contained sites 5, 6, 8, and 9.

2.4 Discussion

2.4.1 Genetic diversity

This study utilized 12 microsatellite loci to investigate the existing genetic diversity of *A. marina* on the Red Sea coast. Other studies with the aim of understanding the genetic diversity of *A. marina* around the world used different numbers of microsatellite loci. For example, three microsatellite loci were used in (Maguire *et al*. 2000 a; Maguire *et al*. 2001; Kahrood *et al*. 2008), five microsatellite loci were used in (Giang *et al*. 2003; Zolgharnein *et al*. 2010; Yoshimori *et al*. 2015), and 6, 7, 8 microsatellite loci were used in Maguire *et al*. 2000 b; Arnaud-Haond *et al*. 2006; and Homer 2009, respectively. In all these studies, the total number of *A. marina* individuals across which microsatellite loci were screened varied between 15 to 303 individuals, while this study used 315 individuals.By using 12 microsatellite loci, a total of 89 alleles were detected with an average of 7.42 allelic diversity ($\bar{A}$) per locus. The allelic diversity of 7.42 found along the Red Sea coastal region of Saudi Arabia was similar to the 7.75 found in the Northern Rivers of New South Wales, Australia (Homer 2009), and with the 6.7 found in New South Wales, Northern Territory, and Western Australia (Maguire *et al*. 2000 b). However, the allelic diversity reported here is greater than those found in the coastal areas of Vietnam, Iran, and Egypt of 4.2, 4.6, and 5, respectively. (Giang *et al*. 2003; Kahrood *et al*. 2008; Yoshimori *et al*. 2015).

When the study areas were broadened, other studies had an increase in the allelic diversity. Maguire *et al*. (2001) sampled throughout six different Australian states and territories resulting in an allelic diversity of 17.3. Similarly, Arnaud-Haond *et al*. (2006) added samples from Philippines and Vietnam to their Australian samples, and the allelic diversity was 16.8. Also, Maguire *et al*. (2000 a) had an allelic diversity of 23.3 with specimens from Australia, New Zealand, New Caledonia, Papua New Guinea, Malaysia, Japan, India, United Arab Emirates, and South Africa.

However, both of Maguire *et al*. (2000 a) and Maguire *et al*. (2001) captured higher averages of numbers of alleles using the most polymorphic microsatellites. By using only the most polymorphic loci, the allelic diversity in this study would increase to 12, but averaging across a greater number of microsatellite loci are more informative for inferring population genetic diversity (Young *et al.* 2000; Frankham *et al.* 2002).

The average number of different alleles per locus for all sites (N_a) ranged from 1.2 to 6.6 with an average of 3.2 which was close to most studies in which (N_a) averages ranged from 2.33 to 4.7 (Maguire *et al*. 2000 a; Giang *et al*. 2003; Kahrood *et al*. 2008; Homer 2009 Zolgharnein *et al*. 2010; and Yoshimori *et al*. 2015). In this study, loci with longer repeats such as M81 (CA)9(CT)16 and M13 (AT)10(GT)12 produced more alleles comparing with other loci with shorter repeats such M98 (CGG)8 and M34 (GCT)14. In general, the number of alleles tends to increase with increasing number of repeats in microsatellite loci (Weber 1990; Maguire *et al*. 2000b; Giang *et al*. 2003).

Along the Red Sea coastal region of Saudi Arabia (an estimated sampling range of 1,345 kilometres), the gene diversity (heterozygosity - H_e) of 315 *A. marina* individuals varied between 0.009 and 0.666 with an average of 0.295, using 12 microsatellite loci. Even though the value of 0.295 gene diversity on the Red Sea was the lowest compared with other studies around the world, a group of considerations should be taken into account such as sampling range, number of samples, and number of loci. For example, Maguire *et al*. (2001) found a gene diversity average of 0.78 Australia wide with 120 individuals and 3 most polymorphic microsatellite loci, but gene diversity decreased to 0.494 with 200 individuals and 3 loci when the sampling area was expanded over 500 kilometres outside of Australia (Maguire *et al*. 2000 a). Gene diversity is anticipated to increase with wider sampling range, but adding more populations that happen to be highly inbred lowers the overall gene diversity.

The southern Indo-Pacific is believed to be *A. marina* centre of distribution, and its origin is in Australia as shown in the earliest fossil pollen records discovered (Ricklefs & Latham 1993). So, places such as South Africa is considered to be the global western edge of the distribution range, while Japan and the Red Sea are the global northern edge. Samples from the Northern Rivers of New South Wales, Australia revealed gene diversity of 0.46 with 220 individuals and 8 loci (Homer 2009); however, going northward direction, the coastal areas of Vietnam had an average of 0.322 with 128 individuals and 5 loci (Giang *et al*. 2003). The Vietnamese populations' gene diversity was the closest to the Red Sea individuals.

Other findings showed greater averages of gene diversity for *A. marina* populations at the edge of the distribution range, but their sampling area, number of samples, and number of loci could be arguably less informative for inferring population genetic diversity. For instance, 10 individuals with 3 loci from United Arab Emirates coast had a gene diversity of 0.816 (Maguire

et al. 2000 a), and 44 individuals with 5 loci from Iran coast had 0.711 with an estimated sampling range of 386 kilometres (Zolgharnein *et al*. 2010). Moreover, 45 individuals with 5 loci from the Red Sea coastal area of Egypt had a gene diversity of 0.635 (Yoshimori *et al*. 2015). Likewise, with the same number of samples and loci in both studies (10 individuals and 3 loci), Dona Paula Goa, India samples had a gene diversity of 0.616, and Durban, South Africa samples had a gene diversity of 0.598 (Maguire *et al*. 2000 a).

The samples from the Red Sea coast of Saudi Arabia had a range of observed heterozygosity (H_o) from 0.202 (site 2) to 0.404 (site 8) with an average of 0.298. This (H_o) average was close to both the Vietnamese populations' (H_o) average of 0.21 (Giang *et al*. 2003) and to Durban, South Africa populations' (H_o) average of 0.233 (Maguire *et al*. 2000 a). However, both of the Vietnamese and the South African populations exhibited significant levels of inbreeding 0.354 and 0.623, respectively, and that was not the case on the Red Sea. Giang *et al*. (2003) suggested that this may be due to repeated bottlenecks and founder effects, while Maguire *et al*. (2000 a) suggested the effects of episodes of glaciation and transgressions in earlier times (Saenger 1998). For most sites, expected heterozygosities (H_e) on the Red Sea coast were close to observed heterozygosities (H_o), and (H_e) ranged from 0.191to 0.401 with an average of 0.295. This led to fixation indices (F_{XX}) very close to zero in most sites, as expected under random mating. The levels of inbreeding ranged from negative 0.044 (site 3) to positive 0.126 (site 7), with an average inbreeding coefficient of positive 0.012 (very low level of inbreeding). On the other hand, the outcrossing rate ranged from 0.77 (site 7) to 1.092 (site 3), with an average of 0.978 (high outcrossing). Overall, *A. marina* individuals on the Red Sea coast were generally outcrossing with low levels of inbreeding. Finally, 31alleles out of the 89 alleles were found to be site-specific, and the number of private alleles ranged from 1 (site 2) to 10 (site 9), and their frequencies fluctuate between 0.014 and 0.171. The percentage of the private alleles on the Red Sea coast samples 34.8% was close to the Vietnamese populations 33.3% (7 out 21) (Giang *et al*. 2003).

2.4.2 Partitioning genetic variation

A. marina samples from the Red Sea coast were assessed using three models of population structure: single panmictic model, isolation by distance model, and discrete subpopulation model. The presence of genetic structure was initially indicated by both of the highly significant

probability values of allelic and genotypic distributions across all sites and among site pairs, and the variation in sites allelic compositions. Moreover, the overall significant high F_{ST} (0.246)/ R_{ST} (0.34) values and the overall low level of gene flow reflected heterogeneity between sites, so a single panmictic model could not be assumed for *A. marina* on the Red Sea coast. Even though Duke *et al*. (1998) suggested the possibility of this model for *A. marina* for its widespread distribution and large numbers of produced propagules, this model could not be confirmed here and other studies. (Maguire *et al*. 2000 a; Giang *et al*. 2003; Arnaud-Haond *et al*. 2006). However, Homer (2009) suggested the occurrence of panmixia over a distance of approximately 620 meters, while Duke *et al*. (1998) reported high values of gene flow between relatively continuous mangrove habitats separated by a few tens of kilometres.

The positive correlations between geographic distances among sites and both of pairwise F_{ST} (borderline significant, *p*-value of 0.046) and Nei's genetic distances (*p*-value of 0.02) revealed the effect of the isolation by distance model (IBD), and this model could explain 12-12.3% of *A. marina* population structure on the Red Sea coast. Both findings of Homer (2009) and Melville and Burchett (2002) supported the isolation by distance model in *A. marina* populations on scales of 200 kilometres and 80 kilometres, respectively. Homer (2009) reported a significant ($p<0.012$) positive correlation of Rxy = 0.737 that explained 54% of the population structure. The estimated sampling range of 1,345 kilometres and the sampling strategy in this study could be the reason for the lower (R^2) values (0.12-0.123). The isolation by distance model assumes a complete continuity of distribution, but interbreeding is limited to short distances resulting in a correlation between geographical distance and migration. For instance, site 5 and site 6, which were geographically the closest sites in this study (59 km), had an F_{ST} value of 0.06, while site 1 and site 9, which were geographically the farthest sites in this study (1,345 km), had an F_{ST} value of 0.154. However, site 7 was a distance of 100 km from the nearest site 8, and site 7-8 pair had F_{ST} of 0.16, but site 5-8 pair had F_{ST} of 0.07 even though they were 452 km apart. This differentiation of site 7-8 pair was obviously not due to geographical distances. Overall, the interbreeding in *A. marina* on the Red Sea was restricted to short distances (IBD), but the variation in distances among sites was not the only factor shaping migration.

Wright's guidelines for diallelic systems suggest that F_{ST} levels less than 0.05 represent a low level of genetic differentiation, levels between 0.051 and 0.15 reflect moderate differentiation, and levels between 0.151 and above are considered to be highly genetically differentiated (Wright

1978). In this study, F_{ST} values ranged from 0.03 (sites 8 and 9) to 0.31 (sites 2 and 7) with an overall of 0.246. As a comparison with other studies, Maguire *et al.* (2000 a) reported a range of (0.05 to 0.82), with an overall F_{ST} of 0.41, and Giang *et al*. (2003) estimated an overall F_{ST} of 0.34. Both of these studies concluded a discrete subpopulations model from their data. On the other hand, estimates for overall F_{ST} values of 0.06 (Homer 2009) and 0.04 (Zolgharnein *et al*. 2010) with gene flow (Nm >1) among populations supported an isolation by distance model in their studies. Over all sites and loci of *A. marina* on the Red Sea coast, the number of migrants was 0.76, 0.48, and 1.9 using F_{ST}, R_{ST}, and the private alleles' method, respectively (Barton & Slatkin 1986).

Moreover, hierarchical analysis of molecular variance (AMOVA) showed that the variation among populations percentage and the variation within individuals in the total population percentage were 41%, 49%, respectively in (Maguire *et al.* 2000 a), but they were 6%, 94%, respectively in (Homer 2009). Maguire *et al.* (2000 a) concluded a discrete subpopulations model form their data, while Homer (2009) findings supported an isolation by distance model. On the Red Sea coast, the variation among populations percentage was 25%, and the variation within individuals in the total population percentage was 75%.

In addition to the significant correlation between genetic distances and geographical distances on the Red Sea coast, both of the overall F_{ST} value and its range, and the among populations variation percentage were not in the realm of discrete subpopulations. Hence, the isolation by distance model was more likely to reflect the structuring of the population. In order to understand what was contributing to the significant 25% among populations variation in this study, all of PCoA, BAPS, *STRUCTURE*, and DAPC plots were compared in the next paragraphs.

Site 7 and (sites 1 and 2 together) were highly differentiated populations based on both of the estimate of grouped allele frequencies (site perspective), and the partitioning of individual genotypes. According to the site by site PCoA plot in figure 2.5-A, site 7 was separated by the second axe which accounted for 30.4% of the variation. Both of BAPS clustering of groups in figure 2.6 and DAPC scatterplot in figure 2.11 showed site 7 as a separate cluster. Moreover, PCoA plot in figure 2.4-A separated individuals from site 7 by the second axe which accounted for 17.2% of the variation. The *STRUCTURE* plots in figures 2.9-A and 2.9-B displayed site 7 as a distinct group. The differentiation of site 7 was not due to geographical distances as it was previously explained by pairwise F_{ST} values. This could represent a sampling artefact which can be tested for

by re-sampling from site 7 at different times, and stable results of the genetic composition are expected if there is a sampling artefact. However, the observed difference on site 7 was most likely due to a sampling of related individuals because site 7 had the highest positive inbreeding coefficient (0.126). Conversely, site 1 and site 2 were the northerly farthest sites in this study, and their differentiations were due to geographical distances (isolation by distance). Based on site by site PCoA plots in figures 2.5-A and B, site 1 and site 2 were separated by the first axes in both plots which accounted for 42.1%, and 54.2% of the variation, respectively. Also, both of the BAPS clustering of groups in figure 2.6 and DAPC scatterplots in figure 2.11 and figure 2.12 showed site 1 and site 2 as one separate cluster. Moreover, PCoA plot in figure 2.4-B distinguished individuals from site 1 and site 2 by the first axe which accounted for 21.4% of the variation. Furthermore, all of *Structure* plots in figures 2.9-A, B, C, and D, and BAPS clustering of individual genotypes in figure 2.7 reflected site 1 and site 2 as almost one group.

Site 5, 6, 8, and 9 were closely placed together based on site by site PCoA plots in figures 2.5-A and B. Also, they were shown as three close intersectional clusters by DAPC scatterplots in figure 2.11 and figure 2.12. Moreover, both of *STRUCTURE* plots in figures 2.9-B and D showed them nearly as one cluster which was in agreement with PCoA plots in figure 2.4-A and B because of the close scattering of their individual genotypes differences.

Site 3 and site 4 represented two different clusters that took intermediate positions between the northern cluster (sites 1 and 2) and the southern clusters (site 5, 6, 8, and 9) in DAPC scatterplots in figure 2.11 and figure 2.12. As well, site by site PCoA plots in figures 2.5-A and B showed a similar positioning, and site 4 was separated in figures 2.5-B by PCoA plot's second axe which accounted for 14% of the variation. Most of *STRUCTURE* plots in figure 2.9 displayed sites 3 and 4 as mixed transitional clusters.

This comprehension of the differentiation pattern, which was explained above, helped in assessing indirectly over what distance gene flow would occur and its transitions or barriers. More specifically, the differentiation of *A. marina* on the Red Sea followed an isolation by distance model, and the differentiation was generally driven by both the grouped allelic frequencies and the differences in individual genotypes found mainly in site 1, 2, and 7. Starting from the south part of the Red Sea coastline and going northward, sites 9, 8, 6, 5 began to isolate by the increase in inter-sites distances, which varied from 59 km (site pair 5-6) to 577 km (site pair 5-9). The differentiation within this geographical range was relatively lower reflecting close intersectional

clusters and a relatively higher gene flow with a gene diversity H_e range of 0.28-0.4. After the range of 577 kilometres, site 4 and site 3 were mixed transitional zones, and these zones were a distance of 768-1000 km from the south with a gene diversity H_e range of 0.26-0.29. Reaching the northerly farthest sites and the edge of distribution, the grouped allelic frequencies and genotypes of site 2 and site 1 diverged as one distinct population, and this population was a distance of 1,150-1,350 km from the south with a gene diversity H_e range of 0.19-0.28. The differentiation of site 7 represented a gene flow barrier, and it was not due to IBD model. Even though 59 km was the shortest inter-sites distance in this study, the presence of panmixia could not be detected because of the highly significant probability values of allelic and genotypic distributions and F_{ST} values among site pairs. The distance scale of panmixia might occur on a smaller scale such as 620 meters (Homer 2009).

Over all sites and loci of *A. marina* on the Red Sea coast, the number of migrants was 0.76, 0.48, and 1.9 using F_{ST}, R_{ST}, and the private alleles' method, respectively (Barton & Slatkin 1986). The last estimate which is based on the private alleles method has been criticized as it is sensitive to sample size and markers. (Young *et al*. 2000). Theoretically, a single migrant per generation can prevent complete differentiation as Wright demonstrated (Frankham *et al*. 2002). However, a level of 5-20 migrants per generation could prevent differentiation as it accounts for fluctuations in population size in nature (Vucetich and Waite 2000; Frankham *et al*. 2002).

In addition to the effect of inter-sites distances, other factors can affect the genetic variation within and among sites such as mating system, pollination range, propagule dispersal, and anthropogenic factors.

For the mating system, *A. marina* is considered to be an outcrossing species based on the species entomophilous and protandrous flowers resulting in limited self-compatibility (Primack & Tomlinson 1980; Tomlinson 1986). The outcrossing rates in *A. marina* on the Red Sea coast ranged from 0.77 (site 7) to 1.1 (site 3), with an average of 0.978 (high outcrossing), whereas levels of inbreeding ranged from negative 0.044 (site 3) to positive 0.126 (site 7), with an average inbreeding coefficient of 0.012 (very low level of inbreeding). This finding was consistent with the studies that showed *A. marina* populations were generally outcrossing with low levels of inbreeding (Duke *et al*. 1998; Maguire *et al*. 2000 a). In general, the majority of the total genetic diversity is proportioned among populations (F_{ST}) in inbreeding species (Hamrick & Godt 1990; Awadalla & Ritland 1997). Site 7 exhibited the highest inbreeding coefficient, and it had the

highest range of pairwise F_{ST} values. In theory, colonization from single propagules comparing to outcrossing helps in establishing populations in isolated areas (Primack & Tomlinson 1980). For example, the strong inbreeding of *A. marina* populations reported by Giang *et al*. (2003) in the southern part of Vietnam was suggested as a process of recovery following disturbances, recent bottlenecks, or recolonizations. Since colonization is a common phenomenon in mangrove habitats (Maguire *et al*. 2000 a), site 7 might be an indication of past colonization events.

For the pollination range, the honeybee *Apis mellifera*, which is one of the most known pollinators of *A. marina*, has shown a fluctuation in space and time regarding its pollination range with a reported potential flight range up to 13.7 kilometres (Homer 2009). In this study, the distances between *A. marina* sites ranged from 59 km to 1,345 km. Therefore, *Apis mellifera* was most likely unable to cover such a range, and pollen dispersal might occur only within sites rather than between sites.

For the propagule dispersal, field experiments on propagule dispersal have shown limitations by ocean currents, the patchy presence of suitable environmental conditions, and the limited longevity of propagules during dispersal (Clarke 1992). On a larger scale, site-specific topography and hydrology could permit or enhance gene flow via propagule dispersal. For example, Giang *et al*. (2003) attributed the low genetic diversity in *A. marina* populations at Canh Duong, Vietnam to the poor development of river deltas. On the Red Sea coast, sites 1 and 2 showed comparatively lower values in their gene diversity, and these sites were located in regions in which steep mountains were relatively close to the sea coast. On a smaller scale, local retention of propagules and an increase in rates of inbreeding would occur when fruits are trapped in the pneumatophores root system (Rabinowitz, 1978; Maguire *et al*. 2000 a; Dodd *et al*., 2002).
Among populations genetic differentiation of chloroplast genomes, which is maternally inherited, could help to determine the relative roles of pollen and propagules to gene flow by comparing it with among populations genetic differentiation of nuclear genome via microsatellites (Ouborg *et al.* 1999; Young *et al.* 2000). Moreover, a site-specific study of the propagule dispersal could reveal the effect of local topography and hydrology on propagule dispersal and recruitment.

Many studies documented the degradation of mangroves by anthropogenic factors such as overdevelopment, pollution and unsustainable use (Farnsworth and Ellison 1997; Blasco *et al.* 2001; Alongi 2002; Saenger 2002). For example, a reduction in the levels of polymorphism was reported by Parani *et al*. (1997) for *A. marina* populations resulting from overuse of foliage for

fodder, grazing, and environmental pollution. Based on the field observations in this study, site 7 and 2 were under pressure from grazing, and site 4 and 5 were under pressure from environmental pollution because site 4 was close to agro-based industries (shrimp ponds), and site 5 was close to a sewage treatment plant. Both of site 7 and 5 had relatively higher inbreeding coefficients.

2.5 Summary

Background

Avicennia marina (Forsk.)Vierh. is the most wide-ranging of all mangrove tree species because it has the largest longitudinal and latitudinal distribution. Furthermore, *A. marina* can grow and reproduce across a wide range of climatic, saline, and tidal conditions which would imply a large genetic variation. The same vast geographic range and a large number of propagules, which can float and disperse with ocean current, suggest also that this species exhibits long-distance gene flow. A possibility that populations throughout the range would be genetically undifferentiated. Utilizing SSR markers, this study examined the genetic variation in *A. marina* along the Saudi Arabian Red Sea coastline, and it determined which model best described the distribution of genetic variation within and among population. That helped in assessing indirectly over what distance gene flow occurred and its transitions or barriers.

Results

A total of 89 different alleles were the outcomes of the 315 *A. marina* individuals utilizing 12 microsatellite loci, resulting in an allelic diversity average ($\bar{A}$) of 7.42. Observed heterozygosity (H_o) was close to expected heterozygosities (H_e) for most sites, and the average (H_o) was 0.298. The levels of inbreeding ranged from negative 0.044 to positive 0.126, with an average inbreeding coefficient of 0.012. On the other hand, the outcrossing rate ranged from 0.77 to 1.092, with an average of 0.978. Also, 31 alleles out of the 89 alleles were found to be unique for specific sites, and their frequencies fluctuated between 0.014 and 0.171. All F_{ST} values were found to be significant at the 99% level, and F_{ST} values ranged from 0.031 (sites 8 and 9) to 0.31 (sites 2 and 7) with an overall of 0.246. Moreover, all R_{ST} values were found to be significant at the 99% level, and R_{ST} values ranged from 0.0088 (sites 8 and 9) to 0.65 (sites 2 and 7) with an overall of 0.34. Over all populations and loci, the number of migrants was 0.76, 0.48, and 1.9 using F_{ST}, R_{ST}, and the private alleles' method, respectively. Results from AMOVA showed that the variation among populations was 25% ($p < 0.001$), within individuals in the total population were 75% ($p < 0.001$). The positive correlations between geographic distances among sites and both of pairwise F_{ST} (borderline significant, *p*-value of 0.046) and Nei's genetic distances (*p*-value of 0.02) revealed the effect of the isolation by distance model (IBD), and this model could explain

12-12.3% of *A. marina* population structure on the Red Sea coast. In addition to the significant correlation between genetic distances and geographical distances on the Red Sea coast, both of the overall F_{ST} value and its range, and the among populations variation percentage were not in the realm of discrete subpopulations. Hence, the isolation by distance model was more likely to reflect the structuring of the population. All plots of PCoA, BAPS, *STRUCTURE*, and DAPC plots demonstrated what was contributing to the significant 25% among populations variation. The differentiation was generally driven by both the grouped allelic frequencies and differences in individual genotypes found mainly in site 1, 2, and 7. Starting from the south part of the Red Sea coastline and going north, site 9, 8, 6, 5 began to isolate by the increase in inter-sites distances, which varied from 59 km (site pair 5-6) to 577 km (site pair 5-9). The differentiation within this geographical range was relatively lower reflecting close intersectional clusters and a relatively higher gene flow with a gene diversity H_e range of 0.28-0.4. After the range of 577 kilometres, site 3 and 4 were mixed transitional zones, and these zones were a distance of 768-1000 km from the south, and they had a gene diversity H_e range of 0.26-0.29. Reaching the northerly farthest sites and the edge of distribution, the grouped allelic frequencies and genotypes of site 1 and 2 diverged as one distinct population, and this population was a distance of 1,150-1,350 km from the south with a gene diversity H_e range of 0.19-0.28. The differentiation of site 7 represented a gene flow barrier, and it was not due to IBD model. Even though 59 km was the shortest inter-sites distance in this study, the presence of panmixia could not be detected because of the highly significant probability values of allelic and genotypic distributions and F_{ST} values among site pairs.

Conclusions

A. marina along the Saudi Arabian Red Sea coastline exhibits one of the lowest value of gene diversity comparing with other studies in the literatures, and the isolation by distance model (IBD) reflects the distribution of genetic variation within and among populations with the existence of transitional zones and one distinct population at the farthest northerly edge of the geographical distribution.

Table 2. 1 Distance Semi-matrix (kilometres) between nine *A. marina* sites on the Red Sea.

	1	2	3	4	5	6	7	8
2	194.38	0						
3	331.77	143.69	0					
4	575.89	384.82	247.41	0				
5	772.26	583.16	439.55	208.07	0			
6	832.61	643.19	499.89	264.33	59.87	0		
7	1,120.08	929.39	788.16	543.32	352.27	292.6	0	
8	1,222.28	1,031.66	890.2	645.69	452.94	393.06	101.77	0
9	1,345.39	1,154.56	1,013.71	768.01	577.5	517.66	225.16	125.25

Table 2. 2 Genetic diversity estimates for 315 *A. marina* individuals from the Red Sea.

Primer	Repeat type	A	N_a	N_e	H_e	H_o
M3	(TG)15	9	3.777	2.214	0.488	0.444
M13	(AT)10(GT)12	17	6.222	2.902	0.585	0.539
M32	(AC)14	14	4.333	1.372	0.224	0.234
M34	(GCT)14	2	1.222	1.019	0.018	0.019
M49	(TG)16	5	2.555	1.203	0.156	0.136
M64	(CAG)8	3	1.555	1.120	0.094	0.101
M73	(TG)15	3	1.555	1.057	0.046	0.031
M75	(TG)14	8	4.555	2.8550	0.621	0.549
M81	(CA)9(CT)16	19	6.666	3.406	0.666	0.939
M85	(GGC)8	3	1.888	1.323	0.207	0.196
M98	(CGG)8	3	1.222	1.009	0.009	0.003
Am07	(CA)3(TG)5(TG)5	3	2.666	1.919	0.431	0.387
Total		89	38.222	21.405		
Mean		(Ā) 7.42	3.185	1.783	0.295	0.298

A = total number of different alleles, N_a = average number of different alleles per site, N_e = number of effective alleles, H_e = expected heterozygosity, H_o = observed heterozygosity. Forward and reverse primer sequences are as per Maguire *et al.* (2000b), Yoshimori *et al.* (2015).

Table 2. 3 Genetic diversity for each site of *A. marina* on the Red Sea and overall.

ID	Latitude (N)	Longitude (E)	A	N_a	N_e	H_e	H_o	F	Outcrossing rate
1	27° 42′ 66″	35° 60′ 57″	31	2.583	1.557	0.281	0.285	0.009	0.982
2	26° 02′ 48″	36° 70′ 58″	31	2.583	1.383	0.191	0.202	0.001	0.998
3	24° 78′ 87″	37° 18′ 21″	38	3.166	1.632	0.264	0.278	-0.044	1.092
4	23° 12′ 05″	38° 80′ 52″	41	3.416	1.756	0.295	0.297	0.002	0.996
5	21° 26′ 65″	39° 12′ 60″	29	2.416	1.541	0.278	0.290	0.068	0.873
6	20° 81′ 89″	39° 45′ 26″	33	2.750	1.855	0.313	0.330	-0.042	1.088
7	18° 80′ 43″	41° 22′ 72″	33	2.750	1.597	0.285	0.25	0.126	0.776
8	17° 99′ 47″	41° 66′ 82″	53	4.416	2.504	0.401	0.404	-0.009	1.018
9	17° 14′ 08″	42° 41′ 52″	55	4.583	2.224	0.349	0.347	0.009	0.982
Mean				3.185	1.783	0.295	0.298	0.012	0.978

A = total number of different alleles, N_a = average number of different alleles per locus, N_e= number of effective alleles, H_e = expected heterozygosity, H_o = observed heterozygosity, F = Fixation Index (inbreeding coefficient).

Table 2. 4 Private alleles for the sites of *A. marina* on the Red Sea.

Sites	Locus	Allele	Frequency
1	**M64**	154	0.157
1	**M75**	205	0.171
2	**M13**	212	0.014
3	**M13**	216	0.029
4	**M32**	166	0.043
4	**M32**	180	0.029
4	**M75**	201	0.086
5	**M49**	175	0.014
5	**M98**	213	0.029
6	**M13**	217	0.029
6	**M85**	79	0.014
7	**M32**	163	0.014
8	**M3**	189	0.086
8	**M3**	195	0.014
8	**M13**	214	0.071
8	**M32**	153	0.086
8	**M81**	138	0.014
8	**M81**	162	0.014
8	**M81**	163	0.143
8	**M81**	165	0.029
8	**M81**	169	0.014
9	**M3**	178	0.057
9	**M13**	189	0.043
9	**M13**	192	0.029
9	**M32**	147	0.014
9	**M32**	159	0.014
9	**M49**	180	0.014
9	**M81**	159	0.014
9	**M81**	160	0.029
9	**M81**	161	0.014
9	**M98**	220	0.014

Table 2. 5 Matrix of pairwise comparisons of site genetic differentiation calculated using the infinite alleles model (FST) for *Avicennia marina* on the Red Sea.

	1	**2**	**3**	**4**	**5**	**6**	**7**	**8**	**9**
1	0.000	0.001	0.001	0.001	0.001	0.001	0.001	0.001	0.001
2	0.064	0.000	0.001	0.001	0.001	0.001	0.001	0.001	0.001
3	0.100	0.092	0.000	0.001	0.001	0.001	0.001	0.001	0.001
4	0.132	0.172	0.102	0.000	0.001	0.001	0.001	0.001	0.001
5	0.212	0.274	0.133	0.124	0.000	0.001	0.001	0.001	0.001
6	0.163	0.237	0.121	0.122	0.060	0.000	0.001	0.001	0.001
7	0.259	0.308	0.231	0.228	0.233	0.232	0.000	0.001	0.001
8	0.123	0.177	0.095	0.080	0.069	0.055	0.159	0.000	0.001
9	0.154	0.214	0.106	0.087	0.043	0.053	0.194	0.031	0.000

FST values below the diagonal. Probability, *p* (rand >= data) based on 999 permutations is shown above diagonal.

Table 2. 6 Matrix of pairwise comparisons of site genetic differentiation calculated using the stepwise mutation model (R_{ST}) for *Avicennia marina* on the Red Sea.

	1	**2**	**3**	**4**	**5**	**6**	**7**	**8**	**9**
1	0.000	0.001	0.001	0.001	0.001	0.001	0.001	0.001	0.001
2	0.0636	0.000	0.001	0.001	0.001	0.001	0.001	0.001	0.001
3	0.0776	0.0700	0.000	0.001	0.001	0.001	0.001	0.001	0.001
4	0.1749	0.3029	0.1841	0.000	0.001	0.001	0.001	0.001	0.001
5	0.3937	0.5388	0.3427	0.1483	0.000	0.001	0.001	0.001	0.001
6	0.3576	0.6134	0.3544	0.1155	0.2635	0.000	0.001	0.001	0.001
7	0.4457	0.6464	0.4631	0.2274	0.4267	0.5793	0.000	0.001	0.001
8	0.3697	0.4173	0.2783	0.2205	0.0698	0.2933	0.3847	0.000	0.001
9	0.5066	0.5850	0.4275	0.3418	0.1343	0.4406	0.5556	0.0088	0.000

R_{ST} values below the diagonal. Probability, *p* (rand >= data) based on 999 permutations is shown above diagonal.

Table 2. 7 Matrix of pairwise comparisons of site genetic differentiation calculated using the multiallelic analog of FST (GST) for *Avicennia marina* on the Red Sea.

	1	2	3	4	5	6	7	8	9
1	0.000	0.001	0.001	0.001	0.001	0.001	0.001	0.001	0.001
2	0.057	0.000	0.001	0.001	0.001	0.001	0.001	0.001	0.001
3	0.093	0.085	0.000	0.001	0.001	0.001	0.001	0.001	0.001
4	0.125	0.165	0.095	0.000	0.001	0.001	0.001	0.001	0.001
5	0.205	0.267	0.126	0.117	0.000	0.001	0.001	0.001	0.001
6	0.156	0.230	0.115	0.115	0.053	0.000	0.001	0.001	0.001
7	0.252	0.302	0.224	0.221	0.226	0.225	0.000	0.001	0.001
8	0.116	0.170	0.088	0.073	0.062	0.048	0.152	0.000	0.001
9	0.147	0.207	0.099	0.079	0.036	0.046	0.186	0.023	0.000

GST values below the diagonal. Probability, p (rand >= data) based on 999 permutations is shown above diagonal

Table 2. 8 Overall genetic differentiation calculated using the infinite alleles model (F_{ST}) and the stepwise mutation model (R_{ST}) of 9 sites of *Avicennia marina* on the Red Sea.

F-Statistics	Value	*p*	R-Statistics	Value	*p*	*Nm*		
								private
F_{ST}	0.246	<0.001	**R_{ST}**	0.339	<0.001	F-Statistics	R-Statistics	alleles*
F_{IS}	0.005	0.366	**R_{IS}**	0.201	<0.001			
F_{IT}	0.249	<0.001	**R_{IT}**	0.472	<0.001	0.76	0.48	1.9

*Number of migrants using private alleles (Barton & Slatkin 1986).

Table 2. 9 Hierarchical analysis of molecular variance of 9 sites of Avicennia marina on the Red Sea.

Source of Variation	d.f	variance components	*p* F_{ST}	variance components	*p* R_{ST}
		F_{ST}		**R_{ST}**	
Among sites	8	25%	<0.001	34%	<0.001
Within sites	306	0%	0.366	13%	<0.001
Within individuals	315	75%	<0.001	53%	<0.001

% Molecular variation percentage explained by the hierarchical level; p, level of significance for the distribution of variation for that hierarchical level being different from random; d.f = degree of freedom.

Table 2. 10 *Avicennia marina* allele frequencies for all sites by locus.

Locus1M3	Allele	Site1	Site2	Site3	Site4	Site5	Site6	Site7	Site8	Site9
	178	0.000	0.000	0.000	0.000	0.000	0.000	0.000	0.000	0.057
	180	0.700	0.800	0.400	0.871	0.000	0.000	0.086	0.171	0.171
	182	0.286	0.200	0.071	0.100	0.371	0.343	0.000	0.329	0.229
	184	0.000	0.000	0.529	0.000	0.629	0.657	0.186	0.286	0.471
	186	0.014	0.000	0.000	0.000	0.000	0.000	0.686	0.029	0.014
	189	0.000	0.000	0.000	0.000	0.000	0.000	0.000	0.086	0.000
	190	0.000	0.000	0.000	0.014	0.000	0.000	0.043	0.014	0.057
	193	0.000	0.000	0.000	0.014	0.000	0.000	0.000	0.071	0.000
	195	0.000	0.000	0.000	0.000	0.000	0.000	0.000	0.014	0.000
Locus2M13	**Allele**	**Site1**	**Site2**	**Site3**	**Site4**	**Site5**	**Site6**	**Site7**	**Site8**	**Site9**
	169	0.014	0.000	0.014	0.000	0.000	0.000	0.000	0.000	0.214
	170	0.057	0.000	0.043	0.086	0.200	0.000	0.029	0.471	0.271
	189	0.000	0.000	0.000	0.000	0.000	0.000	0.000	0.000	0.043
	192	0.000	0.000	0.000	0.000	0.000	0.000	0.000	0.000	0.029
	193	0.000	0.014	0.071	0.086	0.271	0.343	0.000	0.071	0.071
	195	0.000	0.000	0.000	0.000	0.000	0.014	0.000	0.000	0.043
	197	0.000	0.000	0.000	0.071	0.000	0.014	0.100	0.014	0.014
	199	0.414	0.929	0.786	0.400	0.529	0.200	0.286	0.200	0.271
	201	0.043	0.000	0.000	0.029	0.000	0.100	0.586	0.071	0.014
	203	0.000	0.000	0.029	0.000	0.000	0.000	0.000	0.100	0.000
	205	0.000	0.014	0.014	0.000	0.000	0.000	0.000	0.000	0.000
	208	0.471	0.029	0.014	0.043	0.000	0.300	0.000	0.000	0.000
	210	0.000	0.000	0.000	0.286	0.000	0.000	0.000	0.000	0.029
	212	0.000	0.014	0.000	0.000	0.000	0.000	0.000	0.000	0.000
	214	0.000	0.000	0.000	0.000	0.000	0.000	0.000	0.071	0.000
	216	0.000	0.000	0.029	0.000	0.000	0.000	0.000	0.000	0.000
	217	0.000	0.000	0.000	0.000	0.000	0.029	0.000	0.000	0.000
Locus3M32	**Allele**	**Site1**	**Site2**	**Site3**	**Site4**	**Site5**	**Site6**	**Site7**	**Site8**	**Site9**
	147	0.000	0.000	0.000	0.000	0.000	0.000	0.000	0.000	0.014
	153	0.000	0.000	0.000	0.000	0.000	0.000	0.000	0.086	0.000
	155	0.957	0.986	0.986	0.671	0.757	1.000	0.029	0.757	0.829
	157	0.000	0.000	0.000	0.014	0.014	0.000	0.000	0.000	0.086
	159	0.000	0.000	0.000	0.000	0.000	0.000	0.000	0.000	0.014
	163	0.000	0.000	0.000	0.000	0.000	0.000	0.014	0.000	0.000
	166	0.000	0.000	0.000	0.043	0.000	0.000	0.000	0.000	0.000
	168	0.000	0.000	0.000	0.000	0.000	0.000	0.857	0.043	0.014
	170	0.029	0.000	0.014	0.100	0.014	0.000	0.029	0.043	0.014
	172	0.000	0.014	0.000	0.029	0.214	0.000	0.000	0.000	0.014
	174	0.014	0.000	0.000	0.000	0.000	0.000	0.000	0.029	0.014
	176	0.000	0.000	0.000	0.114	0.000	0.000	0.014	0.000	0.000
	178	0.000	0.000	0.000	0.000	0.000	0.000	0.057	0.043	0.000

Continuousness of table 2.10 *Avicennia marina* allele frequencies for all sites by locus.

Locus3M32	Allele	Site1	Site2	Site3	Site4	Site5	Site6	Site7	Site8	Site9
	180	0.000	0.000	0.000	0.029	0.000	0.000	0.000	0.000	0.000
Locus4M34	**Allele**	**Site1**	**Site2**	**Site3**	**Site4**	**Site5**	**Site6**	**Site7**	**Site8**	**Site9**
	190	0.000	0.000	0.000	0.057	0.000	0.029	0.000	0.000	0.000
	191	1.000	1.000	1.000	0.943	1.000	0.971	1.000	1.000	1.000
Locus5M49	**Allele**	**Site1**	**Site2**	**Site3**	**Site4**	**Site5**	**Site6**	**Site7**	**Site8**	**Site9**
	174	0.000	0.000	0.057	0.000	0.171	0.000	0.000	0.014	0.000
	175	0.000	0.000	0.000	0.000	0.014	0.000	0.000	0.000	0.000
	176	0.843	0.986	0.886	0.971	0.800	0.886	0.971	0.971	0.886
	177	0.157	0.014	0.057	0.029	0.014	0.114	0.029	0.014	0.100
	180	0.000	0.000	0.000	0.000	0.000	0.000	0.000	0.000	0.014
Locus6M64	**Allele**	**Site1**	**Site2**	**Site3**	**Site4**	**Site5**	**Site6**	**Site7**	**Site8**	**Site9**
	146	0.000	0.000	0.086	0.043	0.000	0.000	0.000	0.157	0.043
	154	0.157	0.000	0.000	0.000	0.000	0.000	0.000	0.000	0.000
	155	0.843	1.000	0.914	0.957	1.000	1.000	1.000	0.843	0.957
Locus7M73	**Allele**	**Site1**	**Site2**	**Site3**	**Site4**	**Site5**	**Site6**	**Site7**	**Site8**	**Site9**
	167	0.000	0.071	0.000	0.000	0.029	0.029	0.000	0.000	0.000
	169	0.971	0.857	1.000	1.000	0.971	0.971	1.000	1.000	1.000
	170	0.029	0.071	0.000	0.000	0.000	0.000	0.000	0.000	0.000
Locus8M75	**Allele**	**Site1**	**Site2**	**Site3**	**Site4**	**Site5**	**Site6**	**Site7**	**Site8**	**Site9**
	201	0.000	0.000	0.000	0.086	0.000	0.000	0.000	0.000	0.000
	205	0.171	0.000	0.000	0.000	0.000	0.000	0.000	0.000	0.000
	207	0.529	0.371	0.414	0.486	0.629	0.414	0.271	0.343	0.329
	210	0.000	0.014	0.071	0.000	0.343	0.014	0.714	0.200	0.371
	211	0.300	0.471	0.129	0.014	0.000	0.271	0.000	0.014	0.029
	214	0.000	0.000	0.000	0.000	0.000	0.000	0.014	0.071	0.043
	216	0.000	0.129	0.357	0.400	0.029	0.171	0.000	0.200	0.171
	218	0.000	0.014	0.029	0.014	0.000	0.129	0.000	0.171	0.057
Locus9M81	**Allele**	**Site1**	**Site2**	**Site3**	**Site4**	**Site5**	**Site6**	**Site7**	**Site8**	**Site9**
	138	0.000	0.000	0.000	0.000	0.000	0.000	0.000	0.014	0.000
	142	0.000	0.000	0.057	0.000	0.000	0.000	0.014	0.000	0.000
	146	0.000	0.014	0.000	0.000	0.000	0.000	0.000	0.000	0.014
	148	0.457	0.514	0.229	0.057	0.000	0.186	0.086	0.086	0.000
	149	0.457	0.357	0.057	0.014	0.000	0.071	0.071	0.057	0.014
	150	0.029	0.086	0.429	0.543	0.471	0.414	0.386	0.186	0.243
	151	0.000	0.029	0.200	0.357	0.486	0.314	0.443	0.271	0.214
	152	0.000	0.000	0.000	0.014	0.029	0.000	0.000	0.029	0.243
	153	0.000	0.000	0.000	0.000	0.014	0.000	0.000	0.086	0.171
	154	0.057	0.000	0.014	0.000	0.000	0.014	0.000	0.043	0.029
	155	0.000	0.000	0.000	0.000	0.000	0.000	0.000	0.029	0.014
	159	0.000	0.000	0.000	0.000	0.000	0.000	0.000	0.000	0.014
	160	0.000	0.000	0.000	0.000	0.000	0.000	0.000	0.000	0.029

Continuousness of table 2.10 *Avicennia marina* allele frequencies for all sites by locus.

Locus9M81	Allele	Site1	Site2	Site3	Site4	Site5	Site6	Site7	Site8	Site9
	161	0.000	0.000	0.000	0.000	0.000	0.000	0.000	0.000	0.014
	162	0.000	0.000	0.000	0.000	0.000	0.000	0.000	0.014	0.000
	163	0.000	0.000	0.000	0.000	0.000	0.000	0.000	0.143	0.000
	165	0.000	0.000	0.000	0.000	0.000	0.000	0.000	0.029	0.000
	166	0.000	0.000	0.014	0.014	0.000	0.000	0.000	0.000	0.000
	169	0.000	0.000	0.000	0.000	0.000	0.000	0.000	0.014	0.000
Locus10M85	**Allele**	**Site1**	**Site2**	**Site3**	**Site4**	**Site5**	**Site6**	**Site7**	**Site8**	**Site9**
	79	0.000	0.000	0.000	0.000	0.000	0.014	0.000	0.000	0.000
	110	0.900	0.829	0.929	1.000	1.000	0.771	0.586	0.757	0.971
	114	0.100	0.171	0.071	0.000	0.000	0.214	0.414	0.243	0.029
Locus11M98	**Allele**	**Site1**	**Site2**	**Site3**	**Site4**	**Site5**	**Site6**	**Site7**	**Site8**	**Site9**
	213	0.000	0.000	0.000	0.000	0.029	0.000	0.000	0.000	0.000
	217	1.000	1.000	1.000	1.000	0.971	1.000	1.000	1.000	0.986
	220	0.000	0.000	0.000	0.000	0.000	0.000	0.000	0.000	0.014
Locus12Am07	**Allele**	**Site1**	**Site2**	**Site3**	**Site4**	**Site5**	**Site6**	**Site7**	**Site8**	**Site9**
	257	0.814	0.986	0.814	0.229	0.000	0.000	0.629	0.186	0.043
	269	0.086	0.014	0.100	0.443	0.700	0.529	0.086	0.343	0.600
	271	0.100	0.000	0.086	0.329	0.300	0.471	0.286	0.471	0.357

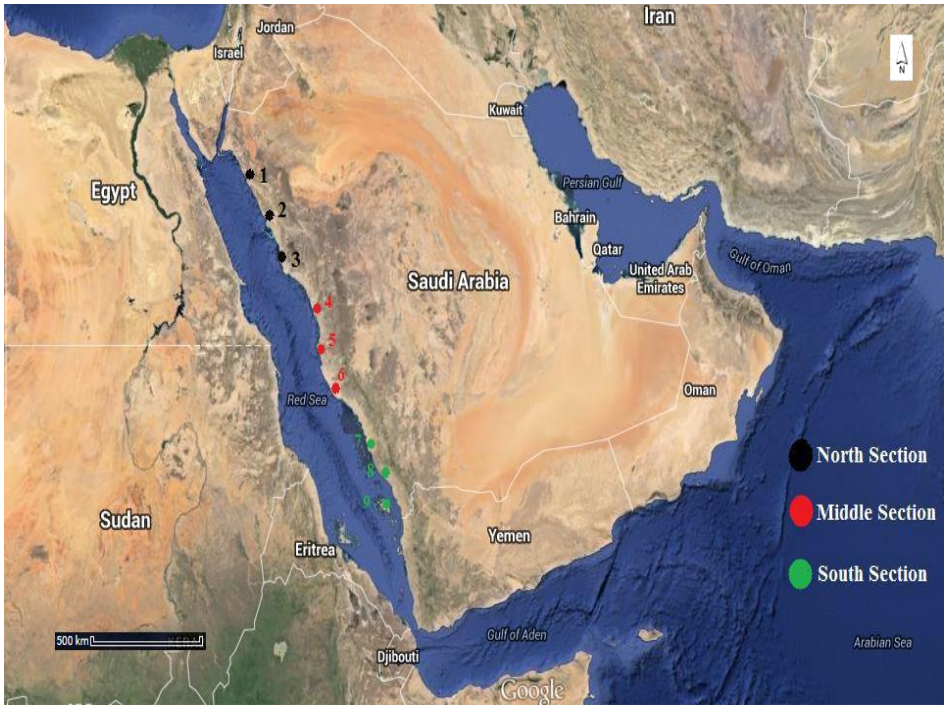

Figure 2. 1 Distribution of *Avicennia marina* sampling sites along the Red Sea, Saudi Arabia.

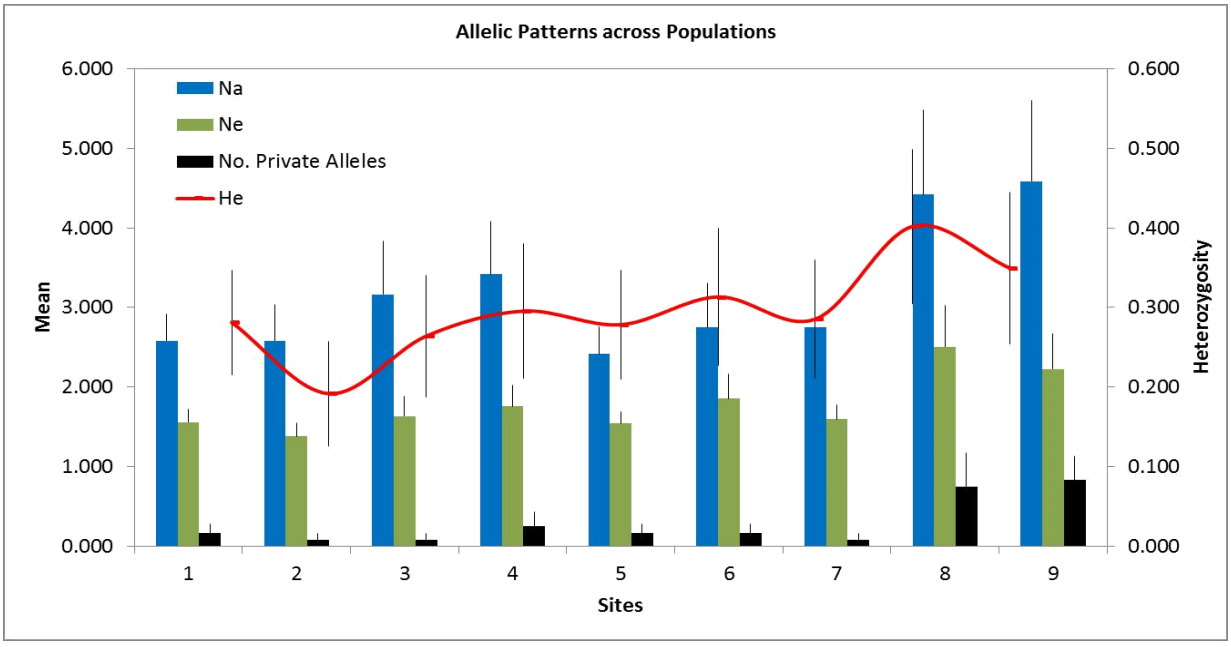

Figure 2. 2 Summary of allelic patterns for *A. marina* sites on the Red Sea.

(A)

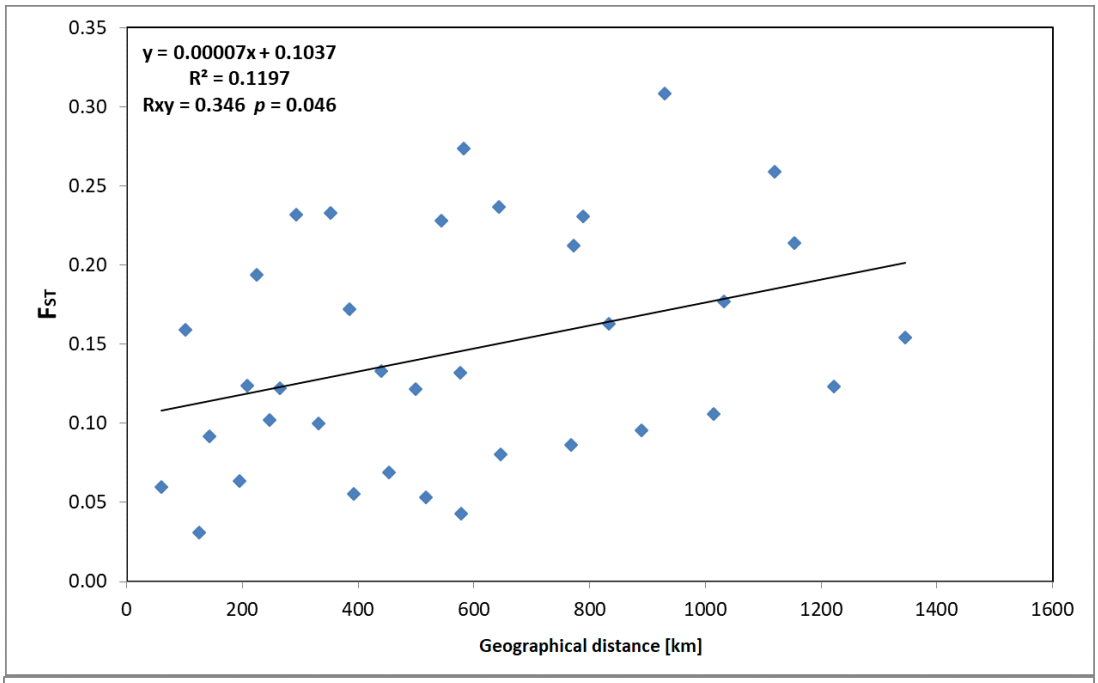

(B)

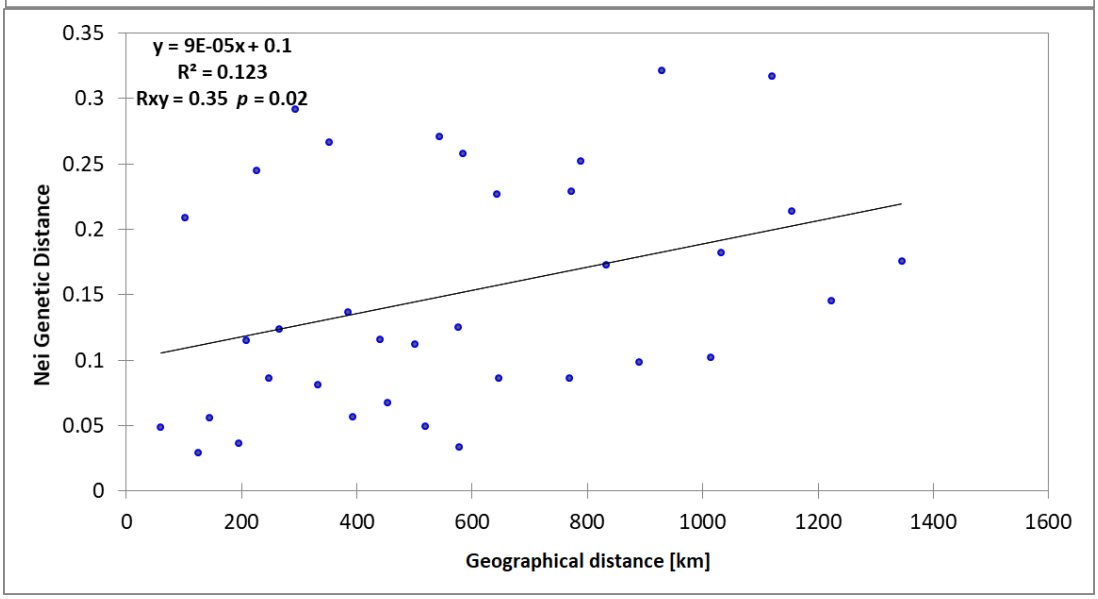

Figure 2. 3 Correlations: (A) geographic distance among *A. marina* sites on the Red Sea and pairwise FST, (B) geographic distance among sites and pairwise Nei genetic distance.

(A)

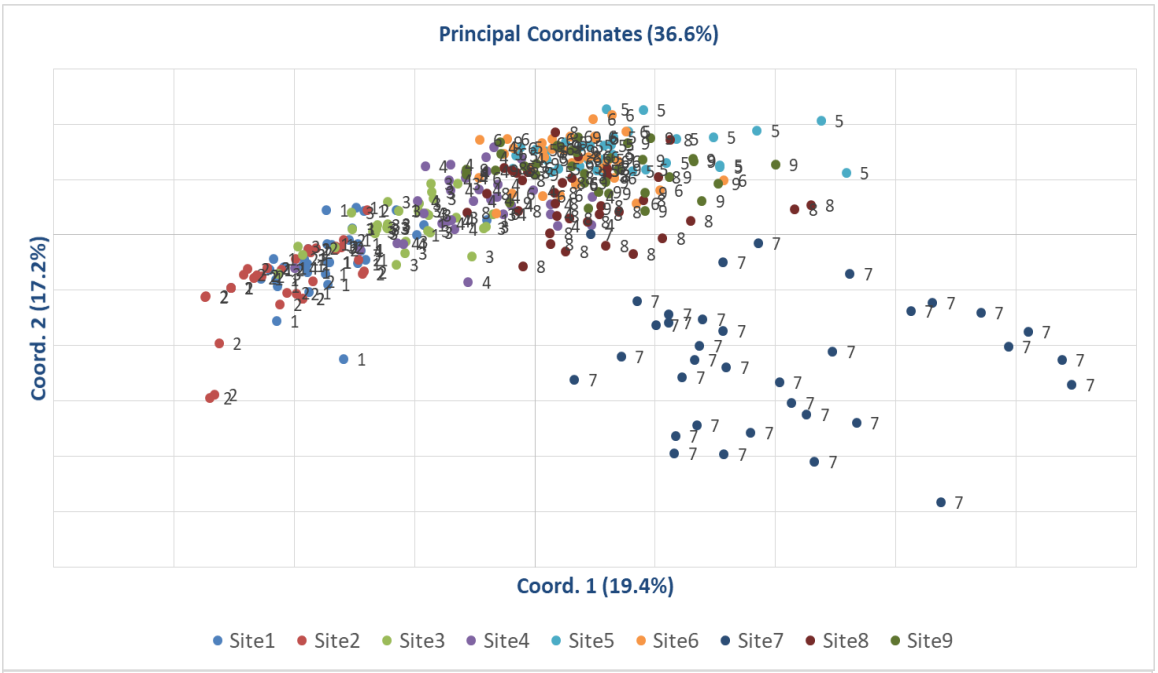

(B)

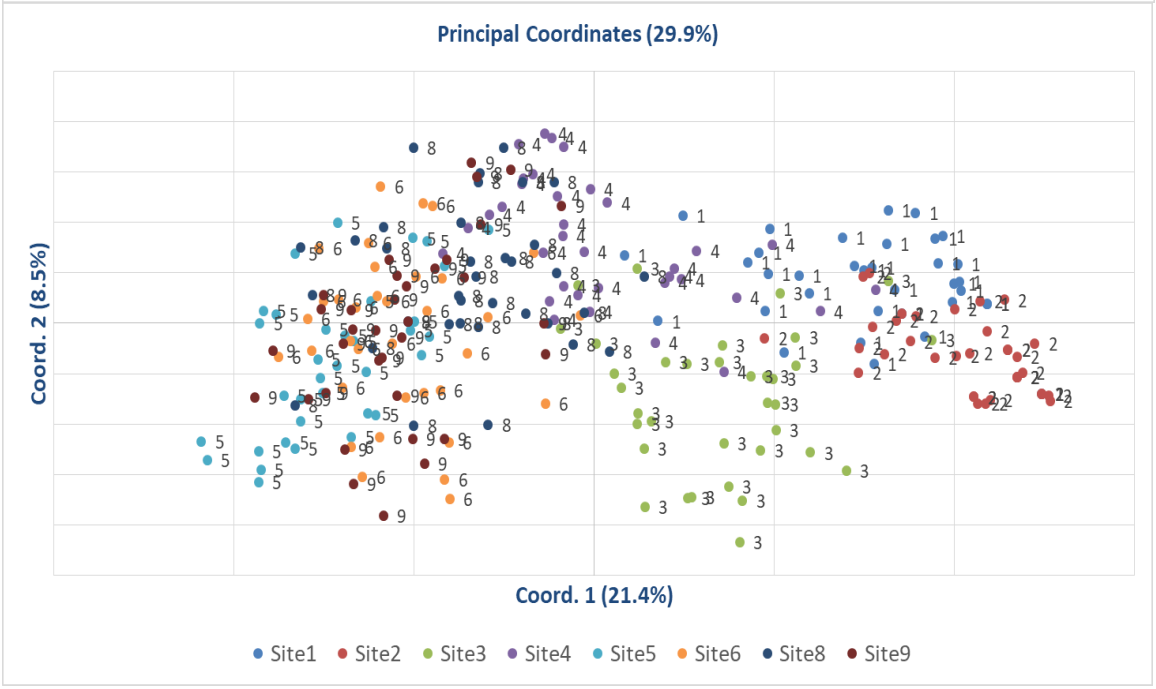

Figure 2. 4 PCA plots using pairwise genetic distance for individuals: (A) all of *A. marina* individuals from the nine sites on the Red Sea, (B) excluding site7

(A)

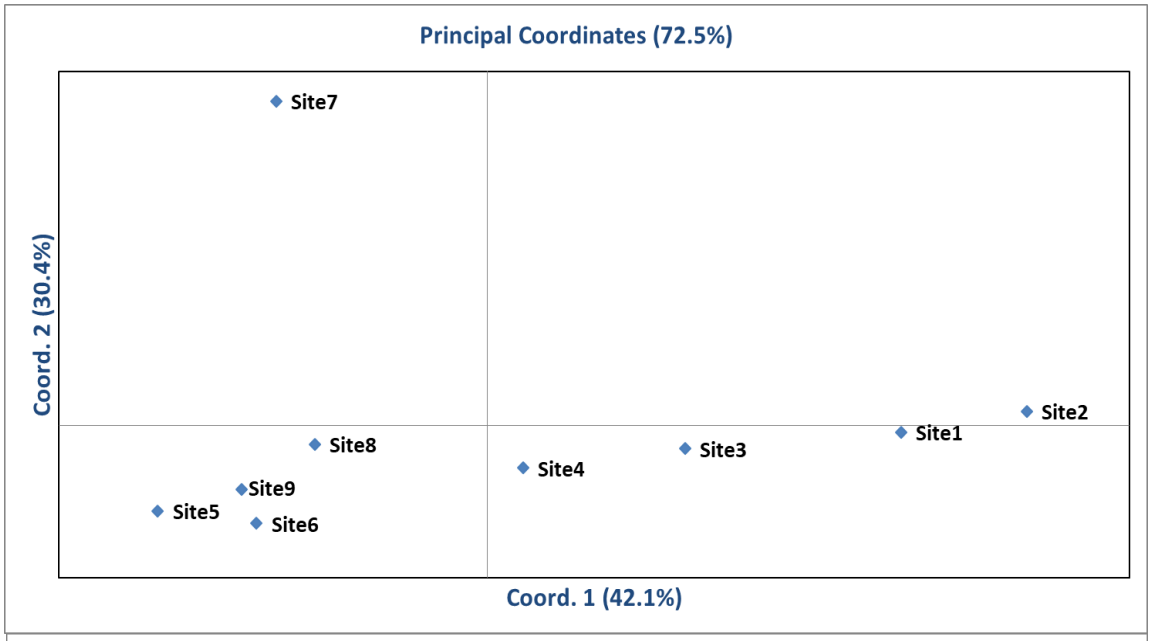

(B)

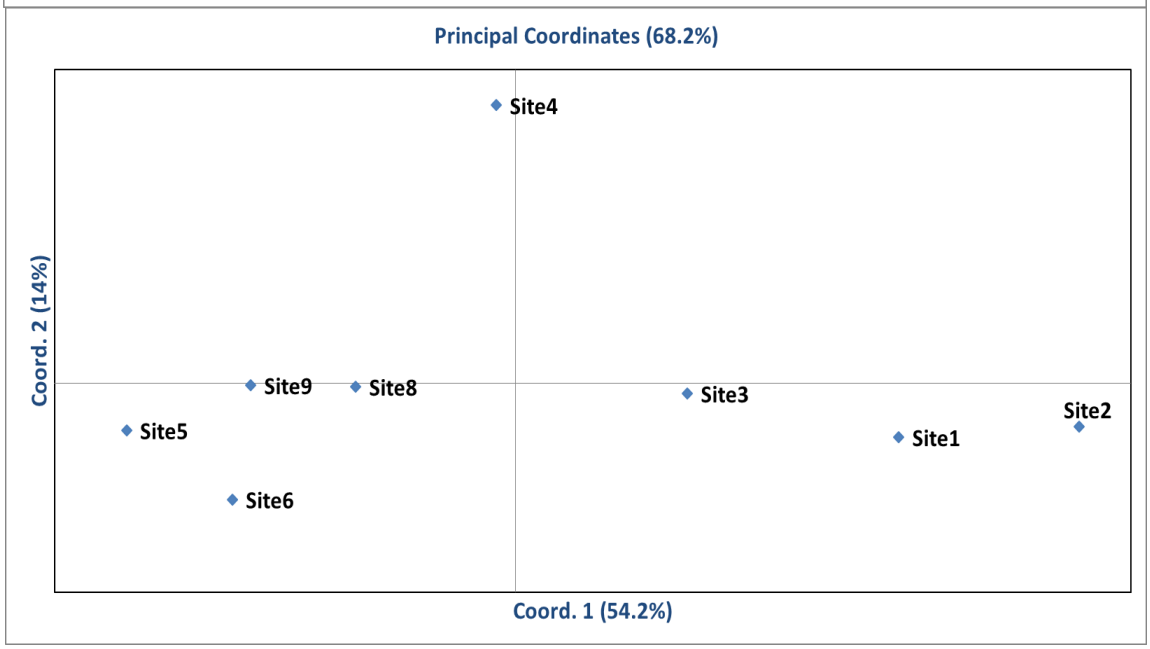

Figure 2. 5 PCA plots using site by site pairwise FST: (A) all of *A. marina* nine sites on the Red Sea, (B) excluding site7

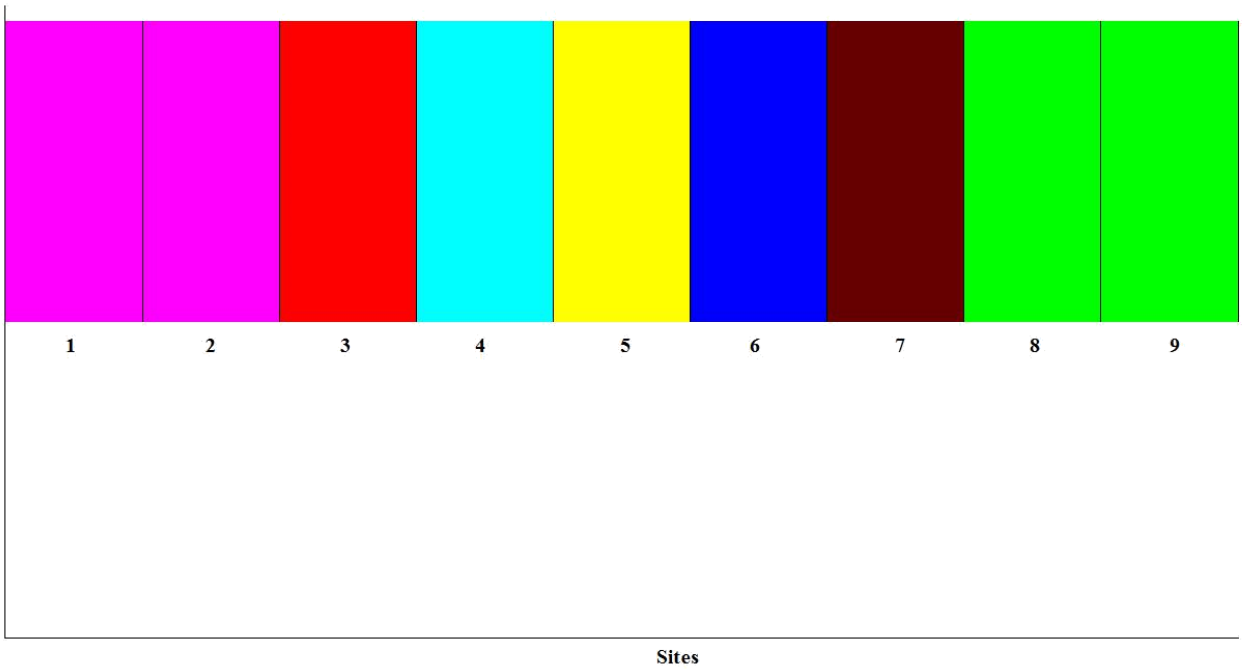

Figure 2. 6 BAPS analysis of genetic mixture differentiation based on group genetic mixture estimates for the 9 sample sites of *A. marina* on the Red Sea.

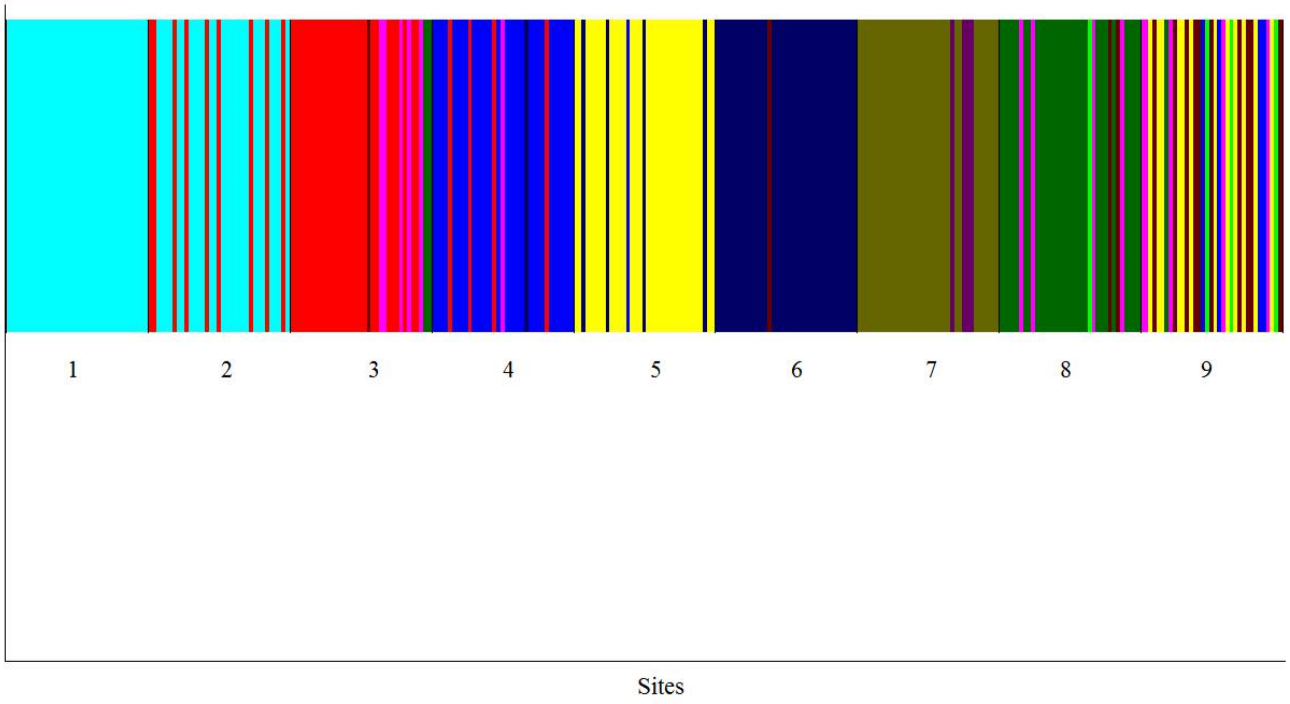

Figure 2. 7 BAPS analysis of genetic mixture differentiation based on individual genotypes of *A. marina* on the Red Sea.

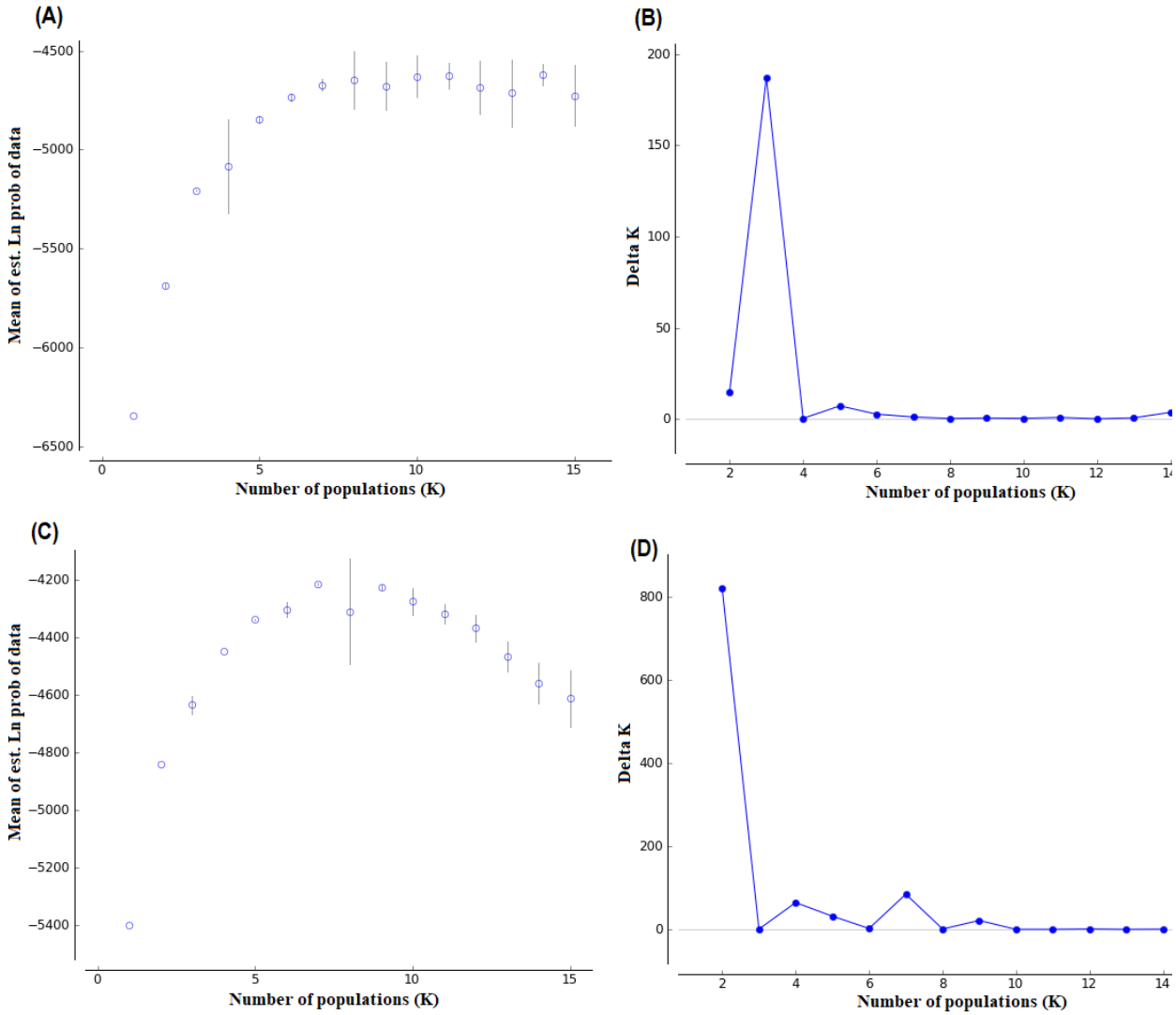

Figure 2. 8 Estimated number of populations (K): (A) all of *A. marina* nine sites on the Red Sea using *STRUCTURE*, (B) all the nine sites following Evanno *et al.* (2005) procedure, (C) excluding site7 using *STRUCTURE*, (D) excluding site7 following Evanno *et al.* (2005) procedure.

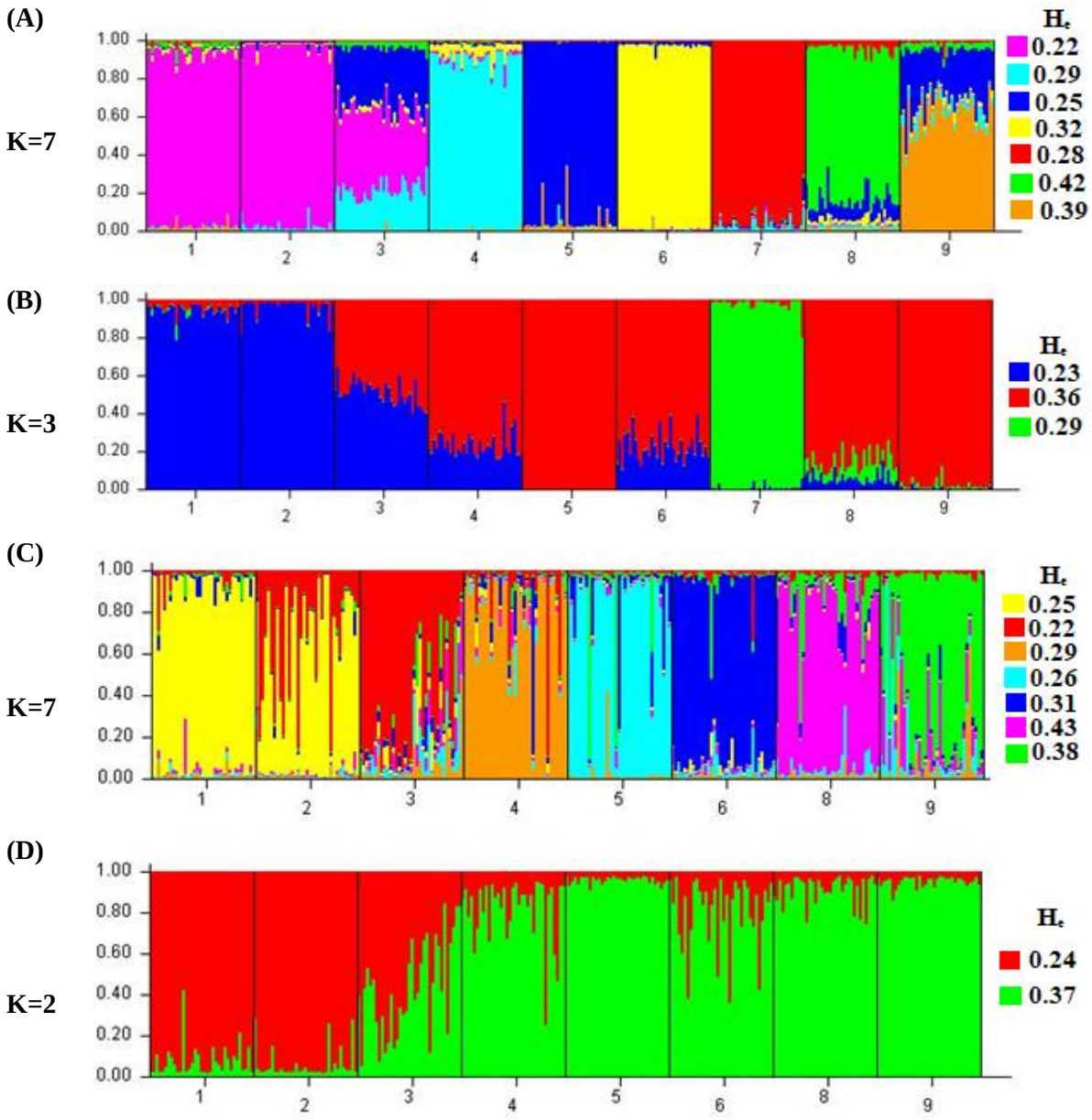

Figure 2. 9 *STRUCTURE* analyses of genetic mixture differentiation for (K) number of populations: (A) all of *A. marina* nine sites on the Red Sea for K = 7, (B) all nine sites for K = 3, (C) excluding site7 for K = 7, (D) excluding site7 for K = 2. H_e=expected heterozygosity (gene diversity)

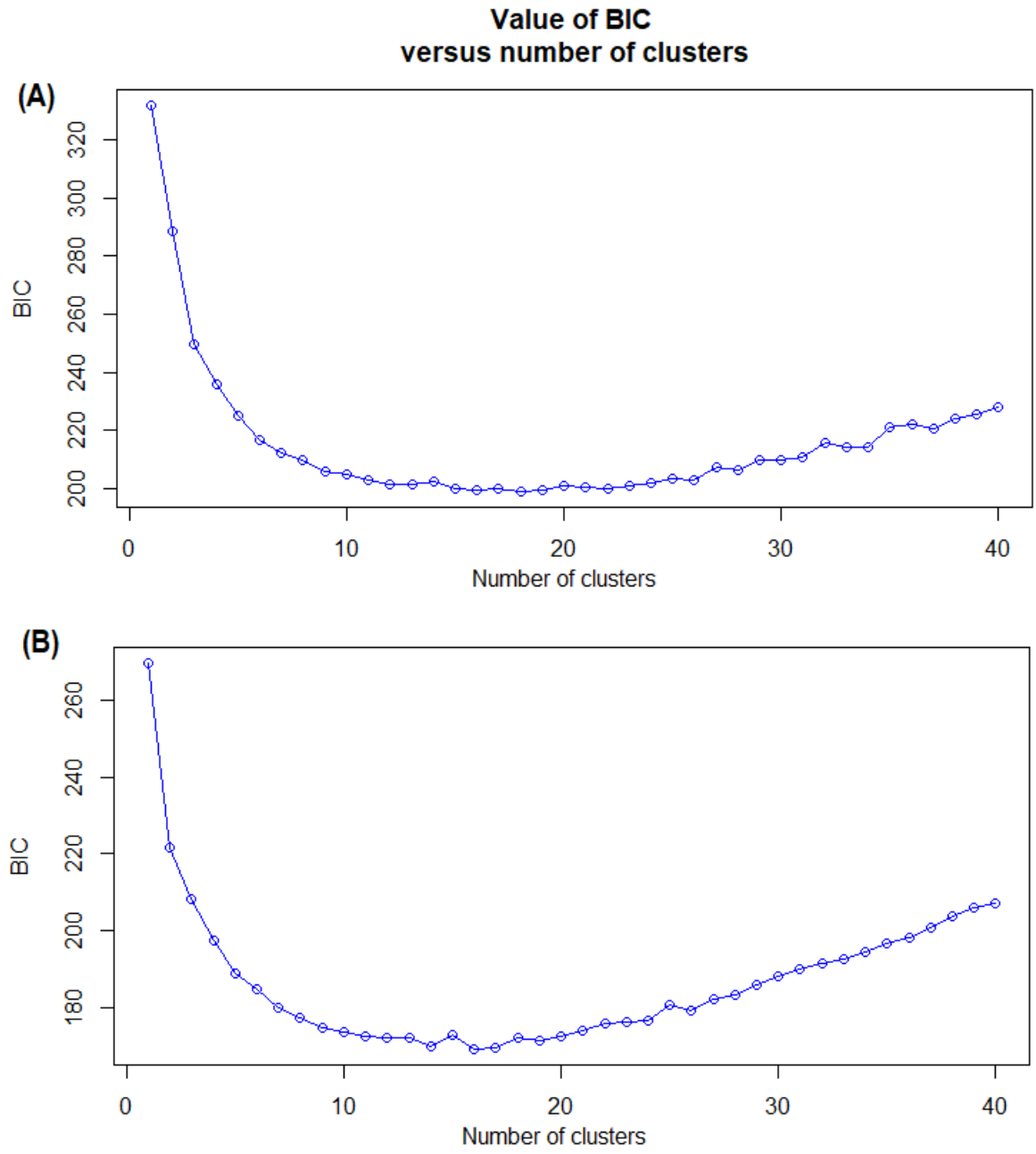

Figure 2. 10 Inference of the number of clusters based on Bayesian Information Criterion (BIC): (A) all of *A. marina* nine sites on the Red Sea, (B) excluding site 7.

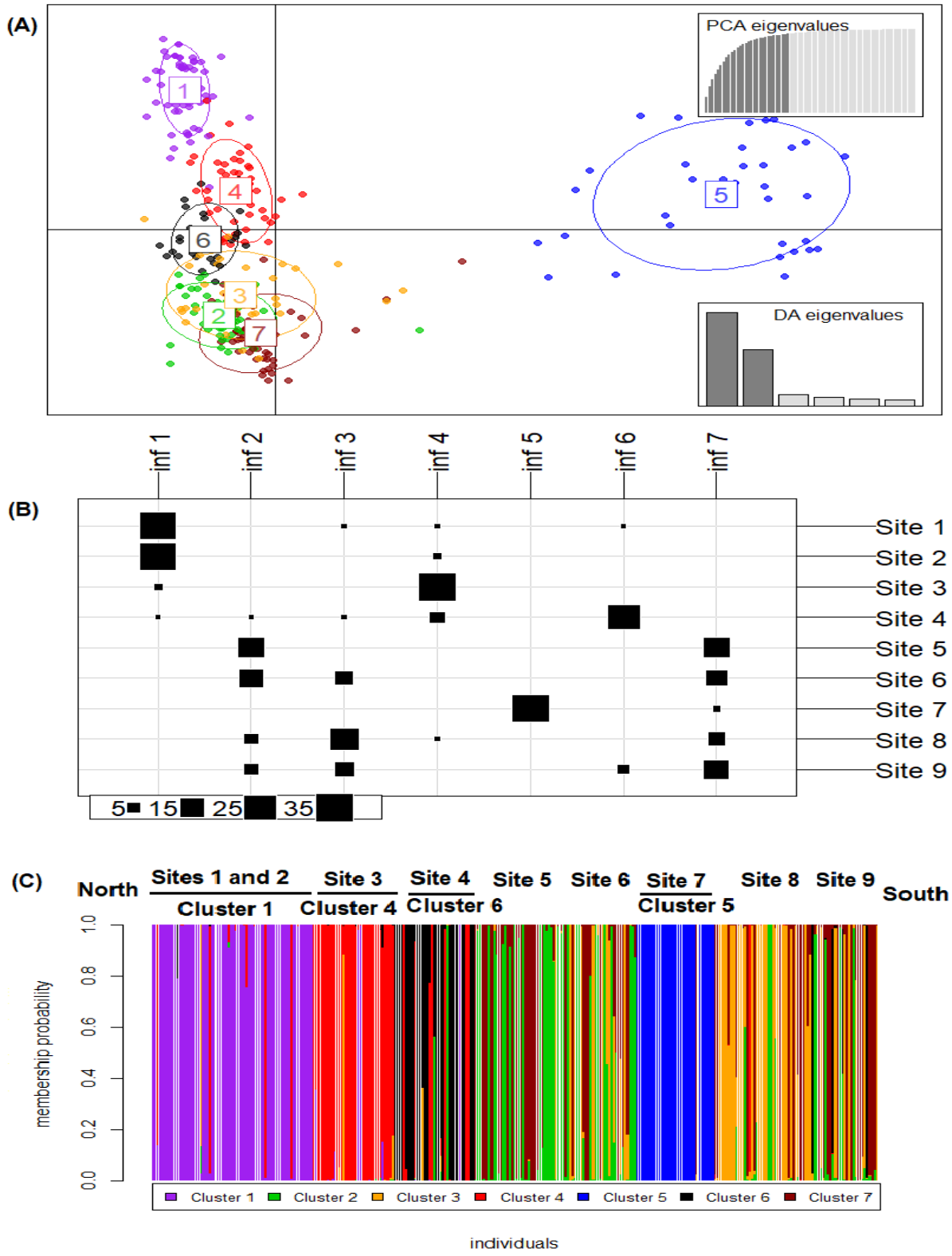

Figure 2. 11 DAPC analysis of all nine sites: (A) scatterplots of DAPC, (B) the number of individuals identified in the inferred clusters-inf, (C) membership probability of *A. marina* individuals on the Red Sea across clusters.

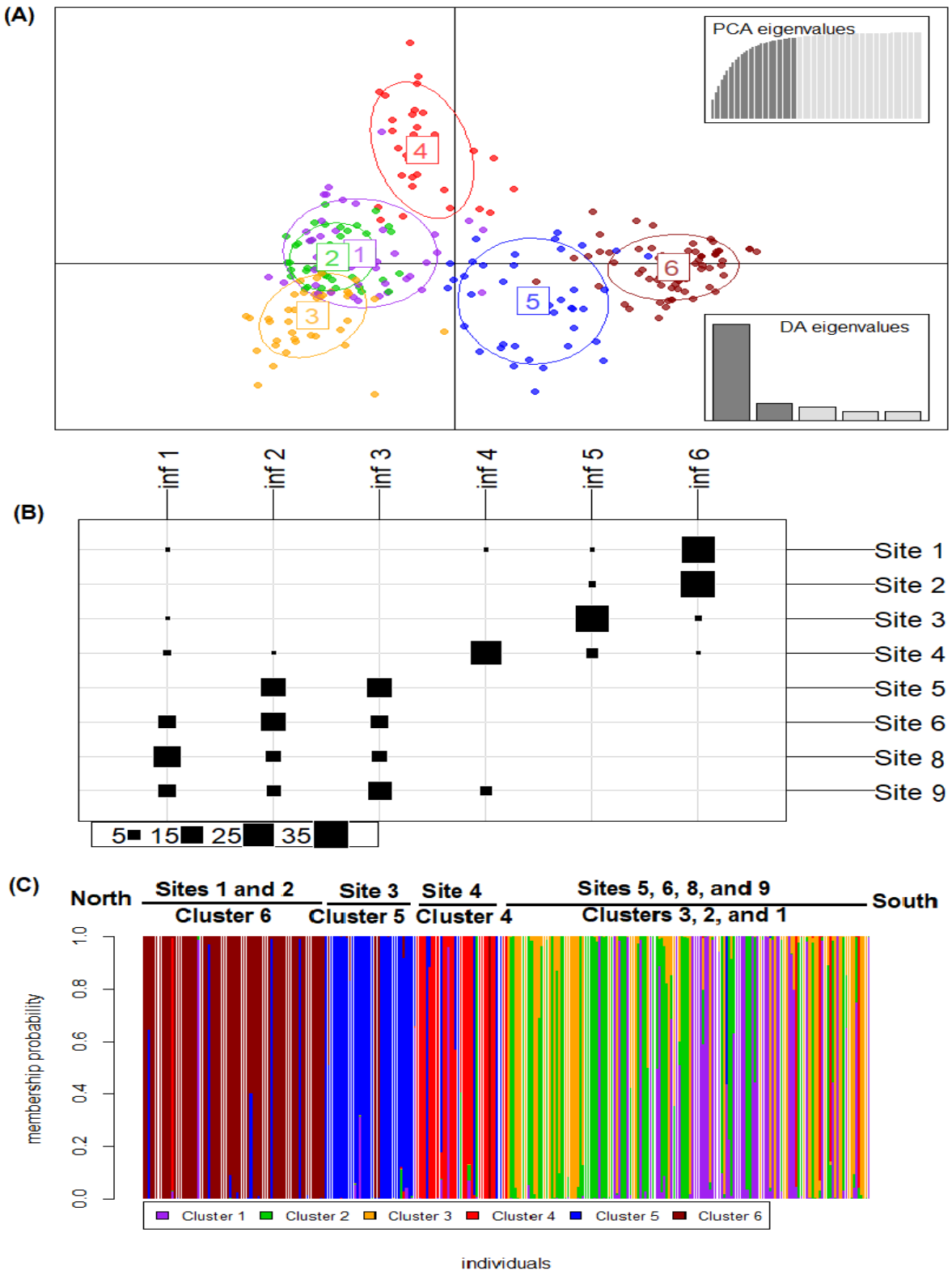

Figure 2. 12 DAPC analysis after excluding site 7: (A) scatterplots of DAPC, (B) the number of individuals identified in the inferred clusters-inf, (C) membership probability of *A. marina* individuals on the Red Sea across clusters.

Chapter 3: Patterns of differential genetic variation among peripheral and core populations of the mangrove species *Avicennia marina* (Forsk.) Vierh. (Acanthaceae) on the Red Sea coast, Saudi Arabia.

3.1 Introduction

The occurrence of *A. marina* on the Red Sea coast is considered as the farthest northwest edge of its global distribution. Thus, their populations are marginal comparing to the central populations in the southern Indo-Pacific. The southern Indo-Pacific is believed to be its centre of distribution, and its origin is in Australia as shown in the earliest fossil pollen records discovered (Ricklefs and Latham 1993). Therefore, places such as South Africa is considered to be the global western edge of the distribution range, while Japan is the global north eastern edge.

At a regional scale, distribution of *A. marina* on the Red Sea coast is patchy and discontinuous, especially in the north part, and its development increases toward the south. This pattern of distribution is in agreement with the abundant centre model in which highly developed and continuous populations with high abundance are often closer to the Equator, while subtropical peripheral populations are less frequent, smaller, and fragmented at the range margins (Brown 1984; Brussart 1984; Brown *et al.* 1995; Saenger 2002). This southern increased development on the Red Sea coast corresponds with the gradual disappearance of stony corals in near shore habitats, a wider continental shelf, warmer temperatures, increased availability of muddier substrate, higher nutrients, and more freshwater (Bruckner *et al.* 2012).

Populations at the limits of species' ranges are often influenced by stronger environmental constraints. However, the subsequent consequences for genetic diversity and structure of peripheral populations are still controversial. Some characteristics of peripheral populations are habitat fragmentation, reduced population size, and genetic isolation which could increase genetic drift and reduce gene diversity lowering the likelihood of adaptation to extreme conditions (Lawton 1993). On the other hand, the fluctuating environmental pressures at the edge of the distribution may favour distinct genotypes and increase genetic diversity in peripheral populations balancing selection effects (Brussart 1984; Safriel *et al*. 1994; Lesica & Allendorf 1995). Another possibility, migration from core populations may sustain relatively high genetic diversity in peripheral populations preventing genetic structuring and adaptation (Peck *et al*. 1998; Kirkpatrick and Ravigne 2002). Within a peripheral-core context, different potential patterns of

genetic diversity and structure might occur over the species distribution range, influencing the distribution range stability or expansion probability.

Historically, mangroves have been expanding along different coastal areas since the last glacial period, following a long period of shrinkage of their ranges (Duke *et al.* 1998; Saenger 1998; Dodd *et al.* 2002). In addition to the effect of historical factors on shaping genetic diversity among central and peripheral populations of mangrove, contemporary mangrove forest distribution data and climate records showed a mangrove expansion and a salt marsh decline at mangrove poleward limits, which were consistent with the poleward extension of temperature thresholds and sea-level rise (Saintilan *et al*. 2014). Triggered by the increase in global average surface temperature of 0.74°C (1906-2005) (Solomon *et al.* 2007), shifts in the structure and distribution of different ecological communities have occurred at a variety of scales (Walther *et al.* 2002; Parmesan and Yohe 2003). Thermally, a global increase of minimum temperatures is at twice the rate of maximum temperatures (Walther *et al.* 2002). Increasing temperature is expected to trigger transitions in the temperature sensitive higher plants distribution (Bakkenes *et al.* 2002; Loarie *et al.* 2008). Even though Avicennia is the most cold-tolerant mangrove genus worldwide, it is been the focus of most changes detected (Saintilan *et al*. 2014). Yet, the effect of these changes on the genetic structuring of mangrove populations especially peripheral ones, which already grow under unstable environmental conditions, is still an open question. The aims of this chapter were to test the hypothesis of lower genetic diversity and higher genetic structure towards the range edges of *A. marina* on the Red Sea coast, and to examine the influence of the distribution limit on the populations' genetic compositions.

3.2 Materials and methods

This chapter used the same data set that contained 12 microsatellite loci screened across 315 *A. marina* individuals from 9 separate sites on the Red Sea from chapter 2. These 9 separate sites were divided into three major sections: north, middle, and south in figure 2.1. Based on the nature of distribution, *A. marina* on the Red Sea coast was hypothesized as core populations in the southern part (relatively close to the Equator), and as peripheral populations in the northern part (pole-ward limit). Following the same division of the coastline and sampling sites, the south section's sites (site 9, 8, and 7) were initially hypothesized as core populations, while the middle section's sites (site 6, 5, and 4) and the north section's sites (site 3, 2, and 1) were peripheral populations. Therefore, each section had 105 individuals coming from 3 separate sites. Within a core-peripheral context, the influence of distribution limit on the genetic composition was inspected on the basis of comparative analyses of the genetic composition of peripheral and core populations.

Sections' gene diversity statistics were estimated using GenAlEx (Peakall and Smouse 2006) with 999 random permutations performed to determine significance for all statistics calculated. Genetic diversity statistics were calculated as follows: the total number of different alleles per locus (A), average number of different alleles per locus and per section (N_a), effective number of alleles ($N_e=1/ pi^2$) where *pi* is the frequency of the *i*th allele at a locus (Frankham *et al.* 2002), the expected heterozygosity or gene diversity ($H_e=1- pi^2$), the observed heterozygosity (H_o)=(number of heterozygotes determined by direct count/ *N* = sample size), the fixation index ($F = (H_e-H_o)/ H_e = 1- (H_o/ H_e)$), and the outcrossing rate = $(1 –F_{IS})/(1 +F_{IS})$ where inbreeding coefficient within individuals, $F_{IS} = (H_e- H_o)/ H_e$. (Weir 1996).

Beside sections' gene diversity statistics, the significance of differences was tested for the average number of different alleles per locus per section (N_a), the expected heterozygosity or gene diversity (H_e), and the fixation index (F) by two one-tailed *t*-tests and a two-tailed *t*-test. These tests reflected a series of comparisons: the south section with the middle section, the south section with the north section, and the middle section with the north section.

Using Genepop 4.0 (Rousset 1997) and/or GenAlEx 6.2 (Peakall and Smouse 2006), the degree of sections differentiation was estimated by testing F_{ST}, R_{ST}, allele frequency histograms. The sections F statistics F_{IS}, F_{IT} and F_{ST} were estimated using both the infinite alleles model (F_{ST})

and the stepwise mutation model (R_{ST}) of microsatellite evolution where F_{IS} and R_{IS} = the average inbreeding of individuals within subpopulations, F_{IT} and R_{IT} = the average inbreeding of individuals relative to the total population, and F_{ST} and R_{ST} = the average inbreeding of subpopulations relative to the total population. F_{ST} and R_{ST} were estimated as per Cockerham (1973) and Weir and Cockerham (1984). The calculation of sections Nei's genetic distances (Nei 1972) was performed by GenAlEx 6.2. Also, cluster dendrograms of hierarchical cluster analysis were constructed by using the matrix of pairwise comparisons of sites and sections genetic differentiation calculated using (F_{ST}), (R_{ST}), and Nei's genetic distances.

Percentages of molecular variance among sections, within sections, and within individuals were calculated with AMOVA (The Analysis of Molecular Variance) using GenAlEx 6.2 (Meirmans 2006). AMOVA procedure in GenAlEx 6.2 follows the method of Peakall *et al* (1995) that brings the estimates for F_{ST} in line with the Weir-Cockerham estimates. When performing AMOVA in GenAlEx, statistical testing by random permutation determines whether the observed value is significantly greater than that expected by chance at a 5% significance level.

The overall gene flow via the number of migrants (*Nm)* was evaluated via Genepop and GenAlEx using both F_{ST} ($Nm = [(1/ F_{ST})-1]/4$), and R_{ST}. Also, the pairwise comparisons of the section number of migrants (*Nm*) based on F_{ST} values were provided. Moreover, the levels of admixture within each individual in each section was analysed using the Bayesian admixture analysis in BAPS 3.1 with the predefined populations option (Corander *et al*., 2003). Using a critical probability level of 0.05, the total immigration was calculated by summing the mean proportion of admixture received from all the other sections. Similarly, the total emigration was computed using the mean proportion of admixture donated to all the other sections, creating immigration–emigration ratio for each section.

To test for a reduction in effective population size linked to bottleneck or founder events, heterozygosity tests used to compare the estimates of expected heterozygosity based on allele frequencies (H_e) and on the number of alleles and sample size (H_{eq}). The number of alleles decreases faster than heterozygosity, resulting in (H_e) > (H_{eq}), which can be used as an indicator of a recent bottleneck event (Cornuet & Luikart 1996). According to Luikart *et al*. (1998), Wilcoxon tests were used with the estimates of (H_{eq}) calculated under the two mutation models: stepwise-mutation model (SMM) and infinite allele model (IAM) in the program bottleneck 1.2.02 (Cornuet & Luikart 1996). Furthermore, a qualitative descriptor of allele frequency distribution

was used to infer bottlenecks (Luikart *et al*. 1998). Bottlenecks can cause a characteristic mode-shift distortion in the distribution of allele frequencies at selectively neutral loci as they cause alleles at low-frequency class (<0.1) to transitorily become less abundant than alleles in 1 or more intermediate allele frequency classes. This method is recommended for sample size exceeds the minimum requested of 30 samples (Luikart *et al*. 1998).

Contemporary effective population size (N_e) mean values with 95% confidence intervals were estimated for each site using both of LDNe (Waples & Do 2008) and NeEstimator (Do *et al.* 2014) programs from a single population sample. LDNe program uses a linkage disequilibrium method initially developed by (Hill 1981) and corrected for small sample size by Waples (2006), whereas the selected method from NeEstimator program uses molecular co-ancestry developed by (Nomura 2008), in which the estimator is obtained from a simple parameter (molecular co-ancestry) of allele sharing among sampled individuals. Calculations were made after dropping one locus per pair that showed LD (M13-M49 pair in site 5), to comply with the conditions forced by the methods, and the lowest allele frequency used was 0.02.

Two categories of environmental parameters (air and sea) were shown in table 3.11. The air parameters were maximum air temperature (annual mean, summer mean, and winter mean) in Celsius, minimum air temperature (annual mean, summer mean, and winter mean) in Celsius, and relative humidity (annual mean, summer mean, and winter mean) as percentages. The sea parameters were Sea Surface Temperature (SST) (annual mean, summer mean, and winter mean) in Celsius and sea surface salinity (annual mean, summer mean, and winter mean) in PSU. The air parameters data set was obtained from local meteorological stations (2015/2016): Duba, Al-Wajh, Umluj, Rabigh, Jeddah, Mastabah, Qunfudhah, Khisa, and Jizan stations, and it reported by World Weather Online.com. The sea parameters data set was obtained (2015/2016) from the Physical Oceanography Distributed Active Archive Centre (PO.DAAC) which is a part of the NASA Earth Science Data and Information System (ESDIS) project.

After variables standardization and checking of multicollinearity among fifteen environmental variables, a multivariate analysis of redundancy (RDA) was performed to assess the relationship between gene diversity statistics: (N_a=average number of different alleles per locus, H_e=expected heterozygosity, F=inbreeding coefficient, O=Outcrossing rate) and a group of variables (all the 15 environmental parameters above, and the (Area) =estimates of the total area of the populations which reflect habitat fragmentation). For each site, an approximation of the total

area of population was estimated by Global Position System (GPS) as the area of a polygon connection trees along the perimeter of the distribution area of population. The significance of the variability explained by each environmental variable was analysed by automatic selection of variables using a Monte Carlo test with 999 permutations, so the variable that best fits the data was selected first, followed by the other variable added to the model in order of goodness of fit (ter Braak and Šmilauer 2002).

3.3 Results

Based on the proposed sectioning of sampling sites, 48, 53, and 72 alleles were detected in the north, middle, and south sections, respectively. Genetic diversity summary statistics of the sections were listed in table 3.1. The average number of different alleles per locus per section (N_a) were 4 in the north, 4.42 in the middle, and 6 in the south. The observed heterozygosity (H_o) ranged from 0.256 (north) to 0.334 (south), and the expected heterozygosities (H_e) were higher than the observed heterozygosities (H_o), and (H_e) ranged from 0.277 (north) to 0.414 (south). This led to positive fixation indices of 0.111, 0.146, and 0.163 in the north, middle, and south sections, respectively. On the other hand, the outcrossing rate ranged from 0.72 (south) to 0.8 (north). The total number of private alleles in each section ranged from 6 (north) to 24 (south), and their frequencies fluctuated between 0.014 and 0.171 in table 3.2. Figure 3.1 showed that the south section exhibited relatively higher values in its N_a, N_e, H_e, and private alleles.

Comparisons (based on *t*-tests) of N_a, H_e, and F (inbreeding coefficient) for the north, middle, and south sections were shown in table 3.3. This comparison detected a significantly higher N_a ($p < 0.001$) in the south section than the north section. However, the rest of the comparisons were not significant.

Table 3.4 displayed matrix of pairwise comparisons of north, middle, and south sections genetic differentiation calculated using the infinite alleles model (F_{ST}), and table 3.5 showed the matrix of pairwise comparisons of genetic differentiation calculated using the stepwise mutation model (R_{ST}). All F_{ST} values were found to be significant at the 99% level, and they ranged from 0.074 (middle and south sections) to 0.192 (north and south sections) with an overall of 0.152. Moreover, all R_{ST} values were found to be significant at the 99% level, and R_{ST} values ranged from 0.112 (middle and south sections) to 0.302 (north and south sections) with an overall of 0.227. Both of F_{ST} and R_{ST} values showed an overall similar pattern of genetic differentiation as they indicated moderate levels of differentiation between middle and south sections, and high levels of differentiation among north-middle pair, and north-south pair. The overall values of F_{IS} and R_{IS} were 0.136 ($p < 0.001$) and 0.344 ($p < 0.001$), respectively, and they indicated a moderate to high level of inbreeding. The overall values of F_{IT} and R_{IT} were 0.268 and 0.493, respectively in table 3.6.

Percentages of molecular variance among sections, within sections, and within individuals were calculated with AMOVA using both theoretical models, the infinite alleles model (F-statistics), and the stepwise mutation model (R-statistics) in table 3.7. The results from AMOVA showed that the variation among sections were (15%, 23%) ($p < 0.001$), within sections were (12%, 27%) ($p < 0.001$), and within individuals were (73%, 50%) ($p < 0.001$). This corresponds to the estimates of both F_{ST} and R_{ST} (0.152 and 0.227, respectively).

Hierarchical cluster analysis dendrograms that used matrices of pairwise comparisons of site genetic differentiation calculated by the infinite alleles model (F_{ST}), the stepwise mutation model (R_{ST}), and Nei's genetic distances were presented in figure 3.2, figure 3.3, and figure 3.4, respectively. In all dendrograms, site 1, 2, and 3 were clustered together reflecting the north section, while the other sites were linked at the highest level of grouping. In addition to the obvious differentiation of site 7 in all dendrograms, site 4 was displayed at higher hierarchical level comparing to site 5, 6, 8, and 9 in figure 3.2 and figure 3.4. When using the pairwise comparisons of section genetic differentiation, hierarchical cluster analysis dendrograms were identical in grouping north section in one group, and middle and south sections in another group in figure 3.5. By examining the alleles frequencies at microsatellite loci that have the highest F_{ST} values: M3, M13, M32, M75, M81, and Am07 among sections in figure 3.6, the north section displayed relatively fewer alleles with higher frequencies, while the south section had relatively more alleles with intermediate frequencies.

The estimates of the number of migrants (*Nm*) varied depending on the levels of genetic differentiation in table 3.6. Over all three sections and loci, the number of migrants was 1.4 and 0.85 using F_{ST} and R_{ST}, respectively. Moreover, the pairwise comparisons of north, middle, and south sections number of migrants (*Nm*) based on F_{ST} values were 1.1 (north-middle), 1 (north-south), and 3.1 (middle-south) in table 3.8. Also, the differences between average proportions of immigrant genetic material compared with emigrant gene flow contributed to other sections in figure 3.7 showed a net negative value for north section reflecting a relative excess of migrants leaving the section, but a net positive value for south section indicating more immigration.

As indicated by both a Wilcoxon sign-rank test in table 3.9 and the mode shift test in figure 3.8, there was no evidence of recent bottleneck except for (site 6 /middle section) which only showed a significant heterozygote excess under infinite alleles model (IAM); however, site 6 did not show a significant distortion of allele frequency distribution. Therefore, there were no strong

pieces of evidence supporting the occurrence of a bottleneck at site 6. The mode shift test showed that the distribution of allele frequencies of all sites fitted the normal "L-shaped" distribution expected from a population in mutation-drift equilibrium.

Mean values of N_e point estimates of contemporary effective population size and associated 95% confidence intervals, which were estimated by two methods: (1) the bias-corrected version of the linkage disequilibrium (LD) method and (2) the molecular co-ancestry method, were reported in table 3.10.

Based on the first method, site 1, 2, and 3 in the north section had N_e values of 14, 49.3, and 104.9, respectively. Site 4, 5, and 6 in the middle section had values of 165.9, 13, and 24.2, respectively. Site 7, 8, and 9 in the south section had values of 11.7, 151.5, and 110.3, respectively. Two sites in the south section had N_e values over 100, while one site in the middle and north sections exceeded the value of 100. Site 1, 5, 7 had the lowest values, while site 3, 4, 8, and 9 had the highest values. Even though the upper confidence intervals in the first method were indistinguishable from infinity in site 2, 3, 4, 8, and 9, the lower confidence intervals were reported for all sites which should be able to provide useful insights for conservation applications.

According to the second method, site 1, 2, and 3 in the north section had N_e values of 1.9, 4.1, and 3.4, respectively. Site 4, 5, and 6 in the middle section had values of 8.7, 4.2, and 1.7, respectively. Site 7 and 8 in the south sections had values of 3.4 and 13.2, respectively. The second method failed to estimate N_e value of site 9, and it was reported as infinity that implied the lack of evidence for variation in the genetic characteristic caused by genetic drift due to a finite number of parents.

Based on the N_e values in table 3.10, the averages of N_e values of sections revealed a northward declining pattern in both methods. In the first method, north, middle, and south sections had averages of N_e values of 56, 68, and 91.2, respectively. Also, north, middle, and south sections had averages values of 3.1, 4.9, and 8.3, respectively in the second method.

After analysing the association between sites' gene diversity statistics (N_a, H_e, F, O) and 16 variables in table 3.11 by multivariate analysis of redundancy (RDA), the total area of the populations (Area) and the Sea Surface Salinity in Winter (SW) were the only variables contributing significantly to the model (Area: $F = 2.35$, $p < 0.05$; SW: $F = 2.4$, $p < 0.05$). After that, (Area) and (SW) were submitted to automatic selection of variables with the rest 14 variables using a Monte Carlo test with 999 permutations. The resulted groups that turned out to be

significant were two groups. The first group consisted of Area, Annual Sea Surface Temperature (SSTAnn), and Annual Relative Humidity (AnnRH) ($F = 2.01$, $p < 0.05$). The explained variation in gene diversity statistics among sites by (Area), (SSTAnn), and (AnnRH) was 60.1% (constrained variation) in figure 3.9. The second group contained Area and Sea Surface Salinity in Winter (SW) ($F = 2.29$, $p < 0.05$). The explained variation in gene diversity statistics among sites by (Area) and (SW) was 53.4% (constrained variation) in figure 3.10. Because of the high variance inflation factor (VIF) of a model containing both of Annual Sea Surface Temperature (SSTAnn) and Sea Surface Salinity in Winter (SW) together, the analyses were done separately on two different groups to avoid multicollinearity issues. The variable Area, which was correlated to the first axis in figure 3.9, had a significantly strong positive correlation with both of (N_a) and (H_e), a weak positive correlation with (O), and a weak negative correlation with (F). On the other hand, the variable SW, which was correlated to the second axis in figure 3.10, had a significantly negative correlation with both of (N_a) and (H_e), a weak positive correlation with (O), and a weak negative correlation with (F).

3.4 Discussion

Within a core-peripheral context, there were a lower genetic diversity and a higher genetic structure towards the range edges of *A. marina* on the Red Sea coast. There was an obvious increasing trend southwards for most gene diversity statistics as the north section had the lowest number of alleles and gene diversity, while the south section had the highest values especially with its significant average number of different alleles per locus (N_a) compared to the north. Even though the south section showed non-significant higher inbreeding value, it had the highest gene diversity. Both of F_{ST} and R_{ST} indicated moderate levels of differentiation between middle and south sections and high levels of differentiation among north-middle pair, and north-south pair. This pattern of a reduced gene diversity and a higher genetic structure was reported by Arnaud-Haond *et al*. (2006) in *A. marina* peripheral populations of northern Vietnam, northern Philippines and southern Australia, comparing to core populations of north and eastern Australia.

In addition to the lower genetic diversity and higher genetic structure of the north section, all of hierarchical cluster analysis dendrograms supported the grouping of site 1, 2, and 3 together reflecting the north section's sites as peripheral populations. However, there was no evidence supporting the initial assumption of the middle section's sites as peripheral populations because they exhibited a relatively similar level of genetic diversity and structure to the south section, and they could be termed as core populations. This demonstrated in the gene flow exchange among sections because pairwise comparisons of the number of migrants (*Nm*) based on F_{ST} values were 1.1 (north-middle), 1 (north-south), and 3.1 (middle-south).

Both of Peck *et al*. (1998) and Kirkpatrick and Ravigne (2002) suggested that migration from core populations may sustain relatively high genetic diversity in peripheral populations preventing genetic structuring, but this pattern of migration was not observed on the Red Sea coast. The differences between average proportions of immigrant genetic material compared with emigrant gene flow contributed to other sections in figure 3.7 showed a net negative value for the north section peripheral sites reflecting a relative excess of migrants leaving the north section, but more immigration was indicated by a net positive value for the south section core sites. This asymmetry in immigration–emigration pattern on the Red Sea coast manifested in the relatively higher gene diversity of south section core sites. Arnaud-Haond *et al*. (2006) suggested that *A. marina* of northern Vietnam and northern Philippines, which displayed a high level of genetic

structure and a low level of gene diversity, were operating as independent evolutionary units more than as components of a metapopulation system connected by gene flow.

Interestingly, the sectioning of the Red Sea coastline and sampling sites into three major sections maintained relatively a comparable amount of the genetic variations among sections and within sections. This represented an advantage for conservation planning and reforestation decisions. Percentages of molecular variance (AMOVA) among sections were (15%, 23%) ($p < 0.001$), and within sections percentages were (12%, 27%) ($p < 0.001$). This corresponds to the estimates of both F_{ST} and R_{ST} (0.152 and 0.227, respectively).

Maguire *et al*. (2000a) observed a higher number of private alleles in the United Arab Emirates' peripheral population of *A. marina* comparing to North and Eastern Australia' core populations suggesting that environmental pressures at the edge of the distribution may favour distinct genotypes and increase genetic diversity in peripheral populations. This was not observed on the Red Sea coast as 24 private alleles were found in the south section core populations comparing to 6 alleles in the genetically less diverse north peripheral populations. This might suggest a higher severity of the environmental pressures at the edge of the distribution on the Red Sea coast.

Two sites in the south section had N_e values over 100, while one site in the middle and north sections exceeded the value of 100. Also, the averages of N_e values of sections revealed a northward declining pattern. This pattern of the lower effective population size of peripheral north section's sites manifested in both of the lower gene diversity and the alleles frequencies at microsatellite loci that had the highest F_{ST} values among sections. The north section loci had relatively fewer alleles with higher frequencies (tendency to fixation or loss), while the south section loci had relatively more alleles with intermediate frequencies. This suggested the effect of genetic drift, a characteristic of peripheral populations.

Regarding the environmental conditions of the Red Sea, Red Sea is a narrow and relatively deep oceanic trough extending for over 1,900 km, between 13º and 28º N latitude. It is the world's northernmost tropical sea, with extensive shallow shelves that support complex coral reefs and associated ecosystems. At its southern end, water exchange between the Red Sea and the Indian Ocean occurs through the Gulf of Aden, Babel-Mandeb Strait. At its northern end, the Red Sea splits into the Gulf of Suez and the Gulf of Aqaba. Even though the Red Sea is connected to the

Mediterranean Sea through the Suez Canal in the Gulf of Suez, there is very little exchange of Red Sea and Mediterranean waters (Morcos 1970).

A northeasterly monsoon (winter) and a southwesterly monsoon (summer) are the main factors controlling the climate of the Red Sea. In summer, the direction of surface water flow tends to be south, whereas in winter the flow is reversed bring in the inflow of water from the Gulf of Aden into the Red Sea. The annual means of air maximum temperatures (30-36℃) and minimum air temperatures (17-30℃) vary with a northwards decreasing tendency which is consistent with the sea surface temperature trends. The overall salinity of the Red Sea is higher than the world average as a result of high rate of evaporation and very little precipitation, the absence of rivers draining into the sea, and narrow connection with the Indian Ocean. The salinity varies across the Red Sea with higher averages in its northern parts (40%, or greater) and lower ones in its southern parts (around 37.5%).

Based on this study findings about the underlying main environmental factors influencing the gene diversity statistics of *A. marina* on the Red Sea coast, the variable (Area), which reflected the level of habitats fragmentation, had a significantly strong positive correlation with both of the average number of different alleles per locus (N_a) and the gene diversity (H_e). On the other hand, Sea Surface Salinity in Winter (SW), which was higher than summer season, had a significantly negative correlation with both of (N_a) and (H_e). For example, site 8 and 9 in the south section, which had relatively larger area (284.8, 519.2 hectares, respectively), warmer sea surface temperature (SSTAnn: 29.5℃, 30.1℃, respectively), more humidity (AnnRH: 46.3%, 62.7%, respectively), and less salinity (SW: 38.46 PSU, 38.16 PSU, respectively), were characterized by higher values in their (N_a) and (H_e), whereas site 1 and site 2 in the north section, which had relatively smaller area (4.3, 36.1 hectares, respectively), colder sea surface temperature (SSTAnn: 26.7℃, 27℃ respectively), less humidity (AnnRH: 26.2%, 46.1%, respectively), and more salinity (SW: 40.24 PSU, 40.14 PSU, respectively), were characterized by lower values in their (N_a) and (H_e).

Triest (2008) suggested that this pattern is shaped by mangrove populations' response to colder climate and arid conditions at the limit of their ranges. For instance, Japanese populations of *A. marina* exhibited three monomorphic microsatellites and significant levels of inbreeding, while populations belong to tropical Papua New Guinea revealed 14 alleles for the same three markers and a high level of genetic variation (Maguire *et al*. 2000a). Mangroves distribution are

supposed to be limited in areas where mean air temperatures of the coldest months are higher than 20°C (Walsh 1974; Chapman 1975, 1977), and they grow usually well in (28–30℃) air temperature range with tolerance limits as low as 8℃ for short periods of time and as high as 42℃ (Teas 1984). As a genus, Avicennia is the most cold-tolerant of mangrove worldwide, and *Avicennia marina* requires relatively warm water and thrives in (26– 28℃) water temperature range. However, *A. marina* would tolerate (16-36℃) water temperature range (Teas 1984). Regarding salinity, mangroves tolerate a high concentration reaching up to 44% of salt (Schmitz *et al*. 2006).

In addition to the effect of contemporary environmental conditions in shaping genetic diversity of central and peripheral mangrove populations, mangroves have been historically expanding along different coastal areas since the last glacial period, following a long period of ranges shrinkage (Duke *et al* 1998; Saenger 1998; Dodd *et al* 2002). For example, the reduction in genetic diversity of *Avicennia germinans* (L.) L. at the northern range limit was explained as a result of northward leading-edge recolonization after late Pleistocene extinction (Nettel and Dodd 2007). Another example, Mildenhall (1994) suggested a link between the loss of *A. marina* from the Poverty Bay, East Cape region of New Zealand and the slight decrease in temperature after the mid-Holocene highstand, 6,000 years BP. Based on glacial-interglacial changes in the hydrographic conditions of the Red Sea, high aridity and eustatically controlled changes resulted in surface water salinities as much as 8.6% higher than at present as the dynamics of water exchange between the Red Sea and the Indian Ocean was effected by changes in the dimensions of the Bab-el-Mandeb Strait (Locke & Thunell 1988). Interestingly, the Gulf of Aden which is relatively close to the south section of the Red Sea had both glacial surface water salinities similar to the present day and slightly warmer surface waters. Thus, the whole area of the Red Sea had dramatic changes in temperatures and salinities especially its northern part. Connection between the Red Sea and the Gulf of Aden was re-established with deglaciation, and surface salinities in the Red Sea decreased after 18,000 years B.P. During the last glacial maximum, *A. marina* on the Red Sea coast may have been subjected to repeated bottleneck or founder effects which were reflected on the present day low level of gene diversity. Moreover, the relatively higher gene diversity statistics of the south section may suggest a lesser level of effect on its populations as they are geographically closer to the Gulf of Aden. It seems that the sea surface salinity has a historical and current substantial role in shaping the genetic diversity of *A. marina* on the Red Sea.

This pattern of reduced levels of heterozygosity in *A. marina* populations at the range edges was reported at places such as Japan, Victoria (Port Albert) in Australia, and Durban (Beachwood) in South Africa by Maguire *et al*. (2000a), and the authors suggested repeated bottleneck or founder effects in earlier times due to episodes of glaciation and transgressions as a potential cause (Saenger 1998).

Along with the effect of contemporary and historical environmental conditions, the climate change is expected to have global and regional impacts on mangrove ecosystems in the future through inter-connected factors (Ellison 2015). These factors are a sea level rise (SLR), an increase in temperature, changes in precipitation regime, changes of ocean currents, and an increase of storminess (McKee *et al*. 2012). The anticipated magnitude and accuracy of these inter-connected factors and their impacts are spatially variable on regional and local scales. Woodworth *et al* (2009) have estimated a local SLR rate of 3.3 mm/year within the Gulf of Aden and the Red Sea. Moreover, SLR rates in the Middle East are either at or below the global average (Ward *et al*. 2016). With this predicted SLR rate on the Red Sea, some areas are more likely to be affected. In the north section, most of the mangrove stands have constrained locations because mountains are relatively close to the sea coast, while the constrained locations of middle section's stands have resulted from the rapid development of the most populated part of the coastline. The constrained locations in the north and middle sections are expected to limit or block the landward migration of mangroves as a result of climate change. Regarding temperatures, an increase up to 7°C by the end of the century is anticipated in the Middle East (Lelieveld *et al*. 2012). Simultaneously, Kostopoulou *et al* (2014) predicted a decrease in precipitation on the Red Sea. The coupling of higher temperatures and less precipitation can limit mangrove growth rates, and the effect on growth will be more profound if salinity increases due to locally higher evaporation rates. However, SLR might counter the effect of evaporation preventing the increase in salinity. If salinity levels increase on the Red Sea, the north section’s mangrove stands are most likely to be affected. Also, the decrease in precipitation will lower the supply of fluvial sediment, which is essential for sustaining surface elevation to cope with SLR (Kostopoulou *et al*. 2014). The Red Sea area is not expected to be affected by storminess. Fluctuations in the rate and severity of storminess are likely to have a greater effect on North America, Central America, Asia, Australia, and East Africa than West Africa and South America (Ward *et al*. 2016).

3.5 Summary

Background

Distribution of *A. marina* on the Red Sea coast is patchy and discontinuous, especially in the north part, and its development increases toward the south. This pattern of distribution is in agreement with the abundant centre model in which highly developed and continuous populations with high abundance are often closer to the Equator, while subtropical peripheral populations are less frequent, smaller, and fragmented at the range margins (Brown 1984; Brussart 1984; Brown *et al.* 1995; Saenger 2002). This southern increased development on the Red Sea coast corresponds with the gradual disappearance of stony corals in near shore habitats, a wider continental shelf, warmer temperatures, increased availability of muddier substrate, higher nutrients, and more freshwater (Bruckner *et al.* 2012). Populations at the limits of species' ranges are often influenced by stronger environmental constraints. However, the subsequent consequences for genetic diversity and structure of peripheral populations are still controversial. The aims of this chapter were to test the hypothesis of lower genetic diversity and higher genetic structure towards the range edges of *A. marina* on the Red Sea coast, and to examine the influence of the distribution limit on the populations' genetic compositions.

Results

There was an obvious increasing trend southwards for most gene diversity statistics as the north section had the lowest number of alleles and gene diversity, while the south section had the highest values especially with its significant average number of different alleles per locus (N_a) compared to the north. Both of F_{ST} and R_{ST} indicated moderate levels of differentiation between middle and south sections and high levels of differentiation among north-middle pair, and north-south pair. This demonstrated in the gene flow exchange among sections because pairwise comparisons of the number of migrants (*Nm*) based on F_{ST} values were 1.1 (north-middle), 1 (north-south), and 3.1 (middle-south). Interestingly, the sectioning of the Red Sea coastline and sampling sites into three major sections maintained relatively a comparable amount of the genetic variations among sections and within sections, and this represented an advantage for conservation planning and reforestation decisions. Percentages of molecular variance (AMOVA) among sections were (15%, 23%) ($p < 0.001$), and within sections percentages were (12%, 27%) ($p < 0.001$). This

corresponds to the estimates of both F_{ST} and R_{ST} (0.152 and 0.227, respectively). Two sites in the south section had N_e values over 100. One site in the middle and north sections exceeded the value of 100. Also, the averages of N_e values of sections revealed a northward declining pattern. On the subject of the underlying main contemporary environmental factors influencing *A. marina* gene diversity statistics on the Red Sea coast, the variable (Area), which reflected the level of habitats fragmentation, had a significantly strong positive correlation with both of the average number of different alleles per locus (N_a) and the gene diversity (H_e), a weak positive correlation with outcrossing rate (O), and a weak negative correlation with inbreeding (F). On the other hand, Sea Surface Salinity in Winter (SW), which was higher than summer season, had a significantly negative correlation with both of (N_a) and (H_e). Also, a discussion of the historical environmental conditions effects in the region, along with the anticipated effects of climate change in the future, was provided.

Conclusions

There is a clear influence of the distribution limit on the genetic composition of *A. marina* on the Red Sea coast that manifests in lower gene diversity, higher genetic structuring, and restricted gene flow. The proposed sites sectioning helps in understanding the magnitude of differentiation, and it will help in guiding conservation management. The north section shows relatively high differentiation, but middle and south sections show relatively more similarity. Thus, translocations between similar vs dissimilar sections should have different priorities.

Table 3. 1 Genetic diversity summary statistics of the north, middle, and south sections of *A. marina* on the Red Sea in figure 2.1.

Sections	A	N_a	N_e	H_e	H_o	F	Outcrossing rate
North	48	4	1.654	0.277	0.256	0.111	0.800
Middle	53	4.42	1.938	0.341	0.306	0.146	0.745
South	72	6	2.555	0.414	0.334	0.163	0.720
Mean		4.8	2.049	0.344	0.299	0.140	0.755

A = total number of different alleles, N_a = average number of different alleles per locus per section, N_e = number of effective alleles, H_e = expected heterozygosity, H_o = observed heterozygosity, F = Fixation Index (inbreeding coefficient).

Table 3. 2 Private alleles of the north, middle, and south sections of *A. marina* on the Red Sea.

Sections	Locus	Allele	Frequency
North (6 alleles)	**M13**	205	0.010
	M13	212	0.005
	M13	216	0.010
	M64	154	0.052
	M73	170	0.033
	M75	205	0.057
	M13	217	0.010
	M32	166	0.014
Middle (8 alleles)	**M32**	180	0.010
	M34	190	0.029
	M49	175	0.005
	M75	201	0.029
	M85	79	0.005
	M98	213	0.010
	M3	178	0.019
	M3	189	0.029
	M3	195	0.005
	M13	189	0.014
	M13	192	0.010
	M13	214	0.024
	M32	147	0.005
	M32	153	0.029
	M32	159	0.005
	M32	163	0.005
South (24 alleles)	**M32**	168	0.305
	M32	178	0.033
	M49	180	0.005
	M75	214	0.043
	M81	138	0.005
	M81	155	0.014
	M81	159	0.005
	M81	160	0.010
	M81	161	0.005
	M81	162	0.005
	M81	163	0.048
	M81	165	0.010
	M81	169	0.005
	M98	220	0.005

Table 3. 3 Comparisons (based on t-test) of N_a = average number of different alleles per locus per section, H_e = expected heterozygosity, and F = Fixation Index (inbreeding coefficient) for north, middle, and south sections of *A. marina* on the Red Sea.

Test	Genetic diversity	Mean ± SE	*p* value
North vs. Middle	**N_a**	4±0.8 ≅ 4.42±0.7	0.8
	H_e	0.277±0.07 ≅ 0.341±0.08	0.4
	F	0.111±0.06 ≅ 0.146±0.1	0.4
North vs. South	**N_a**	4±0.8 ≅ 6±1.6	0.04
		4±0.8 < 6±1.6	< 0.001
	H_e	0.277±0.07 ≅ 0.414±0.09	0.1
	F	0.111±0.06 ≅ 0.163±0.05	0.1
Middle vs. South	**N_a**	4.42±0.7 ≅ 6±1.6	0.08
	H_e	0.341±0.08 ≅ 0.414±0.09	0.4
	F	0.146±0.1 ≅ 0.163±0.05	0.4

Table 3. 4 Matrix of pairwise comparisons of the north, middle, and south sections genetic differentiation of *A. marina* on the Red Sea, calculated using the infinite alleles model (F_{ST})

	North	Middle	South
North	0.000	0.001	0.001
Middle	0.191	0.000	0.001
South	0.192	0.074	0.000

F_{ST} values below the diagonal. Probability, *p* (rand >= data) based on 999 permutations is shown above diagonal.

Table 3. 5 Matrix of pairwise comparisons of the north, middle, and south sections genetic differentiation of *A. marina* on the Red Sea, calculated using the stepwise mutation model (R_{ST})

	North	Middle	South
North	0.000	0.001	0.001
Middle	0.280	0.000	0.001
South	0.302	0.112	0.000

R_{ST} values below the diagonal. Probability, *p* (rand >= data) based on 999 permutations is shown above diagonal

Table 3. 6 Overall genetic differentiation calculated using the infinite alleles model (F_{ST}) and the stepwise mutation model (R_{ST}) of the north, middle, and south sections of *A. marina* on the Red Sea.

F-Statistics	Value	*p*	R-Statistics	Value	*p*	*Nm*	
						F-Statistics	R-Statistics
F_{ST}	0.152	<0.001	R_{ST}	0.227	<0.001		
F_{IS}	0.136	<0.001	R_{IS}	0.344	<0.001		
F_{IT}	0.268	<0.001	R_{IT}	0.493	<0.001	1.4	0.85

Table 3. 7 Hierarchical analysis of molecular variance of the north, middle, and south sections of *A. marina* on the Red Sea.

Source of Variation	d.f	variance components	*p*	variance components	*p*
		F_{ST}		R_{ST}	
Among sections	2	15%	<0.001	23%	<0.001
Within sections	312	12%	<0.001	27%	<0.001
Within individuals	315	73%	<0.001	50%	<0.001

% Molecular variation percentage explained by the hierarchical level; *p* level of significance for the distribution of variation for that hierarchical level being different from random; d.f = degree of freedom.

Table 3. 8. Matrix of pairwise comparisons of number of migrants (N_m) based on F_{ST} values of the north, middle, and south sections of *A. marina* on the Red Sea.

	North	Middle	South
North	0.000		
Middle	1.1	0.000	
South	1	3.1	0.000

Table 3. 9 Wilcoxon sign-rank tests for heterozygosity excess (Luikart *et al.* 1998b) in the *A. marina* 9 sites on the Red Sea. H_e: Hardy-Weinberg expected heterozygosity; IAM: infinite alleles model; SMM: stepwise mutation model; *LH*exc: number of loci with heterozygosity excess; *p*: probability of significant heterozygosity excess.

			Wilcoxon sign-rank test					
			——— IAM ———			——— SMM ———		
			Observed	Expected		Observed	Expected	
Sections	**Sites**	**He (±SE)**	***LH*exc**	***LH*exc**	***p***	***LH*exc**	***LH*exc**	***p***
	1	0.281±0.06	6	4.88	0.246	3	5.48	0.947
North	2	0.191±0.06	4	4.35	0.849	2	4.75	0.997
	3	0.264±0.07	3	4.54	0.714	2	5.01	0.993
	4	0.295±0.08	3	4.71	0.787	1	4.95	0.99
Middle	5	0.278±0.07	5	4.39	0.179	4	4.84	0.787
	6	0.313±0.08	7	4.34	0.024	4	4.72	0.544
	7	0.285±0.07	6	4.15	0.273	2	4.46	0.843
South	8	0.401±0.09	7	4.85	0.179	4	5.09	0.875
	9	0.349±0.09	5	5.25	0.687	1	5.51	0.999

Table 3. 10 Estimated means effective population size (N_e) of *A. marina* at nine sites on the Red Sea inferred from a set of 315 individuals using LDNe and NeEstimator programs. Brackets show 95% confidence intervals.

	Sites	*Ne*	
		LINKAGE DISEQUILIBRIUM METHOD*1 *P*crit (0.02)	**MOLECULAR COANCESTRY METHOD*2**
North Section	**1**	14.0 (7.1-43.4)	1.9 (1.2-5.4)
	2	49.3 (31.6-∞)	4.1 (4.1-24.8)
	3	104.9 (72.3-∞)	3.4 (2.6-11.3)
Middle Section	**4**	165.9 (128.8-∞)	8.7 (8.1-35.9)
	5	13.0 (7.4-42.2)	4.2 (3.7-15.8)
	6	24.2 (12.3-91.1)	1.7 (1.3-5.9)
South Section	**7**	11.7 (5.8-33.4)	3.4 (3-12.8)
	8	151.5 (97.8-∞)	13.2 (10-43.3)
	9	110.3 (62.2-∞)	∞

***1**(Hill 1981; Waples 2006; Waples & Do 2010)
***2**(Nomura 2008). *P*crit = the lowest allele frequency used was 0.02

Table 3. 11 Geographic position, climatic and sea surface information of Avicennia marina sampling sites on the Red Sea. Tmin Ann= annual mean minimum air temperature, Tmin Summer= mean minimum air temperature in summer, Tmin Winter= mean minimum air temperature in winter; Tmax Ann= annual mean maximum air temperature, Tmax Summer= mean maximum air temperature in summer, Tmax Winter= mean maximum air temperature in winter; RH Ann= annual mean of relative air humidity, RH Summer= mean of relative air humidity in summer, RH Winter= mean of relative air humidity in winter; T Ann= annual mean of sea surface temperature, T Summer= mean of sea surface temperature in summer, T Winter= mean of sea surface temperature in winter; S Ann= annual mean of sea surface salinity, S Summer= mean of sea surface salinity in summer, S Winter= mean of sea surface salinity in winter for the period (2015/2016).

Site ID		**1**	**2**	**3**
Site Name		Duba	Al-wajh	Umluj
Geographical Location	Latitude (N)	27° 42′ 66″	26° 02′ 48″	24° 78′ 87″
	Longitude (E)	35° 60′ 57″	36° 70′ 58″	37° 18′ 21″
	*T*min Ann (℃)	17	23.75	25.17
	*T*min Summer (℃)	24.67	27.33	28.33
	*T*min Winter (℃)	7.33	18.67	21
	*T*max Ann (℃)	30.42	33.42	36.42
Climatic Data	*T*max Summer (℃)	39.33	38.67	42
	*T*max Winter (℃)	19	26.33	29
	RH Ann (%)	26.2	46.1	39
	RH Summer (%)	20.33	48.33	36.33
	RH Winter (%)	37.67	44.33	39.67
	T Ann (℃)	26.7	27	26.7
	T Summer (℃)	29.51	29.95	25.11
Sea Surface Data	*T* Winter (℃)	24.56	24.33	28.86
	S Ann (PSU)	39.72	39.84	39.64
	S Summer (PSU)	38.32	39.12	39.29
	S Winter (PSU)	40.24	40.14	39.93
Total Population Area	(Hectares)	4.3	36.1	10.1

Continuousness of table 3. 12 Geographic position, climatic and sea surface information of *Avicennia marina* sampling sites on the Red Sea. *T*min Ann= annual mean minimum air temperature, *T*min Summer= mean minimum air temperature in summer, *T*min Winter= mean minimum air temperature in winter; *T*max Ann= annual mean maximum air temperature, *T*max Summer= mean maximum air temperature in summer, *T*max Winter= mean maximum air temperature in winter; *RH* Ann= annual mean of relative air humidity, *RH* Summer= mean of relative air humidity in summer, *RH* Winter= mean of relative air humidity in winter; *T* Ann= annual mean of sea surface temperature, *T* Summer= mean of sea surface temperature in summer, *T* Winter= mean of sea surface temperature in winter; *S* Ann= annual mean of sea surface salinity, *S* Summer= mean of sea surface salinity in summer, *S* Winter= mean of sea surface salinity in winter for the period (2015/2016).

Site ID		**4**	**5**	**6**
Site Name		Rabigh	Jeddah	Mastabah
Geographical Location	Latitude (N)	23° 12′ 05″	21° 26′ 65″	20° 81′ 89″
	Longitude (E)	38° 80′ 52″	39° 12′ 60″	39° 45′ 26″
Climatic Data	*T*min Ann (℃)	25.58	18.58	18.58
	*T*min Summer (℃)	29.33	24.33	24.33
	*T*min Winter (℃)	21	12.33	12.3
	*T*max Ann (℃)	36.67	30	30.08
	*T*max Summer (℃)	42.67	36	36.33
	*T*max Winter (℃)	29	23	23
	RH Ann (%)	39	36.2	36.23
	RH Summer (%)	36.33	22.3	22.33
	RH Winter (%)	39.67	53.6	53.7
Sea Surface Data	*T* Ann (℃)	28.4	28.7	28.8
	T Summer (℃)	30.49	28.94	30.22
	T Winter (℃)	26.19	28.45	26.96
	S Ann (PSU)	39.26	38.78	38.59
	S Summer (PSU)	38.95	38.17	37.87
	S Winter (PSU)	39.57	39.24	39.11
Total Population Area	(Hectares)	24.9	11.4	166.7

Continuousness of table 3. 13 Geographic position, climatic and sea surface information of *Avicennia marina* sampling sites on the Red Sea. *T*min Ann= annual mean minimum air temperature, *T*min Summer= mean minimum air temperature in summer, *T*min Winter= mean minimum air temperature in winter; *T*max Ann= annual mean maximum air temperature, *T*max Summer= mean maximum air temperature in summer, *T*max Winter= mean maximum air temperature in winter; *RH* Ann= annual mean of relative air humidity, *RH* Summer= mean of relative air humidity in summer, *RH* Winter= mean of relative air humidity in winter; *T* Ann= annual mean of sea surface temperature, *T* Summer= mean of sea surface temperature in summer, *T* Winter= mean of sea surface temperature in winter; *S* Ann= annual mean of sea surface salinity, *S* Summer= mean of sea surface salinity in summer, *S* Winter= mean of sea surface salinity in winter for the period (2015/2016).

Site ID		**7**	**8**	**9**
Site Name		Qunfudhah	Khisa	Jizan
Geographical Location	Latitude (N)	18° 80′ 43″	17° 99′ 47″	17° 14′ 08″
	Longitude (E)	41° 22′ 72″	41° 66′ 82″	42° 41′ 52″
Climatic Data	*T*min Ann (℃)	18.75	16.58	30.33
	*T*min Summer (℃)	24.67	21.33	33
	*T*min Winter (℃)	12.33	11.67	26.67
	*T*max Ann (℃)	29.33	25.33	35.92
	*T*max Summer (℃)	35	30	39.33
	*T*max Winter (℃)	23.67	20.33	31.33
	RH Ann (%)	32.3	46.3	62.7
	RH Summer (%)	23	39	58.67
	RH Winter (%)	45.67	61.33	69
Sea Surface Data	*T* Ann (℃)	29.9	29.5	30.1
	T Summer (℃)	30.84	27.56	31
	T Winter (℃)	28.18	31.41	27.69
	S Ann (PSU)	38.31	38.36	34.93
	S Summer (PSU)	37.41	38.05	37.84
	S Winter (PSU)	38.65	38.46	38.16
Total Population Area	(Hectares)	103.8	284.8	519.2

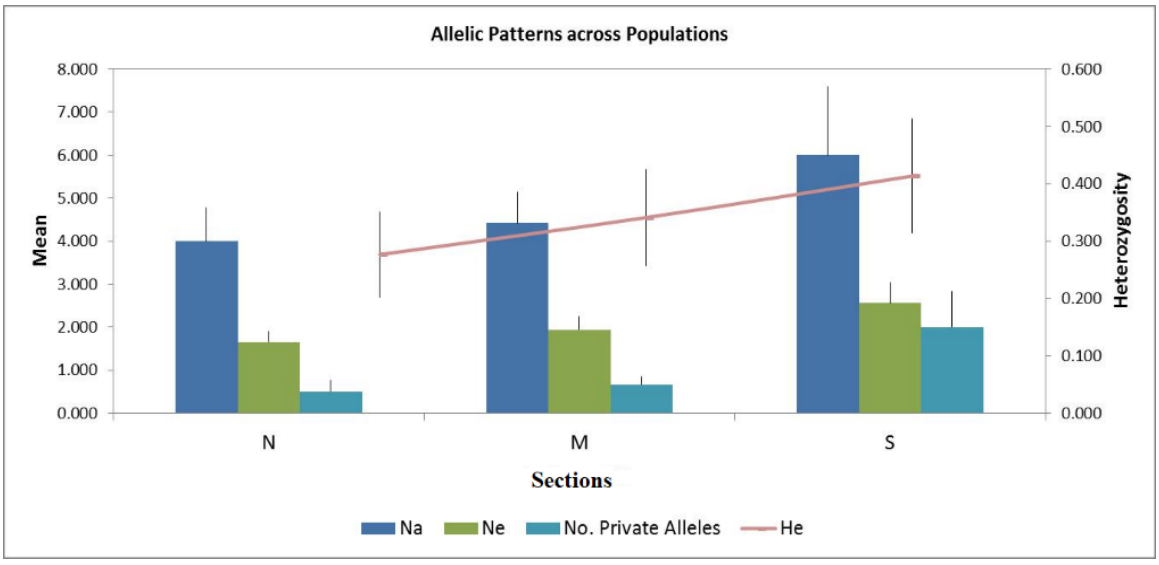

Figure 3. 1 Summary of allelic patterns for the North (N), Middle (M), and South (S) sections of *A. marina* on the Red Sea.

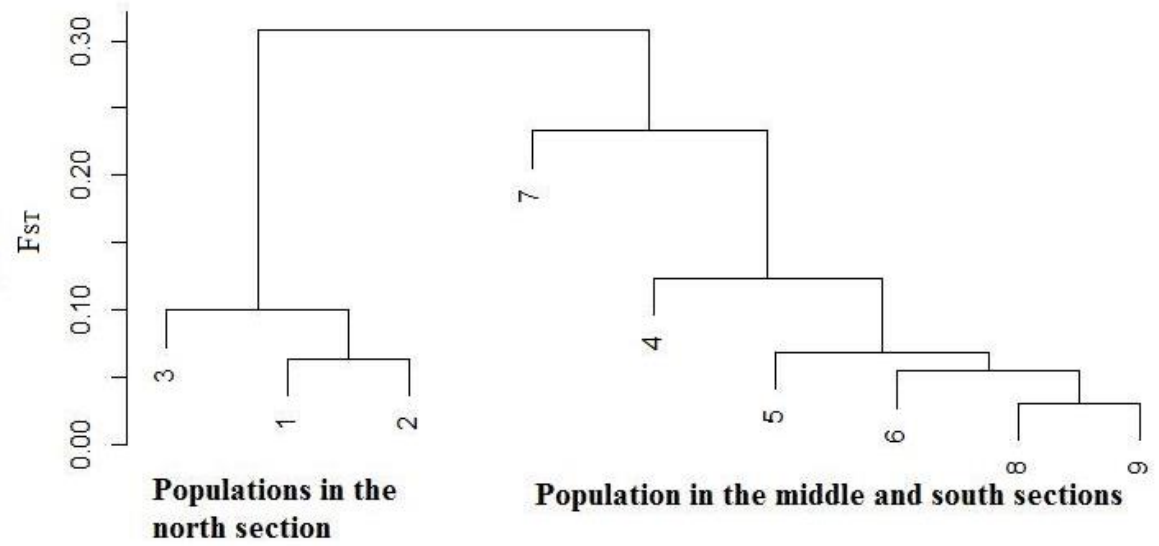

Figure 3. 2 Cluster dendrogram of hierarchical cluster analysis, by using matrix of pairwise comparisons of site genetic differentiation calculated using the infinite alleles model (FST) for *Avicennia marina* populations on the Red Sea.

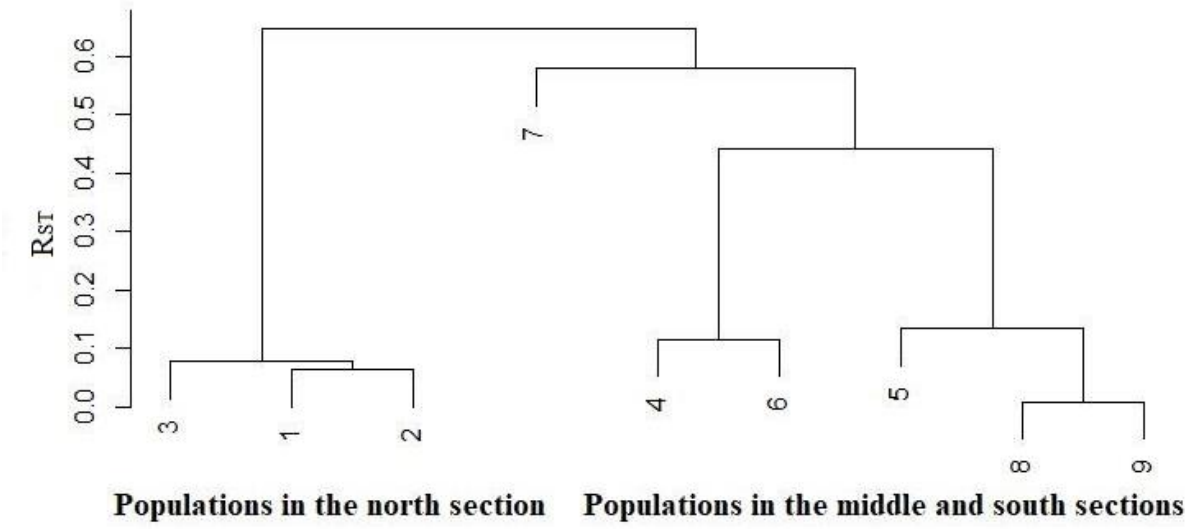

Figure 3. 3 Cluster dendrogram of hierarchical cluster analysis, by using matrix of pairwise comparisons of site genetic differentiation calculated using the stepwise mutation model (RST) for *Avicennia marina* populations on the Red Sea.

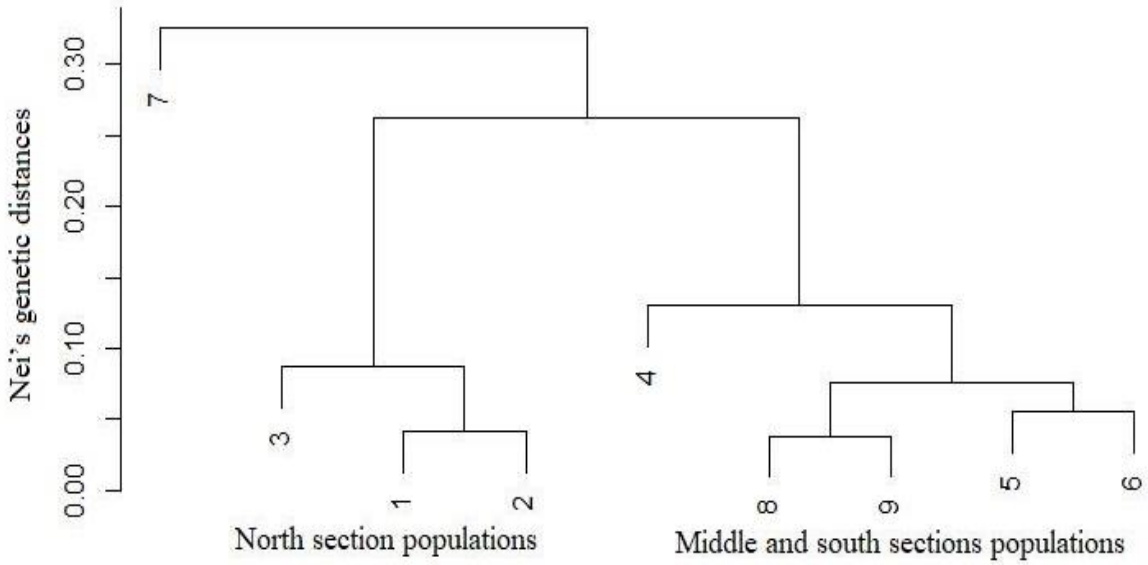

Figure 3. 4 Cluster dendrogram of hierarchical cluster analysis, by using matrix of pairwise comparisons of site genetic differentiation calculated by Nei's genetic distances for *Avicennia marina* populations on the Red Sea.

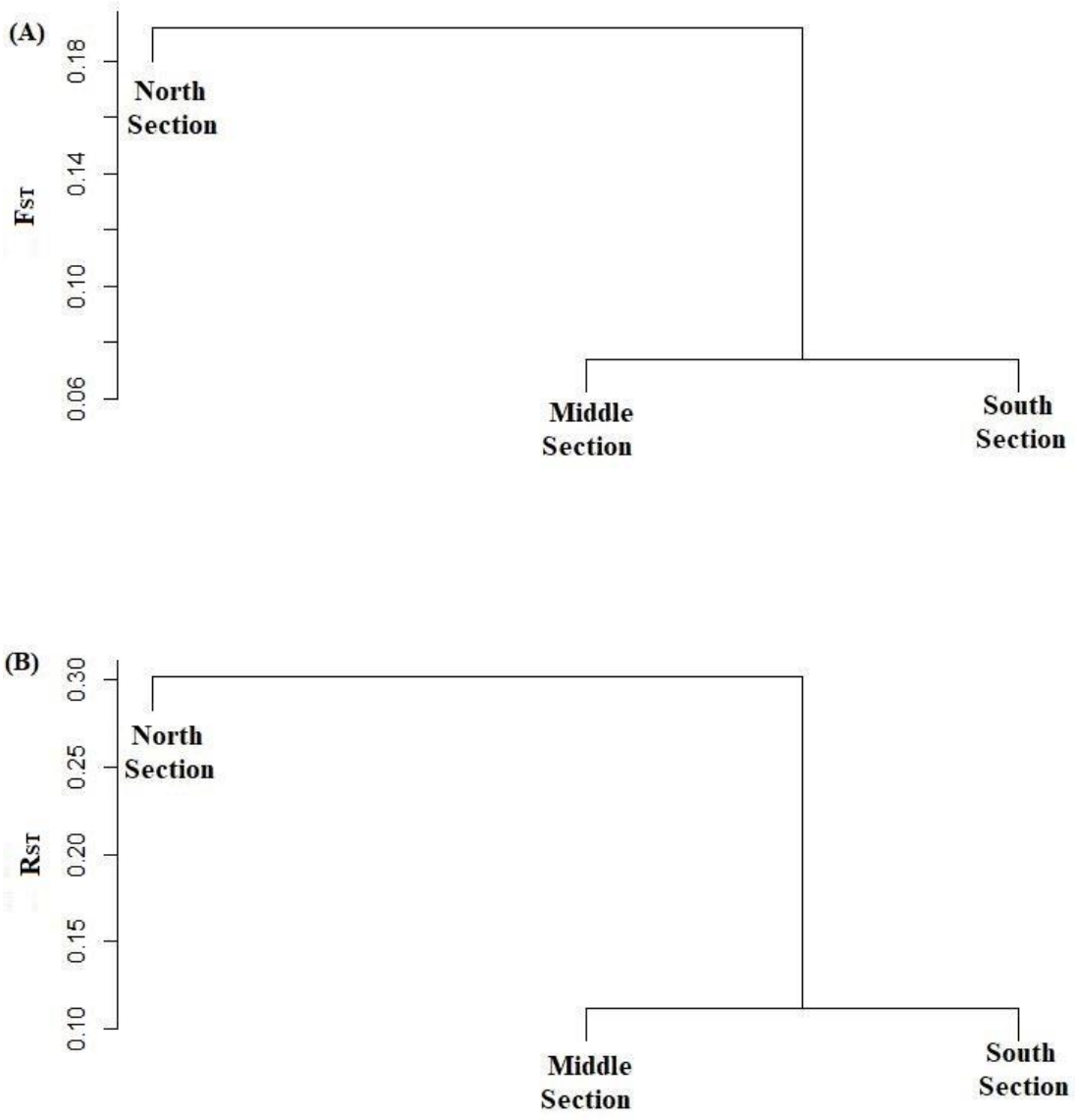

Figure 3. 5 Cluster dendrogram of hierarchical cluster analysis, by using matrix of pairwise comparisons of sections genetic differentiation of *A. marina* on the Red Sea calculated by both: (A) the infinite alleles model (FST), and (B) the stepwise mutation model (RST).

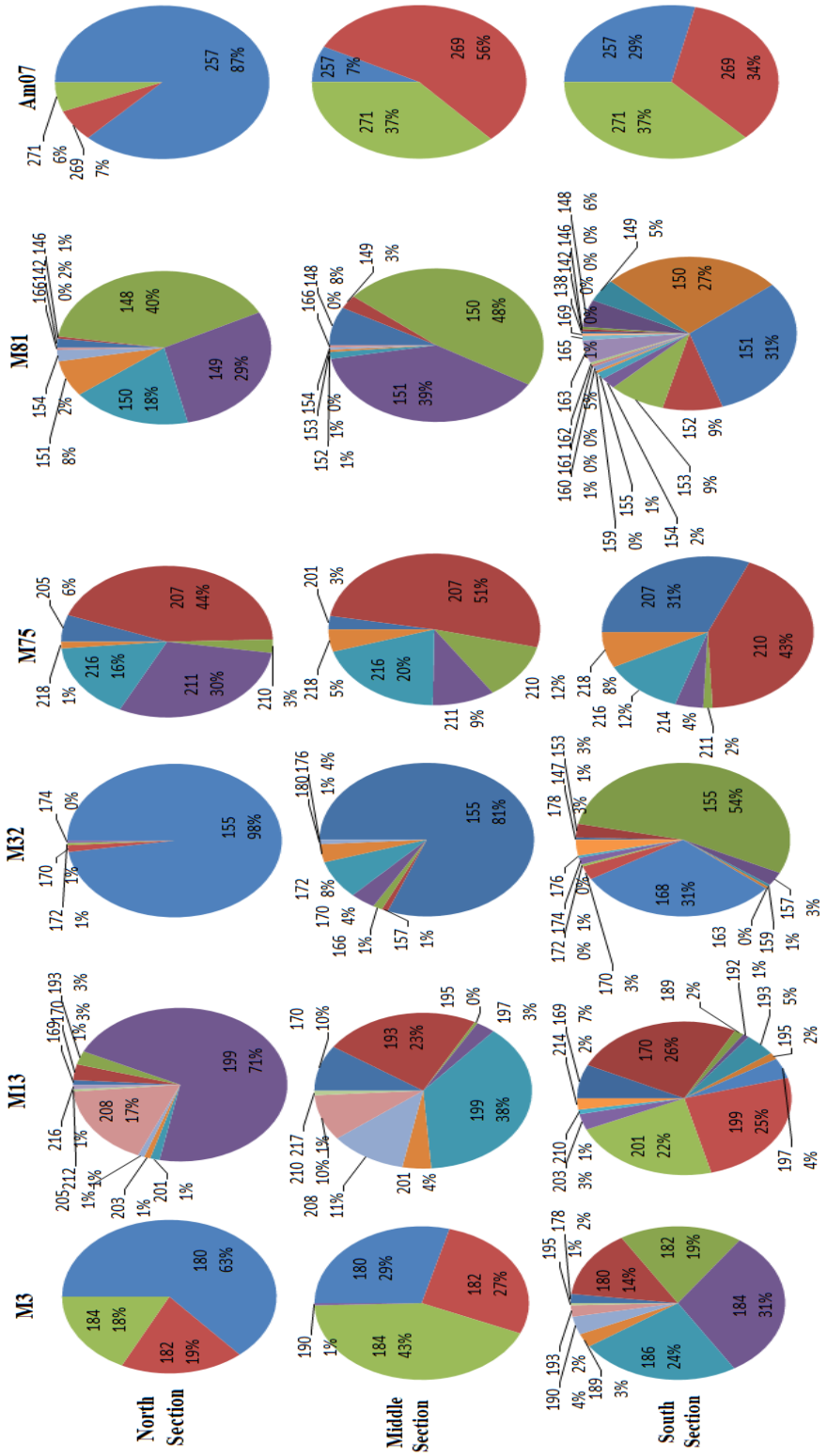

Figure 3. 6 Frequencies of alleles at microsatellite loci that shows the highest FST values: M3, M13, M32, M75, M81, and Am07 among north, middle, and south sections of *A. marina* on the Red Sea.

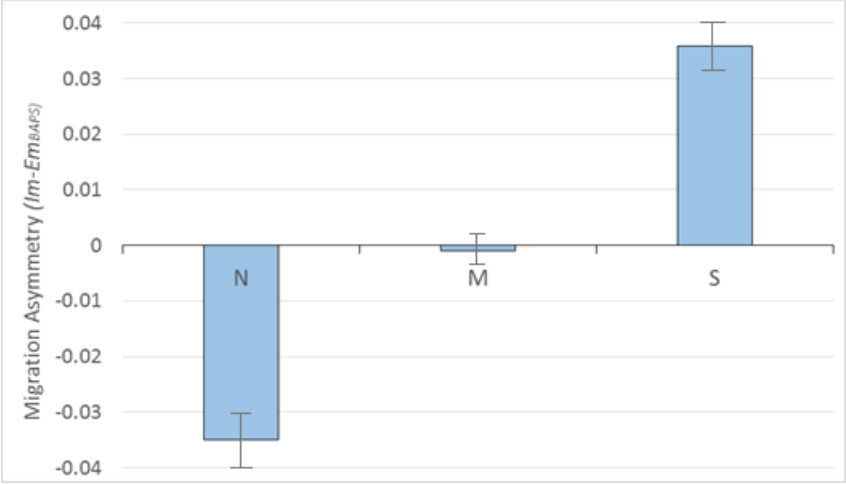

Figure 3. 7 Differences between average proportions of immigrant genetic material compared with emigrant gene flow contributed to other sections based on Bayesian admixture analysis. Net negative values reflect a relative excess of migrants leaving the section and positive values are characterized by immigration. (N) North, (M) Middle, and (S) South sections of *A. marina* on the Red Sea.

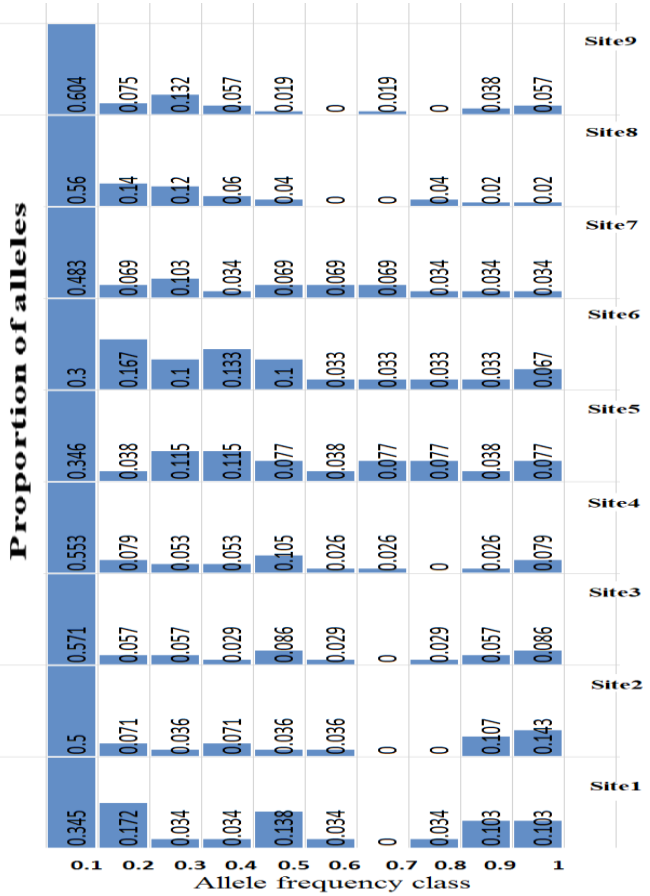

Figure 3. 8 Distribution of allele frequencies in each *A. marina* site on the Red Sea to detect mode-shift distortions which indicate recent bottlenecks following the method in (Luikart *et al.* 1998).

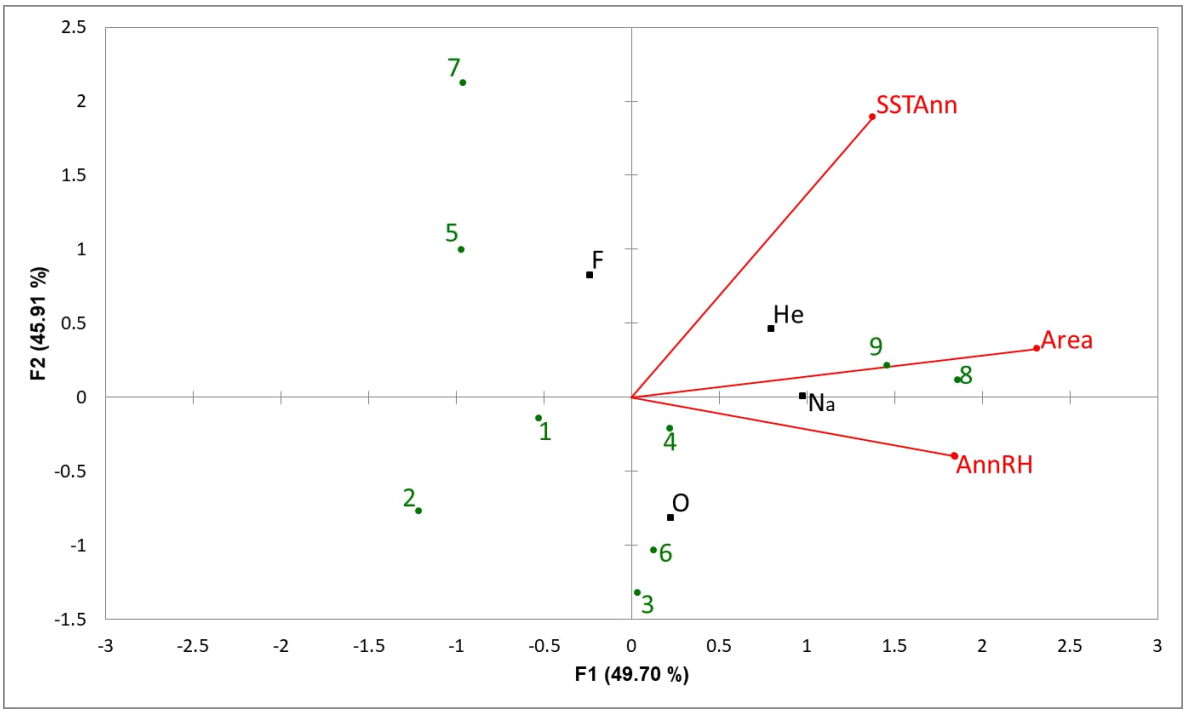

Figure 3. 9 Triplot of the first two axes of the RDA ordination of the 9 sampling sites of *Avicennia marina* based on four gene diversity statistics: N_a=average number of different alleles per locus, H_e=expected heterozygosity, F=Fixation Index (inbreeding coefficient), O=Outcrossing rate, including the explanatory environmental factors: Area=estimates of the total area of the populations, Annual Sea Surface Temperature (SSTAnn), Annual Relative Humidity (AnnRH) (red arrows). The global model of (SSTAnn, Area, and AnnRH) was significant (p<0.05) with (60.1% constrained inertia). Area correlated with the first axis and SSTAnn with the second. Eigenvalues associated with each axis are Axis 1 (1.194), Axis 2(1.103), and constrained inertia (%) with each axis are provided in brackets. Axis 1 (49.70), Axis 2(45.91), (4.4% of the constrained inertia is not shown-third axe).

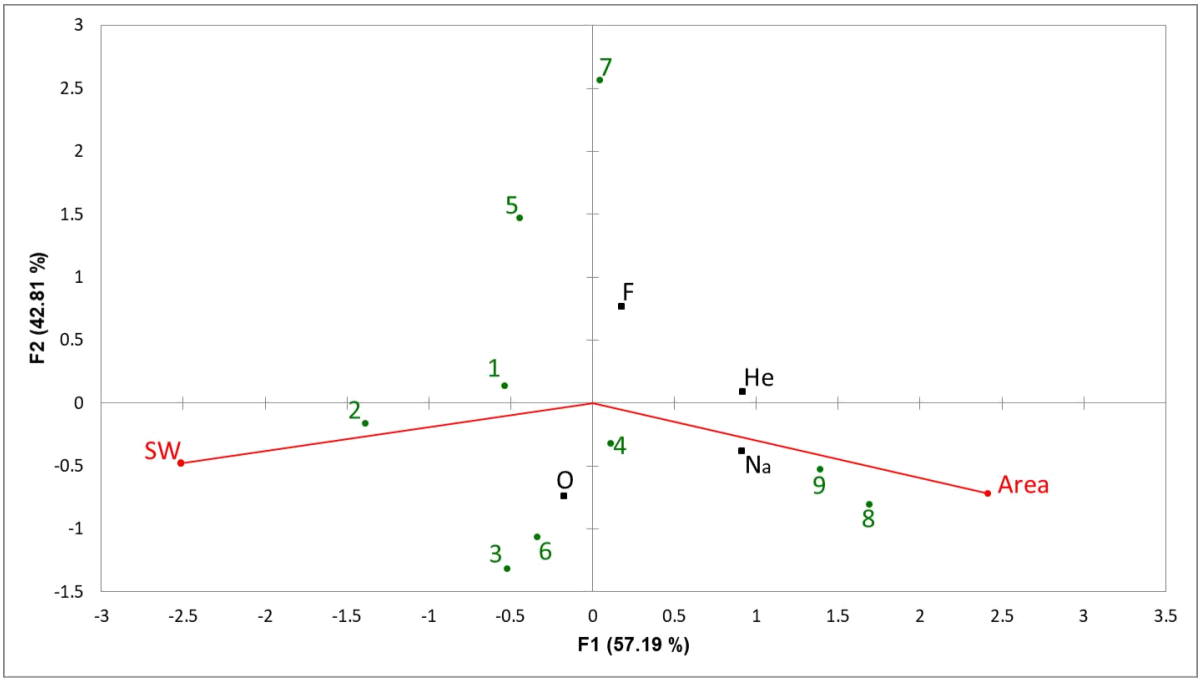

Figure 3. 10 Triplot of the first two axes of the RDA ordination of the 9 sampling sites of *Avicennia marina* based on four gene diversity statistics: N_a=average number of different alleles per locus, H_e=expected heterozygosity, F=Fixation Index (inbreeding coefficient), O=Outcrossing rate, including the explanatory environmental factors: Area=estimates of the total area of the populations, Sea Surface Salinity in Winter (SW) (red arrows). The significant global model of (Area and SW, $p < 0.05$) had (53.4% constrained inertia). Area correlated with the first axis and SW with the second. Eigenvalues associated with each axis are Axis 1 (1.221), Axis 2(0.914), and constrained inertia (%) with each axis are provided in brackets. Axis 1 (57.19), Axis 2(42.81).

Chapter 4: Phenotypic leaf variation in the mangrove species *Avicennia marina* (Forsk.) Vierh. (Acanthaceae) on the Red Sea coast, Saudi Arabia.

4.1 Introduction

As the most widely distributed of all mangrove tree species, *A. marina* reveals a substantial variability in morphological forms across its entire range of distribution. This species can vary from rugged shrubbery on dry coast shores and coral reefs, to closed forests up to 40 m tall in coastal tropical regions (Duke *et al*. 1998). The phenotypic leaf variation in *A. marina* was reported across its Australian range (Melville and Burchett 2002; Saenger and Brooks 2008). These observed differences in phenotypic leaf traits in natural populations are expected whether they reflect phenotypic trait variation, phenotypic plasticity (active or adaptive plasticity), or an interaction between them (Pigliucci *et al*. 1995; Auld *et al*. 2010; Pichancourt & Klinken 2012). Many confounding factors would cause these observed differences, including environmental factors, genetic factors relating to additive genetic variances, dominance genetic variances, and epistatic, or an interaction between the factors of environment and genetics (Pujol *et al*. 2008). Generally, assessments of these phenotypic differences are usually emphasized on traits that have a direct genetic evidence, but phenotypic traits, for which no direct genetic evidence is identified, are assumed to be having a slight significance in conservation planning (Vogler and DeSalle 1994; Rohlf 1994). However, traits that are mostly stimulated by the environment are indirectly controlled by genetics because the phenotype's genes that let on the phenotype to be formed by the environment. Even though no changes in gene frequencies directly occur after the effects of natural selection on these phenotypes, the phenotypic changes that arise without genetic changes can be beneficial, and may be maintained by indirect genetic mechanisms (Falconer and Mackay 1996; Grant 1963; Mayr 1970).

Although it has been anticipated that core and peripheral populations will exhibit a different degree of phenotypic variation, the direction of this variation has contrasting expectations. Theoretically, peripheral populations, which have been subjected to stronger environmental conditions over the course of generations, may reveal higher phenotypic variation than core populations, and plastic genotypes will be advantageous (Volis *et a*l. 1998; Balaguer *et al*. 2001; Valladares *et al*. 2007). Conversely, phenotypic variation and plasticity have been

suggested to be lower across the range margins than near range centres as a consequence of small population sizes, genetic drift, founder effects, or genetic isolation (Berg *et al*. 2005; Becker *et al*. 2006; Mägi *et al*. 2011). In other words, assuming the adaptive value of the phenotypic plasticity, the advantage of conserving plasticity in peripheral populations' stressful environments may lose its benefit comparing to the relative metabolic and intrinsic genetic costs of phenotypic variation and plasticity (Hoffmann 1990; Parsons 1991).

Therefore, understanding the natural phenotypic variation within a widespread species such as *A. marina* is the initial step to define the relative influence of different factors underlying phenotypic differentiation (Domínguez *et al*. 1998; Boyd 2002; Mascó *et al*. 2004; Herrera 2005; Chalcoff *et al*. 2008; Pérez- Barrales *et al*. 2009). Although the phenotypic leaf variation in *A. marina* was reported in different regions across its global distribution (Melville and Burchett 2002; Saenger and Brooks 2008), it has been rarely investigated on the Red Sea coast. Utilizing measurements of leaf dimension (leaf area, length, maximal width, and the ratio of length: width), this study examined the field observed phenotypic leaf variation in *A. marina* along the Saudi Arabian Red Sea coastline, and it determined which model best described the distribution of phenotypic leaf variation within and among populations (isolation by distance, discrete subpopulation). Also, it examined the influence of the distribution limit on the phenotypic leaf variation.

4.2 Materials and methods

4.2.1 Morphological Characteristics

Avicennia marina (Forssk.) Vierh.

Family: Acanthaceae.

Synonyms: *Avicennia officinalis* auct. non L.

Vernacular names: White mangrove, grey mangrove, olive mangrove.

Evergreen coastal tall shrub to small tree up to 5 m tall; roots producing pneumatophores sticking upright out of the mangrove floor; stem usually low-branching, up to 40 cm in diameter, bark surface smooth, brownish or yellowish; crown dense and rounded; Leaves decussately opposite, simple and entire; stipules absent; shortly petiolate; blade ovate to elliptic-oblong, cuneate at base, acute or acuminate at apex, leathery, minutely whitish hairy below, dark-green glabrous on the upper side. Flowers yellow to orange, waxy, in short pedunculated, terminal and axillary, capitate cymes. Bract, and bracteoles smaller than calyx. Calyx short, 5-lobed. Corolla tube short, the limb 4-lobed, c.6 mm across. Fruit a fleshy compressed capsule, leathery, scaly hairy, green-almond like, c. 2.5 cm long, 1-seeded, dehiscing by 2 valves. Seedling with epigeal germination, viviparous; hypocotyl elongated; cotyledons thick and fleshy, folded; radicle usually glabrous, with short hairy collar (Chaudhary 2001).

4.2.2 Field Collection and Measurements

From the same nine sampling sites of *A. marina* in chapter 2 and figure 2.1, leaf dimensions (leaf area, length, maximal width, and the ratio of length: width) were measured in the field. In each site, only the most fully expanded leaf pairs at the mid-point and bottom of stems were measured from the same 35 adult trees that were chosen for the genomic DNA isolation in chapter 2. From each tree, replicates of fifteen leaves were recorded using a Li-Cor portable leaf area meter resulting in 4,725 data set for each leaf dimension (15 replicates*35 trees*9 sites), and a total of 18,900 database for all four leaf dimensions.

4.2.3 Data analyses

The leaf traits data sets were transformed to natural logarithms to normalize their distributions before all the analyses in this chapter, unless otherwise indicated. All the analyses were performed in the R software (R Development Core Team 2015). The first analysis was about the significant differences in leaf traits means among sites. After checking the data for any violations of one-way ANOVA assumptions (implicit factors within a sample/lack of independence between samples/apparent non-normality by a few data points (Outliers)/ non-normality of entire samples/ unequal variances), I performed one-way ANOVAs with one fixed factor (site), which had 9 levels (9 sites) and the random factor (tree), followed by the Tukey's post-hoc Honestly Significant Difference (HSD) tests (Byrkit 1987) to identify significant differences between the sites.

Secondly, mixed effects models were constructed by using the package "nlme" in R software (Pinheiro & Bates, 2000). The purpose was to inspect the components of variation in the leaf trait measurements (area, length, maximal width, and L: W ratio; all in natural log scale) among replicate leaves within each tree, among trees within each site, and among sites. For each leaf trait measurement, there were 15 replicate leaves within each tree, 35 trees within each site, and 9 sites in total. Thus, each leaf trait was partitioned according to its differences among sites, among individuals within sites, and among leaves within individuals (the latter level was the error term).

$Y_{aps} = \mu$ (overall mean) + α_a (effect for $_a$th site) + $\beta_{p(a)}$ (effect for $_p$th tree within $_a$th site) + $\epsilon_{s(ap)}$ (random error).

Also, the components of variance (CV): among site CV/within site CV ratios were compared for each leaf trait over all sites. For each site, the estimated coefficients of variation (CVs = standard deviation divided by mean and multiplied by 100) of leaf traits were used as a measure of site variability.

The third analysis was an evaluation of whether latitudes could explain differences in leaf dimensions, and mixed effects models with latitudes were constructed by using the package "nlme" in R software (Pinheiro & Bates, 2000). Before fitting the linear mixed effects models of

leaf traits with latitudes, the unconditional means models were examined, and a comparison between a model with a random intercept and a model without a random intercept was used to justify the use of multi-level regressions with nested structure, which would be indicated by the significant intercept variations. After that, I fitted linear mixed effects models with latitudes as fixed effects and the variances of intercept residuals (random intercepts) of sites (among sites), trees within sites (within sites), and leaves within trees (within individuals) as random effects.

Next, the clinal patterns of leaf traits variation along latitudes were inspected by using regression models. Fitting three regression models on the site transformed mean values for each leaf trait (dependent variable) with the latitudes as the predictor variable. These models were: an intercept only model ($y_t = \beta 1 + €_t$), a linear model ($y_t = \beta 1 + \beta 2 x_t + €_t$) and a quadratic model ($y_t = \beta 1 + \beta 2 x_t + \beta 3 x_t^2 + €_t$). Akaike Information Criterion (AIC) was used to select the best model for each phenotypic trait. The goodness of fit of the intercept-only model would indicate a non-clinal variation, whereas a good linear regression fit or a quadratic regression fit would suggest a clinal differentiation along latitudes (Sugiyama 2003).

All the previous analyses provided an indication of whether latitudinal broad-scale environmental factors' influences were involved in leaf traits variations. Using the same air and sea environmental parameters in table 3.11, a multivariate analysis of redundancy (RDA) was performed to assess the relationship between leaf traits variations and a group of variables (all the 15 environmental parameters in table 3.11, and the (Area) = estimates of the total area of the populations, which reflect habitat fragmentation). The significance of the variability explained by each environmental variable was analysed by automatic selection of variables using a Monte Carlo test with 999 permutations, so the variable that best fits the data was selected first, followed by the other variable added to the model in order of goodness of fit (ter Braak and Šmilauer 2002).

The next analyses assessed the presence of distance-based patterns of variation in leaf traits phenotypes. First, Mantel tests were performed for each one of the leaf traits correlating two matrices: phenotypic distances (Euclidean distances) and geographic distances among sites (Mantel 1967). After that, a spatial autocorrelation analysis was performed for each leaf trait using the library "ncf" of the R package. Autocorrelograms were constructed using distance classes of 100 km. Significance levels of Moran's *I* coefficients of spatial autocorrelation were obtained by Monte Carlo methods with 999 simulations. To test whether the observed pattern of leaf trait being

analysed was randomly distributed among sites; the spatial processes were random chance. Next, estimated sites' means of leaf traits (natural log scale) were re-scaled (0–1), and a hierarchical cluster analysis performed to examine whether the multivariate similarities of sites over the set of leaf traits corresponded with a geographical grouping of these sites. Finally, the sites' means correlation matrix was submitted to principal components analysis. Two components with eigenvalues >1 were extracted, which between them mapped 99.94% of the variance among the leaf traits variables. The solution was rotated by the varimax method, and scores for the sites on the two components were obtained by the regression method. The variable loadings and the site's scores were plotted together in the component space to produce a bi-plot, in which the leaf traits were represented as vectors through the origin and the sites as points.

The next analyses examined the influences of distribution limit on the leaf traits. The nine sampling sites were divided into three major sections: north, middle, and south in figure 2.1. Based on the nature of distribution, *A.marina* on the Red Sea coast was hypothesized as core populations in the southern part (relatively close to the Equator), and as peripheral populations in the northern part (pole-ward limit). Following the same division of the coastline and sampling sites, the south section's sites (site 9, 8, and 7) were initially hypothesized as core populations, while the middle section's sites (site 6, 5, and 4) and the north section's sites (site 3, 2, and 1) were peripheral populations. Therefore, each section had 105 individuals coming from 3 separate sites. Within a core-peripheral context, the influences of distribution limit on the leaf traits were inspected on the basis of comparative analyses of leaf traits between peripheral and core populations.

For each natural-log transformed leaf trait section data set, I performed one-way ANOVAs with one fixed factor - 3 levels (sections) and the random factor (trees), followed by the Tukey's post-hoc Honestly Significant Difference (HSD) tests (Byrkit 1987) when the data set did not violate one-way ANOVA assumptions. When the data set was heteroscedastic, I used the Welch correction, followed by The Games-Howell post-hoc test for pairwise multiple comparisons with unequal variances (Games & Howell 1976). This step showed the significant differences between the sections. Also, the estimated coefficients of variation (CVs) of leaf traits were calculated for each section, and they were used as a measure of section variability.

After that, I performed comparative analyses of the sections leaf dimensions by using two one-tailed *t*-tests and one two-tailed *t*-test for each leaf traits, and a series of comparisons reflected pairs of (north-middle), (north-south), and (middle –south) sections.

The last part of this chapter was a comparison of the phenotypic differentiation and the genetic differentiation. After standardization of leaf traits variables, a matrix of morphological distances based on squared Euclidean distances between sites was calculated using the four leaf traits together, and Mantel test was performed correlating two matrices: pairwise Nei's genetic distances among sites matrix (from chapter 2) and pairwise morphological distances among sites matrix (Mantel 1967). After that, the significance of correlations (Pearson's *r*) between sites' means of leaf traits (natural log scale) and sites inbreeding coefficients (F=Fixation Index) were evaluated. Finally, the hierarchical cluster analysis dendrograms of genetic distances and morphological distances and their components of variations were used in this comparison.

4.3 Results

For all leaf traits, the one-way ANOVAs results showed that there were at least two sites means that were statistically significantly different from each other. The *F*-values and it associated *p*-values for leaf traits were as following: leaf area $F(8,306) = 51.65$, $p < 0.05$, leaf length $F(8,306) = 61.79$, $p < 0.05$, leaf width $F(8,306) = 40.34$, $p < 0.05$, leaf length: width ratio $F(8,306) = 45.47$, $p < 0.05$. In these one-way ANOVAs results, the fixed factor (from which site the data comes) explained 57% of leaf area variations, 62% of leaf length variations, 51% of leaf width variations, and 54% of leaf length: width ratio variations. Table 4.1 summarized mean values of non-transformed leaf area (cm^2), length (cm), width (cm) and length: width ratio (L: W) for the 9 sites, and mean values followed by the same letters were not significantly different ($p < 0.05$, n = 315) with Tukey's HSD test. For each leaf trait, 36 comparisons among 9 sites were the total number of comparisons in Tukey's HSD test. For leaf area and length, 10 comparisons out of 36 were not significant, but leaf width and length: width ratio had 12 insignificant comparisons out of 36. For example, site 6 was significantly the largest in leaf width among all sites, whereas site 7 was significantly the smallest in leaf area and length. Also, the pairs of sites (1 and 3), (4 and 8), and (5 and 9) were not significant in all their leaf traits.

The components of variation for leaf traits in figure 4.1-A showed that most variation 36.7%, 47.9%, and 49.9% occurred among sites for leaf width, area, and length, respectively. The percentages of within sites variations for leaf traits ranged from 26.4 to 31.8%, but the variation among sites percentages had a larger range (36.6-49.9%). Moreover, the components of variance ratios: among-sites CV/within-sites CV ratios in figure 4.1-B were the highest for leaf area and length, while it was the lowest for leaf width.

Table 4.2 showed that models with random intercepts fitted the data significantly better than models without random intercepts, so there were significant intercept variations in terms of leaf dimensional differences scored across the 9 sites which justified the use of multi-level regression with nested structure. The results of linear mixed effects models with latitudes in table 4.3 revealed that leaf area, length, and length: width ratio were significantly and positively correlated with latitudes, but leaf width was not significant. Using the predictor, latitudes, in these models decreased the variance in among-sites intercepts, and latitudes explained 29%, 40%, 61% of the among-sites intercept variance in leaf area, length, and length: width ratio, respectively.

According to table 4.4 and figure 4.2, leaf area, length, and length: width ratio had clinal patterns of variation along latitudes as variation in leaf area and length better fitted to linear models, and variation in length: width ratio better fitted to a quadratic model. However, leaf width had a non-clinal pattern, and it better fitted to an intercept-only model.

After analysing the association between leaf traits (area, length, maximal width, and L: W ratio) and 16 variables in table 3.11 by multivariate analysis of redundancy (RDA), the Annual Sea Surface Temperature (SSTAnn) and the Sea Surface Salinity in Winter (SW) were the only environmental variables contributing significantly to the model (SSTAnn: $F = 6.19$, $p = 0.02$; SW: $F = 7.79$, $p = 0.01$). However, because of the high variance inflation factor (VIF>25) of the model indicating multicollinearity issue, each one of them was separately submitted to automatic selection of variables with the rest 14 variables using a Monte Carlo test with 999 permutations. The resulted groups that turned out to be significant were two groups. The first group consisted of Annual Sea Surface Temperature (SSTAnn) and Relative Humidity in Winter (RHW) ($F = 4.56$, $p= 0.02$). The explained variation in leaf traits among sites by SSTAnn and RHW was 60% (constrained variation) in figure 4.3. The second group contained Sea Surface Salinity in Winter (SW) and Relative Humidity in Winter (RHW) ($F = 4.86$, $p = 0.02$). The explained variation in leaf traits among sites by SW and RHW was 62% (constrained variation) in figure 4.4. The variable SSTAnn, which was correlated to the first axis in figure 4.3, had significant negative correlations with all leaf traits starting with leaf width, area, length, and length: width ratio, and the last trait had the strongest negative correlation with SSTAnn. On the other hand, the variable SW, which was correlated to the first axis in figure 4.3, had significant positive correlations with all leaf traits. For example, sites 5, 7, 8, and 9 that had warmer SSTAnn and lower percentages of SW were characterized by small leaf area, length, and width, whereas sites 1, 2, 3 that had colder SSTAnn and higher percentages of SW were characterized by large leaf area and length. However, site 6 as an exception had large leaf traits even with its warmer SSTAnn and relatively lower SW, and site 4 as an exception had small leaf area, length, and width even with its colder SSTAnn and relatively higher SW.

Based on Mantel tests' results, the correlation between spatial distances and Euclidean leaf length: width ratio distances was significant ($r = 0.53$, $p< 0.05$), and the observed correlation suggested that the two matrices were positively associated, so smaller differences in leaf length: width ratio were generally seen among pairs of sites that were geographically close to each other

than far from each other. The rest of leaf traits, the null hypotheses were failed to be rejected; leaf length ($r = 0.29$, $p = 0.058$), leaf area ($r = 0.031$, $p = 0.38$), and leaf width ($r = -0.22$, $p = 0.91$).

According to the spatial autocorrelation analysis in figure 4.5, leaf width showed an overall disruptive pattern as sites located at distances greater than 200 km had significantly dissimilar phenotypes (dispersed pattern), but sites located at distances around 600-700 km had a significant increase in leaf width similarity (possibility of a correlated pattern over space). The residual spatial autocorrelation almost disappeared after distance unit of around 750 km indicating a nature of randomness for leaf width. Leaf area showed a significant increase in dissimilarity with distances as sites located at distances of (200-300 km) were significantly different in their leaf area, and after this distance unit, the pattern became unclear with no significant Moran's I coefficients. Leaf length: width ratio showed a significant increase in similarity within a distance unit of 650 km, and the similarity decreased monotonically after 650 km. Leaf length was the only trait that did not show a significant differentiation from zero, but it had an overall decreasing trend with distance units.

Hierarchical cluster analysis showed that there were coherent geographical groupings of sites in figure 4.6, and the dendrogram indicated that sites do follow a differentiation by distance model to a certain extent based on multivariate similarities of sites over the whole set of leaf traits. The dendrogram showed the lowest level of groupings (more similarities) as following: (site 2 and site 3, 143.7km apart), (site 4 and site 5, 208km apart), and (site 7 and site 8, 101km apart). Also, table 4.1 showed that the pairs of sites (1 and 3, 331.7km apart), (4 and 8, 645.7km apart), and (5 and 9, 577.5km apart) were not significant in all their leaf traits. Morphologically, the differentiation by distance model was more apparent within a distance range of 100-650 km.
Based on the bi-plot of the principal components analysis in figure 4.7, site 1, 2, 3, and 6 could be grouped by their large leaf area and length, while site 4, 5, and 8 could be grouped by their small leaf area, length, and width. Site 9 had a relatively intermediate position in regards to all leaf dimensions, whereas site 7 had the lowest position in terms of all leaf dimensions.

For the leaf traits data sets of north, middle, and south sections, the one-way ANOVAs results rejected the null hypotheses indicating that there were at least two sections' means that were significantly different from each other. The F-values and it associated p-values for leaf traits were as following: leaf area $F(2,312) = 53.28$, $p < 0.05$, leaf length $F(2,312) = 97.48$, $p < 0.05$, leaf width $F(2,312) = 24.62$, $p < 0.05$, leaf length: width ratio $F(2,312) = 98.74$, $p < 0.05$. In these one-

way ANOVAs results, the fixed factor (from which section the data comes) explained 25% of leaf area variations, 38% of leaf length variations, 14% of leaf width variations, and 39% of leaf length: width ratio variations. Table 4.5 summarized mean values of non-transformed leaf area (cm^2), length (cm), width (cm) and length: width ratio (L: W) for the north, middle, and south sections. The section mean values in table 4.5 followed by the same letters were not significantly different ($p < 0.05$, $n = 315$) with Tukey's HSD test or Games-Howell post-hoc test. Also, table 4.6 showed the estimated coefficients of variation (CVs) of leaf traits in each site and in each section, and they were used as measures of their within-site and within-section variabilities. Furthermore, table 4.7 displayed comparisons of the north, middle, and south sections leaf traits based on t-tests. Based on table 4.5 and table 4.7, all leaf traits of the south section were significantly smaller than the north section and the middle section, whereas leaf area, length, and length: width ratio of the north section were significantly larger than the middle section and the south section. The overall geographical direction of leaf traits mean values had northwards increasing tendency. However, the leaf traits variabilities were not in proportion to the northwards increasing tendency of leaf traits mean values, and that was illustrated in the next paragraphs.

For each leaf trait, 36 comparisons among 9 sites were the total number of comparisons in Tukey's HSD tests in table 4.1. For leaf area and length, 10 comparisons out of 36 were not significant, but leaf width and length: width ratio had 12 insignificant comparisons out of 36. Therefore, leaf area and leaf length as leaf dimensions were more variable than leaf width and length: width ratio. Also, this variability mirrored in the wider ranges of sites estimated coefficients of variation (CVs) of leaf area (15-26) and leaf length (10-17) in table 4.6, whereas leaf width and length: width ratio had narrower ranges of (7-9) and (8-12), respectively.

For all four leaf traits, 12 comparisons among 3 sections were the total number of comparisons in table 4.5. In the north section, 8 comparisons out of 12 were not significant, but the middle section and the south section had only 2 insignificant comparisons. Therefore, the north section showed more phenotypical similarity within its sites comparing to the middle section and the south section. For example, the pair of sites (1 and 3) in the north section was insignificant in all their leaf traits, but no insignificant pairs of sites in all their leaf traits were found within the middle section (sites 4, 5, and 6) or within the south section (sites 7, 8, and 9) in table 4.1. These increased section variabilities of the middle and south sections mirrored in the section estimated

coefficients of variation (CVs) of only two leaf dimensions: leaf area and leaf length in table 4.6 as both of the middle and south sections had higher values than the north section.

Thus, the leaf traits mean values of the north section were significantly larger and less variable than the south section that had significantly smaller leaf traits mean values and higher section variability. Interestingly, the middle section had the northwards increasing tendency of leaf traits mean values, but the middle section preserved the high section variability. Because of the northwards increasing tendency of leaf traits mean values of the middle section, the hierarchical cluster analysis in figure 4.6 grouped the middle section with the north section.

As a comparison of the phenotypic differentiation and the genetic differentiation, there was no significant correlation between pairwise Nei's genetic distances and pairwise morphological distances among sites based on the Mantel test in figure 4.8.

For the correlations (Pearson's r) between sites' means of leaf traits (natural log scale) and sites inbreeding coefficients (F=Fixation Index), there was only a significant negative correlation between the leaf length and inbreeding ($r = -0.72$, $R^2 = 0.52$, $p=0.028$). The rest of leaf traits results were ($r = -0.65$, $R^2 = 0.43$, $p=0.054$) for leaf area, ($r = -0.43$, $R^2 = 0.18$, $p=0.25$) for leaf width, and ($r = -0.65$, $R^2 = 0.42$, $p=0.06$) for leaf length: width ratio.

Morphologically, the components of variation for leaf traits in figure 4.1-A showed that most variation 47.9% and 49.9% occurred among sites for leaf area and leaf length, respectively. Moreover, the components of variance ratios: among-sites CV/within-sites CV ratios in figure 4.1-B were the highest for leaf area and length. Genetically, percentages of molecular variance (AMOVA) among sites were (25%, 34%) ($p < 0.001$), within sites were (0%, 13%), and within individuals were (75%, 53%) ($p < 0.001$). This corresponds to the estimates of both F_{ST} and R_{ST} (0.246 and 0.339, respectively).

Morphologically, the hierarchical cluster analysis showed that there were coherent geographical groupings of sites in figure 4.6. The dendrogram showed the lowest level of groupings as following: (sites 2 and 3), (sites 4 and 5), and (sites 7 and 8). Also, the dendrogram grouped the middle section with the north section. Genetically, the hierarchical cluster analysis dendrograms that used matrices of pairwise comparisons of site genetic differentiation calculated by the infinite alleles model (F_{ST}), the stepwise mutation model (R_{ST}), and Nei's genetic distances were presented in figure 3.2, figure 3.3, and figure 3.4, respectively. In all these dendrograms, site 1, 2, and 3 were clustered together reflecting the north section, while the other sites were linked at

the highest level of grouping with an obvious higher differentiation of site 7. When using the pairwise comparisons of section genetic differentiation, hierarchical cluster analysis dendrograms were identical in grouping north section in one group, and middle and south sections in another group in figure 3.5.

Both of Annual Sea Surface Temperature (SSTAnn) and Sea Surface Salinity in Winter (SW) influenced the genetic and morphological differentiation. The (SSTAnn) had significantly negative correlations with all leaf traits, but it had positive correlations with both of the average number of different alleles per locus (Na) and the gene diversity (He). The (SW) had significantly positive correlations with all leaf traits, but it had significant negative correlations with both of (Na) and (He). The estimates of the total area of the populations (Area), which reflected the level of habitats fragmentation, had significant positive correlations with both of (Na) and (He) only with no effects on leaf traits.

4.4 Discussion

Understanding the natural phenotypic variation within a widespread species such as *A. marina* is the initial step to define the relative influence of different factors underlying phenotypic differentiation (Domínguez et al. 1998; Boyd 2002; Mascó et al. 2004; Herrera 2005; Chalcoff et al. 2008; Pérez- Barrales et al. 2009). Even though the phenotypic leaf variation in *A. marina* was reported in different regions across its global distribution (Melville and Burchett 2002; Saenger and Brooks 2008), it has been rarely investigated on the Red Sea. This study showed that *A. marina* on the Red Sea exhibited more pairwise significant differences in their leaf traits mean values. All the evidences of the significant relationships with latitudes, the high components of variation among sites (47.9% for leaf area, and 49.9% for leaf length), and the clinal patterns of variation along latitudes suggested that geographical broad-scale factors were more likely involved in these significant differences in the various leaf characters among the 9 sites. This was similar to other studies in which A. marina leaves exhibited marked phenotypic differences among three estuaries of Sydney, Australia with no significant differences within sites (Melville and Burchett 2002). Leaf traits are highly expected to be susceptible to environmental variation of abiotic variables (Cunningham et al. 1999; Hobbie and Gough 2002; Wright et al. 2005; Souto et al. 2009). In agreement with the suggestion of geographical broad-scale factors, both of the Annual Sea Surface Temperature-SSTAnn (negatively correlated) and the Sea Surface Salinity in Winter-SW (positively correlated) had significant correlations with all leaf traits in this study. On the Red Sea, sites such as site 8 and site 9, which had warmer sea surface temperature (SSTAnn: 29.5°C, 30.1°C, respectively), and less salinity (SW: 38.46 PSU, 38.16 PSU, respectively), were characterized by small leaf area, length, and width. On the other hand, site 1 and site 2, which had colder sea surface temperature (SSTAnn: 26.7°C, 27°C respectively), and more salinity (SW: 40.24 PSU, 40.14 PSU, respectively), were characterized by large leaf area and length. However, site 6 as an exception had large leaf traits even with its warm SSTAnn and relatively low SW, and site 4 as an exception had small leaf area, length, and width even with its cold SSTAnn and relatively high SW. That suggested a more of a site-specific influence on these two sites.

The geographical distribution patterns of environmental factors such as temperatures might be reflected into geographical patterns of phenotypic variation. Based on the results of different analyses (Mantel tests, the spatial autocorrelation analysis, the hierarchical cluster analysis, and

the principal components analysis), differences in overall leaf phenotypes of *A. marina* on the Red Sea were geographically structured, and the differentiation by distance model was more apparent within a distance range of 100-650 km. These findings contradicted the findings within estuarine neighbourhoods in tropical Queensland, Australia, in which inter-site distances could not explain the phenotypic differences of A. marina, and no coherent geographical groupings of populations were obtained, and phenotypic structuring suggested to arise over quite short distances, less than100 km (Saenger and Brooks 2008).

Within a core-peripheral context, the distribution limit of *A. marina* on the Red Sea coast had an evident influence on the leaf traits mean values and their variations. The leaf traits mean values of the north section (peripheral populations, pole-ward limit) were significantly higher and less variable than the south section (core populations, relatively closer to the Equator) that had significantly smaller leaf traits mean values and higher section variability. Interestingly, the middle section had the northwards increasing tendency of leaf traits mean values, but the middle section preserved the high section variability.

Regarding the leaf traits variations, phenotypic variation and plasticity have been suggested to be lower across the range margins than near range centres as a consequence of small population sizes, genetic drift, founder effects, or genetic isolation (Berg et al. 2005; Becker et al. 2006; Mägi et al. 2011). The advantage of conserving plasticity in peripheral populations' stressful environments may lose its benefit comparing to the relative metabolic and intrinsic genetic costs of phenotypic variation and plasticity (Hoffmann 1990; Parsons 1991). Both of the stressful environmental conditions and the lower gene diversity (from chapter 3) of the north section might explain its lower phenotypic variations. However, the higher gene flow among the middle section and the south section (from chapter 3) might help in preserving the high phenotypic variations of the middle section.

Regarding the leaf traits mean values, the northwards increasing tendency might be a reflection of the geographical distribution patterns of environmental factors because the surface temperatures in the Red Sea rises southward in response to latitudes, but salinity declines southward in response to the intrusion of low salinity water of the Gulf of Aden into the Red Sea especially in winter (Edwards and Head 1987). In general, leaves have a tendency to be smaller in areas under decreasing averages of temperature and/or soil nutrient availability, which reflect the environmental conditions of the northern part of the Red Sea (Cunningham et al. 1999; Hobbie

and Gough 2002; Wright et al. 2005). When it comes to salinity, Halophytes utilize one of two main mechanisms to cope with salinity; avoidance mechanisms and tolerance mechanisms. *A. marina* has salt glands, specialized in salt extrusion, as an adaptive characteristic in its leaf to avoid high concentrations of ions in their leaves. These glands have a higher frequency on the leaf's lower surface (Abdel-Bari et al. 2007). The larger leaf traits in the northern part of the Red Sea comparing with its southern part might be a result of the plant's needs to increase the number of salt glands in response to the higher salinity in the northern part since the number of salt glands and leaf surface have a positive correlation. Another possibility, *A. marina* exhibits the capability to accumulate higher concentrations of Na^+, Cl^-, and Ca^{2+} ions (Yasseen and Abu-Al-Basal 2008). Studies on the accumulation of Ca^{2+} in the plants under saline environment suggested the effect of the increased plasticity of plant tissues (Nilsen and Orcutt 1996; Orcutt and Nilsen 2000; Taiz and Zeiger 2006).

The morphological differentiation of *A. marina* on the Red Sea coast did not increase or decrease strictly based on the genetic differentiation, indicating by the insignificant correlation between pairwise Nei's genetic distances and pairwise morphological distances among sites. Many confounding factors would cause these observed morphological differences in natural populations, including environmental factors, genetic factors relating to additive genetic variances, dominance genetic variances, and epistatic, or an interaction between the factors of environment and genetics (Pujol et al. 2008). However, the significant negative correlation between the mean values of leaf length and inbreeding coefficients might explain the case of site 7 in this study. Site 7 was significantly the smallest in leaf area and length comparing with all sites, and site 7 had the highest inbreeding coefficients (positive 0.126). Thus, site 7 was most likely an indication of inbreeding depression. Although the morphological differentiation and the genetic differentiation were not correlated, both differentiations followed a differentiation by distance model and were significantly influenced by the same geographical broad-scale environmental factors, specifically Annual Sea Surface Temperature (SSTAnn) and Sea Surface Salinity in Winter (SW). However, the estimates of the total area of the populations (Area), which reflect the level of habitat fragmentation (site- specific influences), had a significant effect on the genetic differentiation only. Also, the increased level of variation within sites at the phenotypic level comparing with the absence of the variation within sites at the genetic level suggested an effect of localized environmental influences (site-specific influences) on the morphological differentiation. Overall,

the broad-scale environmental heterogeneity among sites imposed similar structuring processes at the genetic and phenotypic levels, resulting in the presence of a differentiation by distance model.

4.5 Summary

Background

As the most widely distributed of all mangrove tree species, *A. marina* reveals a substantial variability in morphological forms across its entire range of distribution. It can vary from rugged shrubbery on dry coast shores and coral reefs, to closed forests up to 40 m tall in coastal tropical regions (Duke *et al*. 1998). The phenotypic leaf variation in *A. marina* was reported across its Australian range (Melville and Burchett 2002; Saenger and Brooks 2008), but it has been rarely investigated on the Red Sea coast. Utilizing measurements of leaf dimension (leaf area, length, maximal width, and the ratio of length: width), this study examined the field observed phenotypic leaf variation in *A. marina* along the Saudi Arabian Red Sea coastline, and it determined which model best described the distribution of phenotypic leaf variation within and among populations (isolation by distance, discrete subpopulation). Also, it examined the influence of the distribution limit on the phenotypic leaf variation.

Results

This study showed that *A. marina* on the Red Sea coast exhibited more pairwise significant differences in their leaf traits mean values. All the evidences of the significant relationships with latitudes, the high components of variation among sites (47.9% for leaf area, and 49.9% for leaf length), and the clinal patterns of variation along latitudes suggested that geographical broad-scale factors were more likely involved in these significant differences in the various leaf characters among the 9 sites. In agreement with the suggestion of geographical broad-scale factors, both of Annual Sea Surface Temperature-SSTAnn (negatively correlated) and Sea Surface Salinity in Winter-SW (positively correlated) had significant correlations with all leaf traits. Differences in overall leaf phenotypes were geographically structured, and the differentiation by distance model was more apparent within a distance range of 100-650 km. Within a core-peripheral context, the distribution limit of *A. marina* on the Red Sea had an evident influence on the leaf traits mean values and their variations. The leaf traits mean values of the north section (peripheral populations, pole-ward limit) were significantly larger and less variable than the south section (core populations, relatively closer to the Equator) that had significantly smaller leaf traits mean values and higher section variability. Interestingly, the middle section had the northwards increasing

tendency of leaf traits mean values, but the middle section preserved the high section variability. The morphological differentiation of *A. marina* on the Red Sea did not increase or decrease strictly based on the genetic differentiation, indicating by the insignificant correlation between pairwise Nei's genetic distances and pairwise morphological distances among sites. However, the significant negative correlation between the mean values of leaf length and inbreeding coefficients might explain the case of site 7 in this study. Site 7 was significantly the smallest in leaf area and length comparing with all sites, and site 7 had the highest inbreeding coefficients (positive 0.126). Thus, site 7 was most likely an indication of inbreeding depression. Although the morphological differentiation and the genetic differentiation were not correlated, both differentiations followed a differentiation by distance model and were significantly influenced by the same geographical broad-scale environmental factors, specifically Annual Sea Surface Temperature (SSTAnn) and Sea Surface Salinity in Winter (SW). However, the estimates of the total area of the populations (Area), which reflect habitat fragmentation (site-specific influences), had a significant effect on the genetic differentiation only. In addition, the increased level of variation within sites at the phenotypic level comparing with the absence of the variation within sites at the genetic level suggested an effect of localized environmental influences (site-specific influences) on the morphological differentiation. Overall, the broad-scale environmental heterogeneity among sites imposed similar structuring processes at the genetic and phenotypic levels, resulting in the presence of a differentiation by distance model.

Conclusion

Phenotypic leaf variation in *A. marina* along the Saudi Arabian Red Sea coastline follows the differentiation by distance model with an obvious influence of the distribution limit on its variation that manifests in a northwards increasing tendency of leaf traits mean values and lower leaf traits variation.

Table 4. 1 Means (and standard deviations) of non-transformed leaf area (cm^2), length (cm), width (cm) and length: width ratio (L: W) of *Avicennia marina* samples from 9 sites. Mean values followed by the same letters are not significantly different ($p < 0.05$, n = 315) with Tukey's HSD test.

Site	Area		Site	Length		Site	Max. width		Site	L :W ratio	
6	13.89±2.13	d	**1**	6.62±0.73	b	**6**	3.03±0.22	e	**1**	2.54±0.27	b
1	12.26±2.24	bd	**6**	6.23±0.61	ab	**5**	2.77±0.2	a	**3**	2.43±0.25	b
2	11.25±1.87	ab	**3**	6.11±0.67	ab	**2**	2.72±0.25	a	**2**	2.16±0.24	a
3	10.97±1.89	ab	**2**	5.86±0.67	a	**9**	2.7±0.23	a	**4**	2.12±0.26	ac
9	10.27±1.6	a	**9**	5.3±0.57	d	**1**	2.64±0.19	ac	**6**	2.07±0.19	ac
5	10.08±1.47	a	**5**	5.07±0.55	cd	**3**	2.54±0.23	bc	**9**	1.97±0.2	ce
4	8.65±2.23	c	**4**	5.05±0.86	cd	**4**	2.39±0.2	bd	**8**	1.96±0.2	ce
8	8.16±1.76	c	**8**	4.66±0.56	c	**8**	2.39±0.21	bd	**5**	1.84±0.15	de
7	6.83±1.1	e	**7**	4.05±0.42	e	**7**	2.28±0.18	d	**7**	1.79±0.16	d

Table 4. 2 The unconditional means models & the comparison between a model with a random intercept and a model without a random intercept justifying the use of multi-level regression with nested structure for *A. marina* leaf traits on the Red Sea.

	Intercept	Parameter variance		Proportion of variance among sites
		Within site	Among sites	
Leaf Area	2.3***	0.031	0.047	0.6***
Leaf Length	1.7***	0.013	0.024	0.64***
Leaf Width	0.9***	0.0064	0.0078	0.55***
Leaf L/W Ratio	0.7***	0.009	0.0128	0.58***

*** $p < 0.001$

Table 4. 3 The results of linear mixed effects models with latitude and loge-transformed *A. marina* leaf dimensions from 9 sites on the Red Sea.

Leaf character	Values	S.E	D.F	t-value	*p* value
Area					
Intercept	1.85	0.067	4410	27.37	< .00
Latitude	0.0174	0.0013	7	13.115	< .00
Length					
Intercept	1.02	0.261	4410	3.92	0.0001
Latitude	0.0294	0.0117	7	2.50	0.0407
Width					
Intercept	0.86	0.203	4410	4.23	< .00
Latitude	0.0041	0.0091	7	0.45	0.668
L/W Ratio					
Intercept	0.17	0.155	4410	1.07	0.2822
Latitude	0.0253	0.007	7	3.62	0.0085

Leaf character	Explained percentage of among-sites intercept variance by using the predictor latitude
Area	29%
Length	40%
L/W Ratio	61%

Table 4. 4 Akaike Information Criterion (AIC) for three regression models (intercept only, linear, and quadratic) examining geographic patterns of four leaf traits in *Avicennia marina* samples from 9 sites on the Red Sea coast along the latitudes of its distribution range. The best fit model for each trait based on AIC values is indicated by the symbol (*).

	Intercept only ($y = \beta 1 + €$)	**Linear** ($y = \beta 1 + \beta 2x + €$)	**Quadratic** ($y = \beta 1 + \beta 2x + \beta 3x^2 + €$)
Leaf Area	1.2	0.72*	2.7
Leaf Length	-4.9	-8.7*	-7
Leaf Width	-14.9*	-13.2	-11.3
Leaf Length: width ratio	-10.5	-18.01	-18.12*

Table 4. 5 Means (and standard deviations) of non-transformed leaf area (cm2), length (cm), width (cm) and length: width ratio (L: W) of *Avicennia marina* samples based on their sections. Mean values followed by the same letters are not significantly different ($p < 0.05$, n = 315) with Tukey's HSD test or Games-Howell post-hoc test.

Sections	Area		Length		L :W ratio		Sections	Width	
North	11.49±2.09	a	6.19±0.76	c	2.37±0.29	c	**Middle**	2.72±0.33	a
Middle	10.87±2.97	a	5.45±0.88[a]	a	2.01±0.23	a	**North**	2.63±0.23	a
South	8.42±2.09	b	4.67±0.73	b	1.91±0.20	b	**South**	2.45±0.27	b

Table 4. 6 The estimated coefficients of variation (CVs) of *A. marina* leaf traits in each site and in each section (measures of their site and section variability).

	Sites ID									Section ID		
Leaf Traits CV	**1**	**2**	**3**	**4**	**5**	**6**	**7**	**8**	**9**	**North**	**Middle**	**South**
Leaf Area	18	17	17	26	15	15	16	22	16	17.3	18.7	18
Leaf Length	11	11	11	17	11	10	10	12	11	11	13	13
Leaf Width	7	9	9	8	7	7	8	9	9	8.3	8.7	8
Leaf Length: width ratio	11	11	10	12	8	9	9	10	10	10.6	11	10

Table 4. 7 Comparisons (based on t-test) of *A. marina* leaf traits for the north, middle, and south sections on the Red Sea.

Sections	Leaf character	Mean ± SE	*p* value
North and Middle Sections	Area	11.49±2.09 ≅10.87±2.97	0.02*w
		11.49±2.09 >10.87±2.97	0.01*w
	Length	6.19±0.76≅5.45±0.88	0.00*w
		6.19±0.76>5.45±0.88	0.00*w
	Width	2.63±0.23≅2.72±0.33	0.02*w
		2.63±0.23<2.72±0.33	0.01*w
	L/W Ratio	2.37±0.29≅2.01±0.23	0.00
		2.37±0.29>2.01±0.23	0.00
North and South Sections	Area	11.49±2.09 ≅8.42±2.09	0.00*w
		11.49±2.09 >8.42±2.09	0.00*w
	Length	6.19±0.76≅4.67±0.73	0.00*w
		6.19±0.76>4.67±0.73	0.00*w
	Width	2.63±0.23≅2.45±0.27	0.00*w
		2.63±0.23>2.45±0.27	0.00*w
	L/W Ratio	2.37±0.29≅1.91±0.20	0.00
		2.37±0.29>1.91±0.20	0.00
Middle and South Sections	Area	10.87±2.97≅8.42±2.09	0.00
		10.87±2.97>8.42±2.09	0.00
	Length	5.45±0.88≅4.67±0.73	0.00
		5.45±0.88>4.67±0.73	0.00
	Width	2.72±0.33≅2.45±0.27	0.00
		2.72±0.33>2.45±0.27	0.00
	L/W Ratio	2.01±0.23≅1.91±0.20	0.001
		2.01±0.23>1.91±0.20	0.0005

*w indicates Welch's correction was applied.

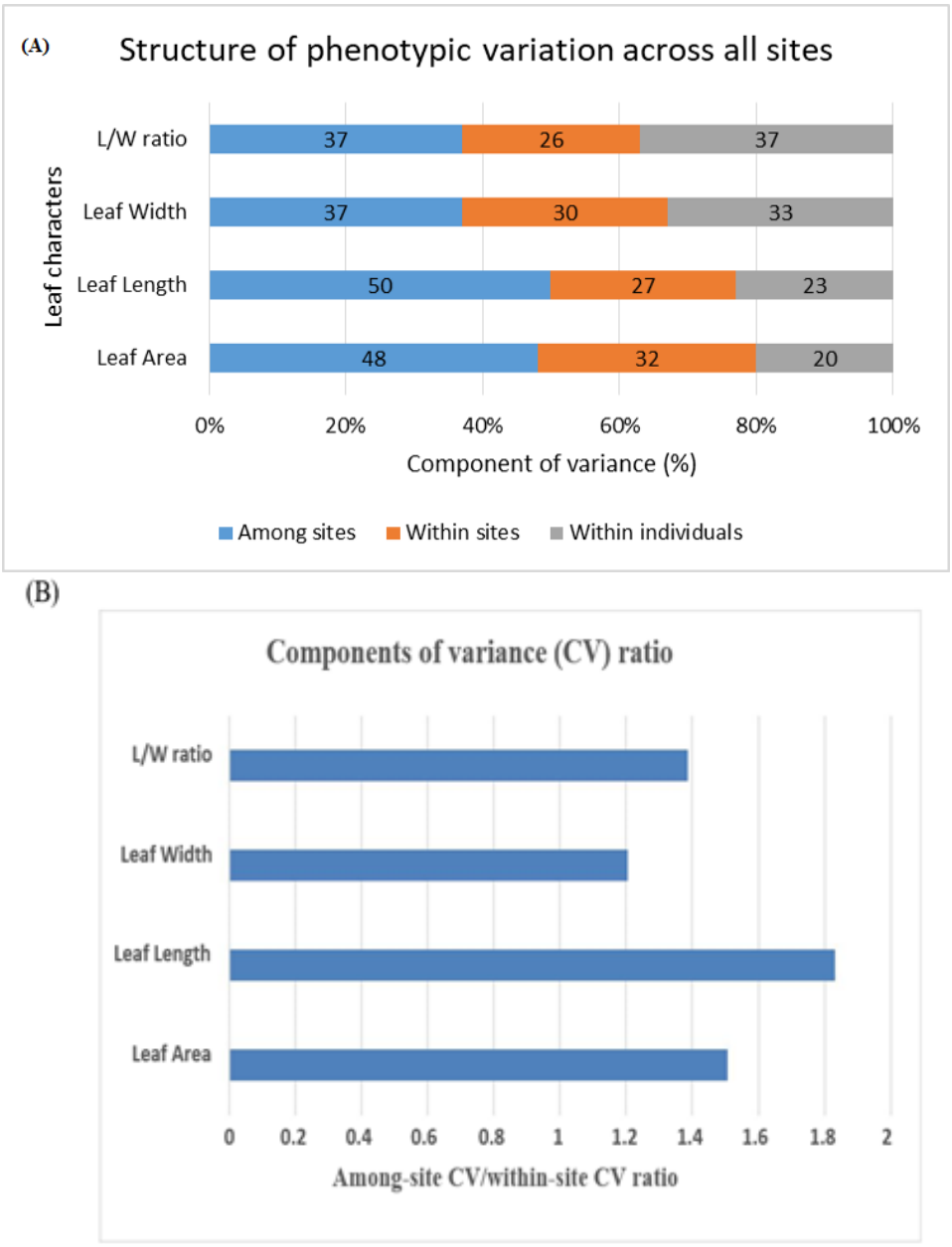

Figure 4. 1 (A) Components of variance expressed as percentages of total variance among sites, within sites, and within individuals. (B) Among-site component of variance /within-site component of variance ratio for each leaf trait of *A. marina* on the Red Sea.

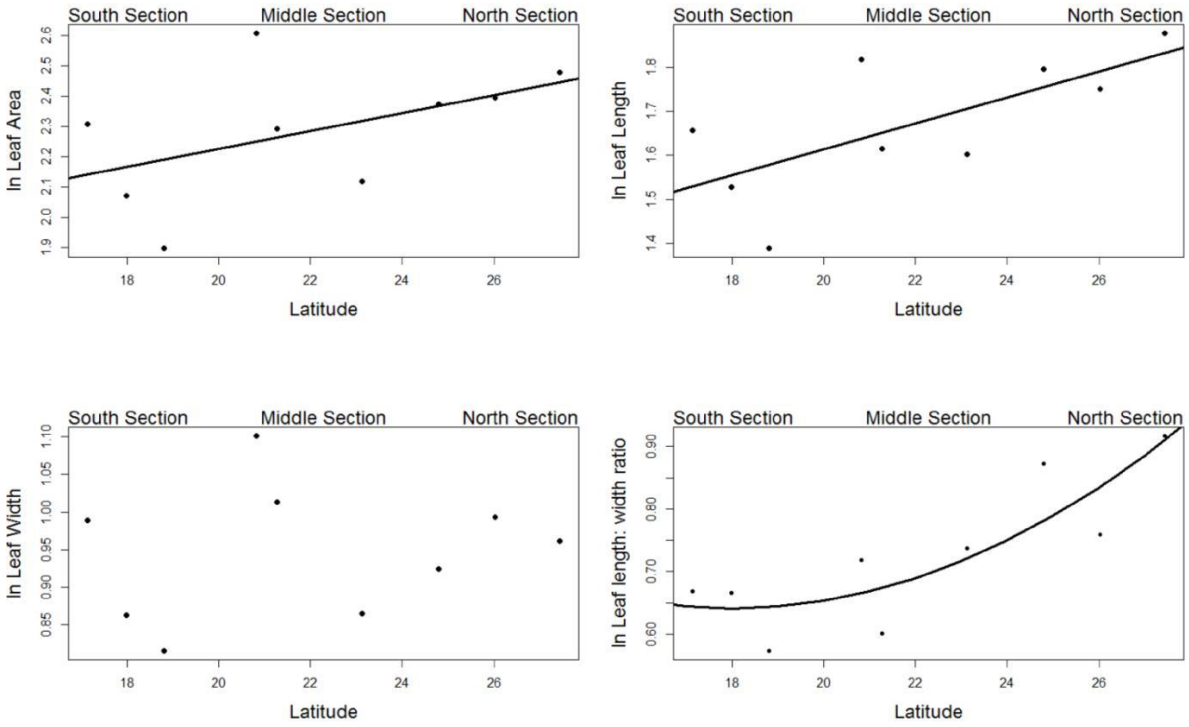

Figure 4. 2 Geographic distribution of *Avicennia marina* leaf traits sampled from 9 sites on the Red Sea coast along the latitudes of its distribution range. Non-clinal (random) or clinal relationships are shown for each trait depending on the regression model (intercept only, linear and quadratic) selected according to the AIC. Leaf Area and Length (Linear), Leaf Width (Intercept only), Leaf Length: width ratio (Quadratic). (see Table4.4).

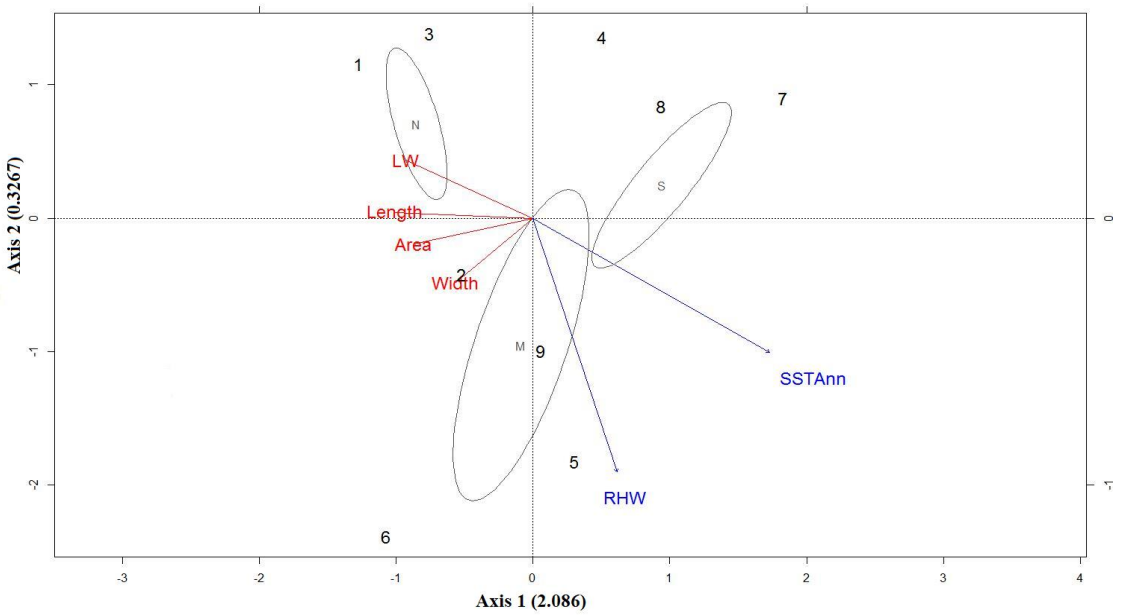

Figure 4. 3 Triplot of the first two axes of the RDA ordination of the nine sites based on four leaf traits variables (red arrows), including the explanatory environmental factors (blue arrows). The global model of Annual Sea Surface Temperature (SSTAnn) and Relative Humidity in Winter (RHW) was significant ($p < 0.05$), and it explained 60% of leaf traits variation. SSTAnn correlated with the first axis. Eigenvalues associated with each axis are provided in brackets. Axis 1 (2.086), Axis 2(0.3267).

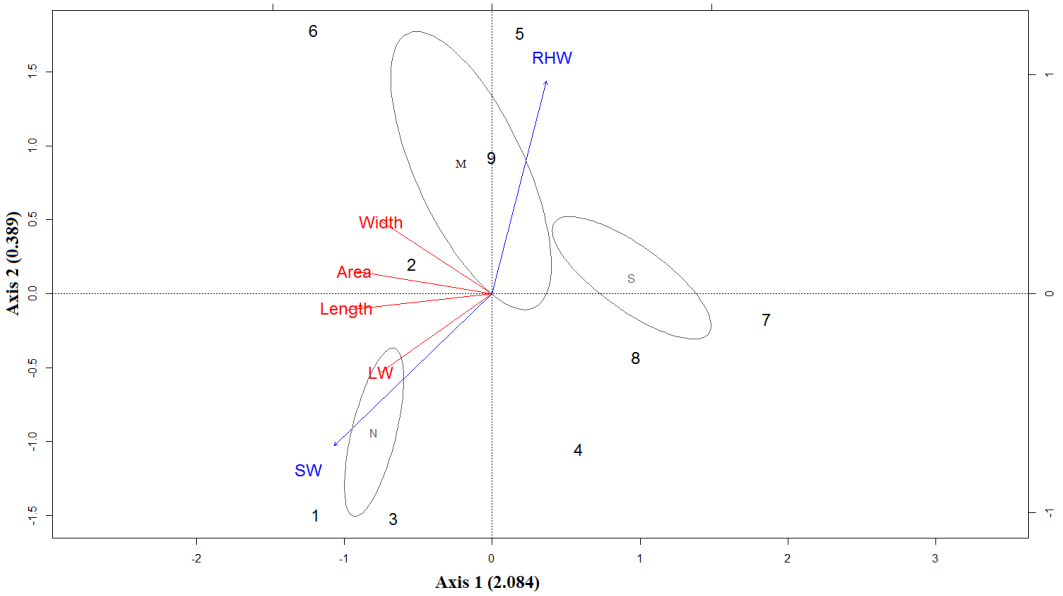

Figure 4. 4 Triplot of the first two axes of the RDA ordination of the nine sites based on four leaf traits variables (red arrows), including the explanatory environmental factors (blue arrows). The global model of Sea Surface Salinity in Winter (SW) and Relative Humidity in Winter (RHW) was significant ($p < 0.05$), and it explained 62% of leaf traits variation. SW correlated with the first axis. Eigenvalues associated with each axis are provided in brackets. Axis 1 (2.084), Axis 2 (0.389).

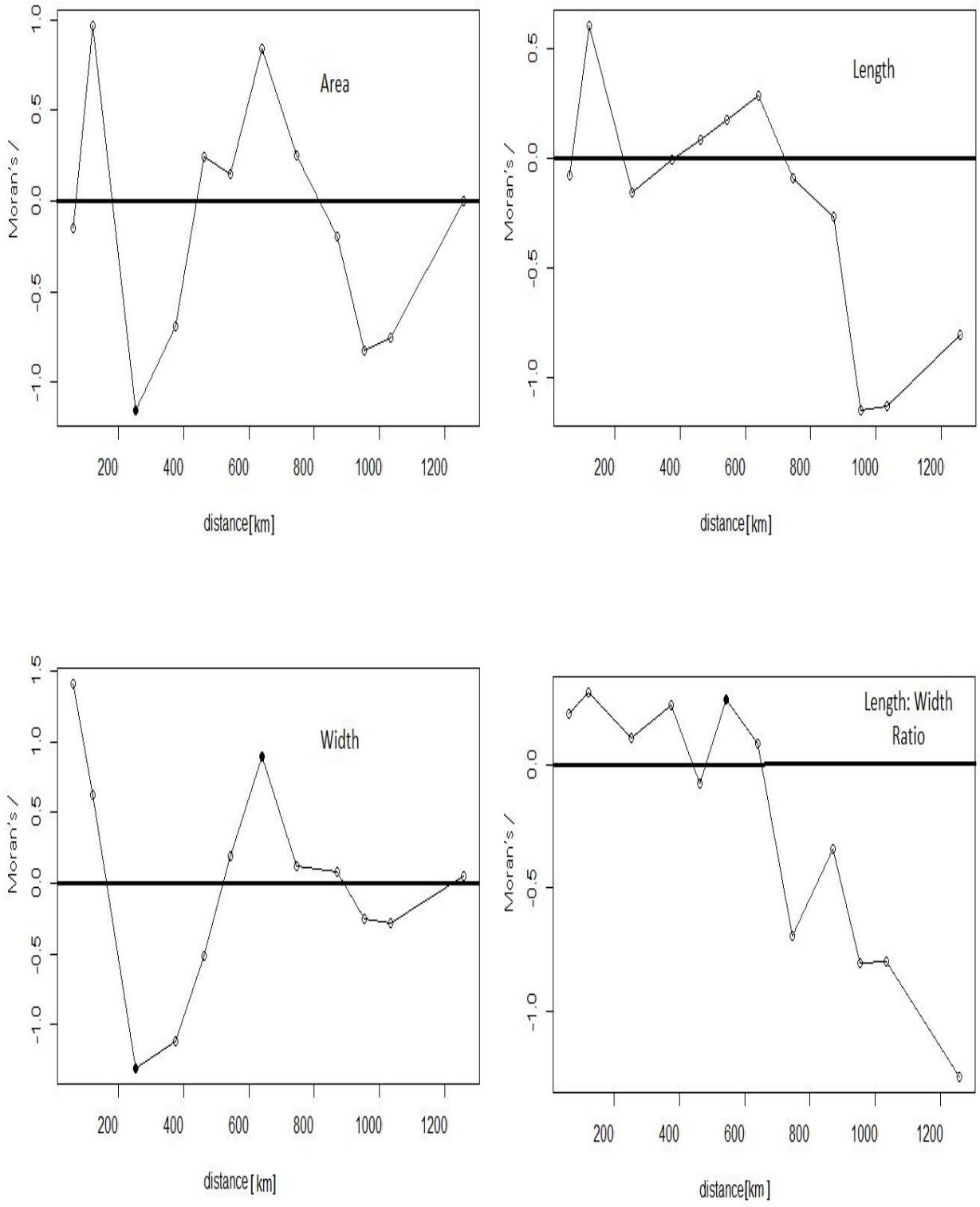

Figure 4. 5 Spatial Autocorrelograms of Moran's I coefficient for *A. marina* leaf traits on the Red Sea as a function of geographical distance among sites. Solid symbols are coefficients that differ significantly from zero (p <0.05); open symbols are non-significant coefficients (p >0.05).

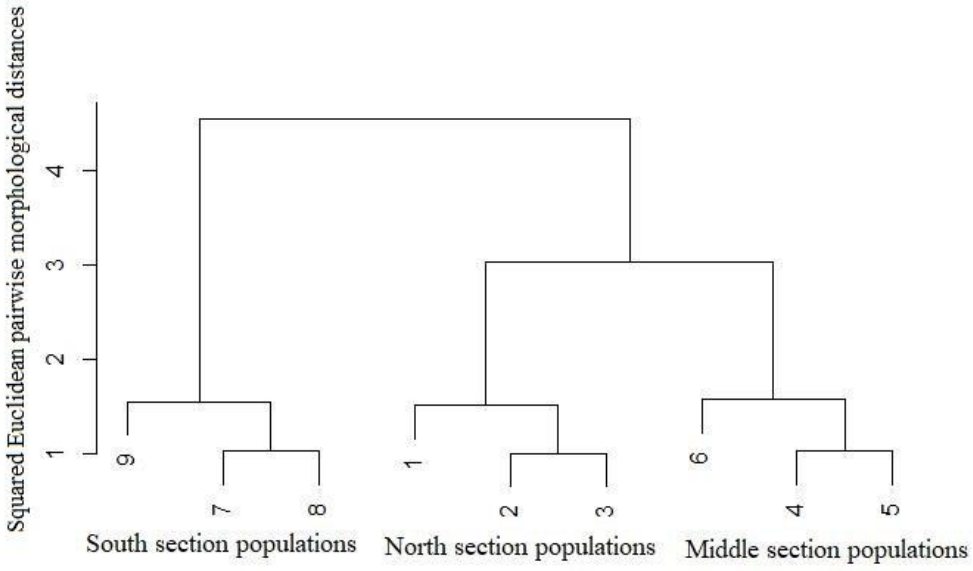

Figure 4. 6 Cluster dendrogram of hierarchical cluster analysis, by using squared Euclidean pairwise morphological distances of *A. marina* on the Red Sea.

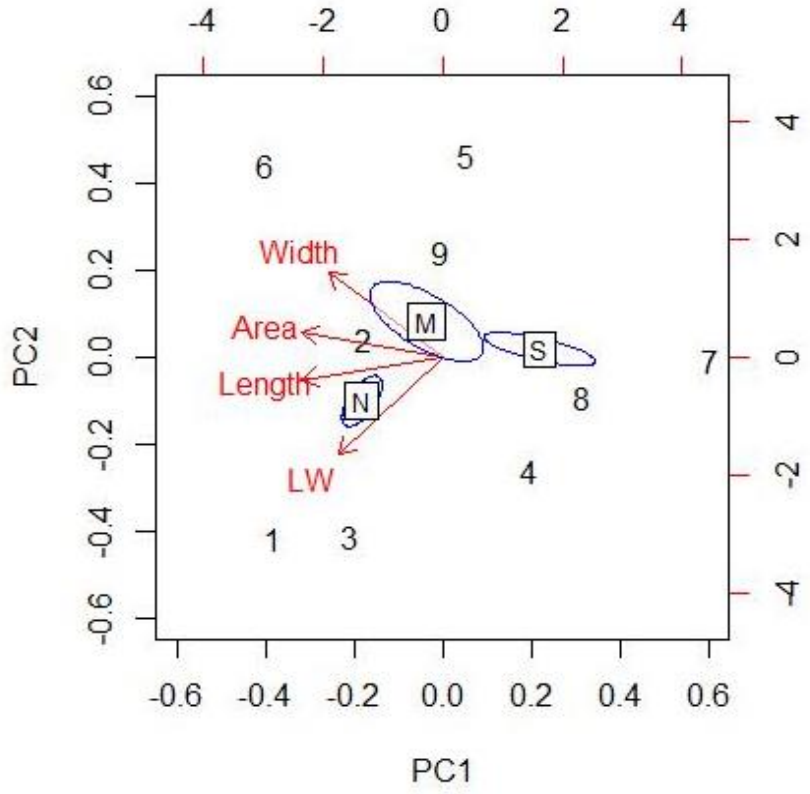

Figure 4. 7 Bi-plot of leaf dimensional variables, represented as vectors through the origin, and the relative positions of the 9 sites to the four vectors following principal components analyses. The relationships among the variables are represented by the angles among their vectors, the relationships among the sites are represented by their inter-point Euclidean distances, and the relationships between the sites and the variables are represented by the orthogonal projections of the site points on the variable vectors.

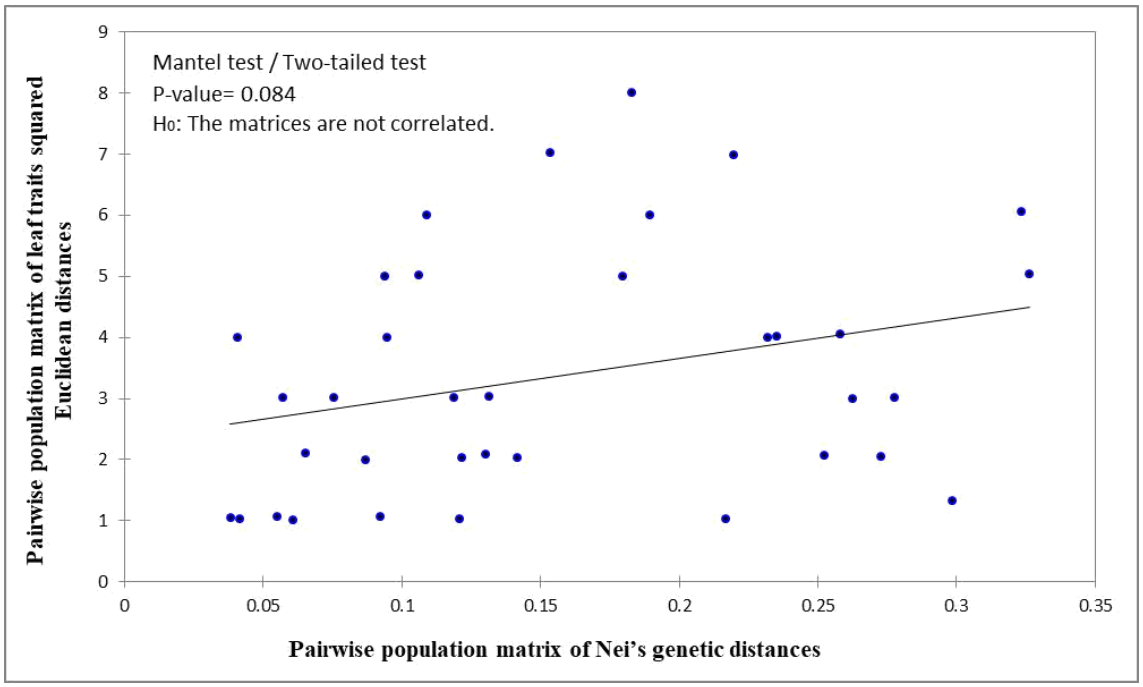

Figure 4. 8 Correlation between genetic distances and morphological distances of *A. marina* on the Red Sea.

Chapter 5: Conclusion

5.1 Research novelties and potential applications

Populations of *A. marina* on the Red Sea coast have rarely ever been genetically investigated for their variation and structure even though the documented status of their degradation anticipates the potential loss of globally and regionally undocumented genetic diversity in mangrove ecosystems. This study is significant to addressing the inadequacies in present-day knowledge, representing one of the first population genetic studies in the farthest northwest edge of *A. marina* global distribution. It will also open avenues for the advancement of the conservation and sustainable management of mangrove ecosystems at local and regional levels on the Red Sea coast which is ultimately a protection of a wide spectrum of globally endangered species. Methodologically, an examination of polymorphism of the 19 microsatellite loci along the entire Red Sea range will provide a direct comparison with other population genetic studies that used some of these markers, and it will offer an evaluation of polymorphism for the markers that have not been used.

5.2 Recommendations for conservation

Mixing seeds from different sites of varying distances throughout the Red Sea coast could be beneficial for gaining the highest adaptive potential, but it could increase the risk of maladaptation and outbreeding depression. Since the local adaptation of *A. marina* has not been studied on the Red Sea coast, the most suitable seed sourcing approach is to establish limits on the geographic distances from which seeds can be sourced for restoration projects in conjunction with an attempt to match the environment of source and recipient sites. Genetically, the differentiation within a geographical range of (59-577 km) at the southern part of the Red Sea coast was relatively lower. Mixed transitional zones arose at a distance of 768-1000 km from the southern part. A distinct population diverged in the northerly farthest sites (1,150-1,350 km from the south). Morphologically, the differentiation by distance model was more apparent within a distance range of 100-650 km. Based on the collective insights from this study, I offer the following recommendations:

As a guideline for a site-level perspective, seed sourcing within 100 kilometres from the site to be restored would be appropriate as a conservative approach.

The sectioning of the Red Sea coastline and sampling sites into three major sections (north, middle, and south) maintained relatively a comparable amount of the genetic variations among sections and within sections. This represented an advantage for conservation planning and reforestation decisions. Also, the north section showed a relatively higher differentiation, but the middle and south sections showed relatively more similarities based on pairwise comparisons of genetic differentiation. Therefore, translocations between similar vs dissimilar sections should have different priorities. Among the middle and south sections, mixing seeds from sites of close and intermediate distance (>100 kilometres) would be appropriate to mimic long-distance gene flow among similar sections. However, it would be proper to mix seeds from sites of an environmental match within the north section, so translocations within the north section should have more priority than among sections.

A group of sites should be prioritized for protection. Site 1 and site 2 reflected a distinct population, and site 8 and site 9 had the highest levels of gene diversity. Based on the field observations in this study, site 7 and site 2 were under pressure from grazing, and site 4 and site 5 were under pressure from environmental pollution due to site 4's proximity to agro-based industries (shrimp ponds) and site 5's proximity to a sewage treatment plant. Both site 7 and site 5 had relatively higher inbreeding coefficients. Site 7 reflected the occurrence of a gene flow barrier and inbreeding depression on its leaf traits mean values.

5.3 Future research directions

On an international scale, an approach that incorporates of both conservation genetics and conservation genomics would be comprehensive in tackling mangrove ecosystems. This will widen the range of the possible questions which can be addressed, such as questions relating to the understanding of the genetic basis of both inbreeding depression and adaptive variation and their association with environmental gradients. On a regional scale, a combination of site-specific approaches would enhance the conservation planning. For example, site-specific studies regarding topography, hydrology, propagule dispersal, and pollinators range are quite informative. Also, a comparison between the genetic differentiations among populations of the maternally inherited

chloroplast genome and the nuclear genome via microsatellites could determine the relative roles of pollen and propagules to gene flow.

Bibliography

Abdel-Bari EM Yasseen BT, Al-Thani RF (2007) Halophytes in the State of Qatar. Environmental Studies Centre. University of Qatar, Doha, Qatar.

Allendorf, FW, Luikart, G (2007). Conservation and the genetics of populations. Blackwell Publishing, Carlton, Australia.

Alongi, DM. (2002). Present state and future of the world's mangrove forests. Environmental Conservation 29(3): 331-349.

Arnaud-Haond, S, Teixeira, S, Massa, SI, Billot, C, Saenger, P, Coupland, G, Duarte, CM. Serrao, EA (2006). Genetic structure at range edge: low diversity and high inbreeding in Southeast Asian mangrove (*Avicennia marina*) populations. Molecular Ecology 15: 3515-3525.

Auld, JR, Agrawal, AA, Relyea, RA (2010). Re-evaluating the costs and limits of adaptive phenotypic plasticity. Proc. Biol. Sci. 277: 503–511.

Awadalla P, Ritland K (1997) Microsatellite variation and evolution in the *Mimulus guttans* species complex with contrasting mating systems. Molecular Biology and Evolution 14: 1023–1034.

Badr, NBE, El-Fiky, AA, Mostafa, AR, Al-Mur, BA (2009). Metal pollution records in core sediments of some Red Sea coastal areas, Kingdom of Saudi Arabia. Environ. Monit. Assess. 155: 509-526.

Bakkenes, M, Alkemade, JRM, Ihle, F, Leemans, R, Latour, JB (2002). Assessing effects of forecasted climate change on the diversity and distribution of European higher plants for 2050. Global Change Biology 8: 390-407.

Balaguer, L, Martınez-Ferri, E, Valladares, F, Perez-Corona, ME, Baquedano, FJ, Castillo, FJ et al. (2001). Population divergence in the plasticity of the response of *Quercus co*ccifera to the light environment. Funct. Ecol. 15: 124–135.

Barbier, EB and Strand, I (1997). Valuing mangrove-fishery linkages: A case study of Campeche, Mexico. The 8th annual conference of European association of environmental and resource economics (EAERE). Department of Agricultural and Resource Economics, University of Maryland, College Park, Maryland 20742, USA, Tilburg University, The Netherlands.

Barton NH, Slatkin M (1986) A quasi-equilibrium theory of the distribution of rare alleles in a subdivided population. Heredity 56: 409–415.

Beaumont, MA and Rannala, B (2004). The Bayesian revolution in genetics. Nature Rev. Genetics 5: 251–261.

Becker, U, Colling, G, Dostal, P (2006). Local adaptation in the monocarpic perennial Carlina vulgaris at different spatial scales across Europe. Oecologia 150: 506–518.

Berg, H, Becker, U, Matthies, D (2005). Phenotypic plasticity in *Carlina vulgaris*: effects of geographical origin, population size, and population isolation. Oecologia 143: 220–231.

Blasco, F, Aizpuru, M, Gers, C (2001). Depletion of the mangroves of Continental Asia. Wetlands Ecology and Management 9: 245–256.

Bodin, N, N′Gom-Kâ, R, Kâ, S, Thiaw, O T, TitodeMorais, L, LeLoc′h, F, Rozuel- Chartier, E, Auger, D, Chiffoleau, JF (2013). Assessment of trace metal contamination in mangrove ecosystems from Senegal West Africa. Chemosphere 90: 150–157.

Boyd A (2002). Morphological analysis of sky land populations of *Macromeria viridiflora* (Boraginaceae). Systematic Botany 27: 116–126.

Brown, JH (1984) On the relationship between abundance and distribution of species. American Naturalist 124: 255–279.

Brown, JH, Mehlman, DW, Stevens, GC (1995) Spatial variation in abundance. Ecology, 76: 2028–2043.
Bruckner, A., G. Rowlands, B. Riegl, S. Purkis, A. Williams, and P. Renaud (2012) Atlas of Saudi Arabian Red Sea marine habitats. Khaled bin Sultan Living Oceans Foundation Panoramic Press, pp. 262.
Brussart. PF (1984) Geographic patterns and environmental gradients: the central-marginal model in Drosophila revisited. Annual Review of Ecology and Systematics 15: 25–64.
Byrkit DR (1987) Statistics today: a comprehensive introduction. The Benjamin-Cummings Publishing Company, Menlo Park, CA.
Chalcoff VR, Ezcurra C, Aizen MA. (2008). Uncoupled geographical variation between leaves and flowers in a South-Andean Proteaceae. Annals of Botany 102: 79–91.
Chapman, Vl (1975) Mangrove biogeography. Proceedings of the International symposium on biology and management of mangroves (Walsh, GE, Snedaker, SC, Teas Hl, eds.). 1: 3–21. University of Florida, Gainesville.
Chapman, Vl (1977) Introduction. Wet coastal ecosystems: ecosystems of the world. (Chapman, Vl, ed.), 1: 1–29. Elsevier, New York.
Chaudhary, S (2001). Flora of the Kingdom of Saudi Arabia. Vol. (2), Part(2). Ministry of Agriculture & Water-Riyadh.
Child, G, Grainger, J (1990). A system plan for protected areas for wildlife conservation and sustainable rural development in Saudi Arabia. National Commission for Wildlife Conservation and Development, Riyadh and IUCN, Gland.
Chmura, GL, Anisfeld, SC, Cahoon, DR, Lynch, JC (2003). Global carbon sequestration in tidal, saline wetland soils. Global Biogeochemical Cycles 17: 1111. doi:10.1029/2002GB001917.
Clarke, PJ (1992). Pre-dispersal mortality and fecundity in the grey mangrove (*Avicennia marina*) in south eastern Australia. Australian Journal of Ecology 17: 161–168.
Cockerham, CC (1973). Analyses of gene frequencies. Genetics 74: 679–700.
Corander, J, Marttinen, P (2006). Bayesian identification of admixture events using multi-locus molecular markers. Molecular Ecology 15: 2833–2843.
Corander, J, Waldmann, P, Sillanpaa, MJ (2003). Bayesian analysis of genetic differentiation between populations. Genetics 163: 367–374.
Corander, J, Waldmann, P, Marttinen, P, Sillanpää, MJ (2004). BAPS 2: enhanced possibilities for the analysis of genetic population structure. Bioinformatics 20(15): 2363-–2369.
Cornuet, J M, Luikart, G (1996) Description and power analysis of two tests for detecting recent population bottlenecks from alleles frequency data. Genetics 144: 2001–2014.
Cunningham SA, Summerhayes B, Westoby M (1999). Evolutionary divergences in leaf structure and chemistry, comparing rainfall and soil nutrient gradients. Ecology 69: 569–588.
Dahdouh-Guebas, F, Hettiarachchi, S, Seen, DL, Batelaan, O, Sooriyarachchi, S, Jayatissa, LP, Koedam, N (2005). Transitions in ancient inland freshwater resource management in Sri Lanka affect biota and human populations in and around coastal lagoons. Current biology 15(6): 579–586.
Do, C, Waples, RS, Peel, D, Macbeth, GM, Tillett, BJ, Ovenden, JR (2014). NeEstimator v2: re-implementation of software for the estimation of contemporary effective population size (Ne) from genetic data. Molecular Ecology Resources 14(1): 209–214.
Dodd, RS, Afzal-Rafii, Z, Kashani, N, Budrick, J (2002) Land barriers and open oceans: effects on gene diversity and population structure in *Avicennia germinan* L. (Avicenniaceae). Mol. Ecol. 11: 1327–1338.

Dodd, RS, Afzal-Rafii, Z, Fromard, F, Blasco, F (1998). Evolutionary diversity among Atlantic coast mangroves. Acta Oecol. 19: 323–330.
Domínguez CA, Eguiarte LE, Núñez-Farfán J, Dirzo R (1998). Flower morphometry of Rhizophora mangle (Rhizophoraceae): geographical variation in Mexican populations. American Journal of Botany 85: 637–643.
Doyle, JJ, Doyle, JL (1990). Isolation of plant DNA from fresh tissue. Focus 12(1): 13-15.
Duke, NC, Benzie, JAH, Goodall, JA, Ballment, ER (1998). Genetic structure and evolution of species in the mangrove genus Avicennia (Avicenniaceae) in the Indo-West Pacific. Evolution 52(6): 1612-1626.
Duke, NC, Meynecke, J-O, Dittmann, S, Ellison, AM, Anger, K, Berger, U, Cannicci, S, Diele, K, Ewel, KC, Field, CD, Koedam, N, Lee, SY, Marchand, C, Nordhaus, I, Dahdouh-Guebas, F (2007). A world without mangroves? Science 317: 41–42.
Edwards, AJ, Head, SM (1987). Red Sea (Key Environments). Pergamon Press in collaboration with IUCN. Oxford. 441pp.
Ellison, JC (2015). Vulnerability assessment of mangroves to climate change and sea-level rise impacts. Wetlands Ecology and Management 23(2): 115–137.
Evanno, G, Regnaut, S, Goudet, J (2005). Detecting the number of clusters of individuals using the software STRUCTURE: a simulation study. Molecular Ecology 14: 2611–2620.
Evans, M. I. (ed.) (1994). Important Bird Areas in the Middle East. Cambridge: Birdlife International.
Falconer, D S, Mackay, TFC (1996). Introduction to quantitative genetics, 4th Edition.
Falush, D, Stephens, M, Pritchard, JK (2003). Inference of population structure using multilocus genotype data: linked loci and correlated allele frequencies. Genetics 164(4): 1567–1587.
Farnsworth, EJ, Ellison, AM (1997). The global conservation status of mangroves. Ambio 26: 328–334.
Frankham, R, Ballou, JD, Briscoe, DA (2002). Introduction to Conservation Genetics. Cambridge University Press, Cambridge, UK.
Games, PA, Howell, JF (1976). Pairwise multiple comparison procedures with unequal N's and/or variances: A Monte Carlo study. Journal of Educational Statistics 1: 113-125.
Giang, LH, Hong, PN, Tuan, MS, Harada, K (2003). Genetic variation of *Avicennia marina* (Forsk.) Vierh. (Avicenniaceae) in Vietnam revealed by microsatellite and AFLP markers. Genes and Genetic Systems 78: 399-407.
Gladstone, W, Tawfiq, N, Nasr, D, Andersen, I, Cheung, C, Drammeh, H, Krupp, F, Lintner, S (1999). Sustainable use of renewable resources and conservation in the Red Sea and Gulf of Aden: issues, needs and strategic actions. Ocean and Coastal Management 42: 671–97.
Glaser, M (2003). Interrelations between mangrove ecosystem, local economy and social sustainability in Caete Estuary, North Brazil. Wetlands Ecology and Management 11: 265–272.
Grant, V (1963). The origin of adaptations. Columbia University Press, New York, NY.
Hamrick, JL, Godt, MW (1990). Allozyme diversity in plant species. In Plant Population Genetics, Breeding, and Genetic Resources. Sinauer Associates Inc., USA p. 43-63.
Hartl, DL, Clark, AG (1997). Principles of Population Genetics, 3rd edition. Sunderland USA, Sinauer Associates Inc. 542 p.
Herrera, J (2005). Flower size variation in Rosmarinus officinalis: individuals, populations and habitats. Annals of Botany 95: 431–437.
Hill, WG (1981). Estimation of effective population size from data on linkage disequilibrium. Genetics Research 38(3): 209–216.

Hobbie SE, Gough L (2002). Foliar and soil nutrients in tundra on glacial landscapes of contrasting ages in northern Alaska. Oecologia 131: 453–462.

Hoffmann, AA (1990). Acclimation for desiccation resistance in Drosophila melanogaster and the association between acclimation responses and genetic variation. Journal of Insect Physiology 36: 885–891.

Homer, LE (2009) Population structure and distance of gene flow in *Avicennia marina* (Forsk.) Vierh. (Avicenniaceae) on a local/regional scale in the Northern Rivers of New South Wales, Australia, PhD thesis, Southern Cross University, Lismore, NSW.

Jombart, T (2008). adegenet: a R package for the multivariate analysis of genetic markers. Bioinformatics, 24(11): 1403–1405.

Kahrood, HV, Korori, SAA, Pirseyedi, M, Shirvany, A, Danehkar, A (2008). Genetic variation of mangrove species *Avicennia marina* in Iran revealed by microsatellite markers. African Journal of Biotechnology 7(17).

Kairo, JG, Dahdouh-Guebas, F, Bosire, J, Koedam, N (2001). Restoration and management of mangrove systems - a lesson for and from the East African region. South African Journal of Botany 67: 383–398.

Kirkpatrick, M, Ravigne, V (2002). Speciation by natural and sexual selection: models and experiments. American Naturalist 159: S22–S35.

Kitamura, S, Anwar, C, Chaniago, A, and Baba, S (1997) Handbook of Mangroves in Indonesia. Saritaksu, Denpasar.

Knowles, P, Perry, DJ, Forster, HA (1992) Spatial genetic structure in two tamarack [*Larix laricina* (do roi) K. Koch] populations with differing establishment histories. Evolution 46: 572–576.

Kostopoulou, E, Giannakopoulos, C, Hatzaki, M, Karali, A, Hadjinicolaou, P, Lelieveld, J, Lange, MA (2014). Spatio-temporal patterns of recent and future climate extremes in the eastern Mediterranean and Middle East region. Natural Hazards and Earth System Sciences 14(6): 1565–1577.

Kotb, MMA, Hanafy, MH, Rirache, H, Matsumura, S, Al-Sofyani, AA, Ahmed, AG, Bawazir, G, Al-Horani, FA (2008). Status of Coral Reefs in the Red Sea and Gulf of Aden Region. International Coral Reef Initiative Forum. PERSGA.

Laegdsgaard, P, Johnson, CR (1995). Mangrove habitats as nurseries: unique assemblages of juvenile fish in subtropical mangroves in eastern Australia. Marine Ecology Progress Series 126: 67–81.

Lakshmi, A, Rajagopalan, R (2000). Socio-economic implications of coastal zone degradation and their mitigation: a case study from coastal villages in India. Ocean and Coastal Management 43: 749-762.

Latch, EK, Dharmarajan, G, Glaubitz, JC, Rhodes Jr, OE (2006). Relative performance of Bayesian clustering software for inferring population substructure and individual assignment at low levels of population differentiation. Conservation genetics 7(2): 295–302.

Lawton, JH (1993). Range, population abundance and conservation. Trends in Ecology and Evolution 8: 409–413.

Lelieveld, J, Hadjinicolaou, P, Kostopoulou, E, Chenoweth, J, El Maayar, M, Giannakopoulos, C, Hannides, C, Lange, MA, Tanarhte, M, Tyrlis, E, Xoplaki, E (2012). Climate change and impacts in the Eastern Mediterranean and the Middle East. Climatic Change 114(3-4): 667–687.

Leonardi, S, Menozzi, P (1996) Spatial structure of genetic variability in natural stands of L. (beech) in Italy. Heredity 77: 359–368.
Leonardi, S, Raddi, S, Borghetti, M (1996) Spatial auto-correlation of allozyme traits in a Norway spruce (*Picea abies*) population. Canadian Journal of Forest Research 26: 63–71.
Lesica, P, Allendorf, FW (1995) When are peripheral populations valuable for conservation? Conservation Biology 9: 753–760.
Loarie, SR, Carter, BE, Hayhoe, K, McMahon, S, Moe, R, Knight, CA, Ackerly, DD (2008). Climate change and the future of California's endemic flora. PLoS ONE 3: e2502.
Locke, S, Thunell, RC (1988). Paleoceanographic record of the last glacial/interglacial cycle in the Red Sea and Gulf of Aden. Palaeogeography, Palaeoclimatology, Palaeoecology 64(3-4): 163–187.
Lovelock, CE, Adame, MF, Bennion, V, Hayes, M, O'Mara, J, Reef, R, Santini, NS (2014). Contemporary rates of carbon sequestration through vertical accretion of sediments in mangrove forests and saltmarshes of South East Queensland, Australia. Estuaries and coasts 37(3): 763-771.
Luikart, G, Allendorf, FW, Cornuet, JM, Sherwin, WB (1998). Distortion of allele frequency distributions provides a test for recent population bottlenecks. Journal of Heredity 89(3): 238–247.
Luikhart, G, England, PR (1999). Statistical analysis of microsatellite DNA data. Trends in Ecology and Evolution 7: 14(7): 253-256.
Mägi, M, Semchenko, M, Kalamees, R, Zobel, K (2011). Limited phenotypic plasticity in range-edge populations: a comparison of co-occurring populations of two Agrimonia species with different geographical distributions. Plant Biol. 13: 177–184.
Maguire, TL, Collins, GG, Sedgley, M (1994). A modified CTAB DNA extraction procedure for plants belonging to the family Proteaceae. Plant Molecular Biology Reporter 12(2): 106-–109.
Maguire, TL, Edwards, KJ, Saenger, P, Henry, R (2000). Characterisation and analysis of microsatellite loci in a mangrove species *Avicennia marina* (Forsk.) Vierh. (Avicenniaceae). Theoretical and Applied Genetics 101(1-2): 279–285.
Maguire, TL, Peakall, R, Saenger, P (2001). Comparative analysis of genetic diversity in the mangrove species *Avicennia marina* (Forsk.) Vierh. (Avicenniaceae) detected by AFLPs and SSRs. Theoretical and Applied Genetics 104: 388–398.
Maguire, TL, Saenger, P, Baverstock, P, Henry, R (2000). Microsatellite analysis of genetic structure in the mangrove species *Avicennia marin*a (Forsk.) Vierh. (Avicenniaceae). Molecular Ecology 9: 1853–1862.
Mantel, N (1967). The detection of disease clustering and a generalized regression approach. Cancer Research 27: 209–220.
Mascó M, Noy-Meir I, Sérsic AN. (2004). Geographic variation in flower color patterns within Calceolaria uniflora Lam. in Southern Patagonia. Plant Systematics and Evolution 244:77–91.
Mayr, E (1970). Populations, species, and evolution. Harvard University Press, Cambridge, MA.
Mazda, Y, Magi, M, Kogo, M, Hong, PN (1997). Mangroves as coastal protection from waves in the Tong King delta, Vietnam. Mangroves and Salt Marshes 1: 127-135.
McKee, K, Rogers, K, Saintilan, N (2012). Response of salt marsh and mangrove wetlands to changes in atmospheric CO 2, climate, and sea level. In Global change and the function and distribution of wetlands (pp. 63–96). Springer, Dordrecht.

Mcleod, E, Chmura, GL, Bouillon, S, Salm, R, Bjork, M, Duarte, CM, Lovelock, CE, Schlesinger, WH, Silliman, B (2011). A Blueprint for Blue Carbon: Towards an improved understanding of the role of vegetated coastal habitats in sequestering CO_2. Frontiers in Ecology and the Environment 9: 552–560.

Meirmans, PG (2006). Using the AMOVA framework to estimate a standardized genetic differentiation measure. Evolution 60(11): 2399–2402.

Melville, F, Burchett, M (2002). Genetic variation in *Avicennia marina* in three estuaries of Sydney, (Australia) and implications for rehabilitation and management. Marine Pollution Bulletin 44(6): 469–479.

Mildenhall, DC (1994). Early to Mid Holocene pollen samples containing mangrove pollen from Sponge Bay, East Coast, North Island, New Zealand. Journal of the Royal Society of New Zealand 24: 219–230.

Milward, NE (1982). Mangrove-dependant biota, in Mangrove ecosystems in Australia. Structure, function and management. (Clough, BF, ed.). pp. 121–139, Australian National University Press, Canberra.

Morcos, SA (1970). Physical and chemical oceanography of the Red Sea. Oceanogr. Mar. Biol. Annu. Rev 8: 73-202.

Nagelkerken, I, van der Velde, G, Gorissen, MW, Meijer, GJ, van't Hof, T, den Hartog, C (2000). Importance of mangroves, seagrass beds, and the shallow coral reef as a nursery for important coral reef fishes, using a visual census technique. Estuarine, Coastal and Shelf Science 51: 31-44.

Nawata, H (2013). A study of human subsistence ecosystem with mangrove in drylands: To prevent a new outbreak of environmental problems. Research Institute for Humanity and Nature, Kyoto, Japan.

Nei, M (1972). Genetic distance between populations. The American Naturalist, 106(949): 283-–292.

Nei, M (1973). Analysis of gene diversity in subdivided populations. Proceedings of the National Academy of Sciences 70(12): 3321–3323.

Nettel, A, Dodd, RS (2007). Drifting propagules and receding swamps; genetic footprints of mangrove recolonization and dispersal along tropical coasts. Evolution 61: 958–971.

Nilsen ET, Orcutt DM (1996). Physiology of plants under stress. Abiotic factors. Wiley, New York.

Nomura, T (2008). Estimation of effective number of breeders from molecular coancestry of single cohort sample. Evolutionary Applications 1(3): 462-474.

Ong, JE (1995). The ecology of mangrove conservation and management. Hydrobiologia 295: 343-351.

Orcutt DM, Nilsen ET (2000) Physiology of plants under stress. Soil and biotic factors. Wiley, New York.

Orloci, L (1978). Multivariate analysis in vegetation research. The Hague: Dr W. Junk B. V.

Ouborg, NJ, Piquot, Y, Van Groenendael, JM (1999). Population genetics, molecular markers and the study of dispersal in plants. Journal of Ecology 87: 551–568.

Parani, M, Lakshmi, M, Elango, S, Ram, N, Anuratha, CS, Parida, A (1997). Molecular phylogeny of mangroves II. Intra- and inter-specific variation in Avicennia revealed by RAPD and RFLP markers. Genome 40: 487–495.

Parmesan, C, Yohe, G (2003). A globally coherent fingerprint of climate change impacts across natural systems. Nature 421: 37–42.

Parsons, PA (1991). Evolutionary rates – stress and species boundaries. Annual Review of Ecology and Systematics 22: 1–18.
Peakall, R, Smouse, PE (2006). GENALEX 6: genetic analysis in Excel. Population genetic software for teaching and research. Molecular Ecology Notes 6: 288–295.
Peakall, R, Smouse, PE, Huff, DR (1995). Evolutionary implications of allozyme and RAPD variation in diploid populations of dioecious buffalograss *Buchloe dactyloides*. Molecular Ecology 4(2): 135–148.
Pearse, DE, Crandall, KA (2004). Beyond FST: Analysis of population genetic data for conservation. Conservation Genetics 5: 585–602.
Peck, JR, Yearsley, JM, Waxman, D (1998). Explaining the geographic distributions of sexual and asexual populations. Nature 391: 889–892.
Pérez-Barrales R, Pino R, Albaladejo RG, Arroyo J. (2009). Geographic variation of flower traits in *Narcissus papyraceus* (Amaryllidaceae): do pollinators matter? Journal of Biogeography 36: 1411–1422.
PERSGA- The Regional Organization for the Conservation of the Environment of the Red Sea and Gulf of Aden, (2005). Mangroves in the RSGA Region. Habitats and Biodiversity, Activities and Programs, Jeddah, Saudi Arabia.
Pichancourt, J-B, Klinken, RD (2012). Phenotypic plasticity influences the size, shape and dynamics of the geographic distribution of an invasive plant. PLoS ONE 7: e32323.
Pigliucci, M, Whitton, J, Schlichting, CD (1995). Reaction Norms of Arabidopsis. 1. Plasticity of characters and correlations across water, nutrient and light gradients. J. Evol. Biol. 8: 421–438.
Pinheiro, JC, Bates, DM (2000). Mixed-effects models in S and S-PLUS. New York: Springer-Verlag.
Primack RB, Tomlinson PB (1980) Variation in tropical forest breeding systems. Biotropica 12: 229–231.
Pritchard, JK, Stephens, M, Donnelly, P (2000). Inference of population structure using multilocus genotype data. Genetics 155: 945-959.
Pritchard, JK, Wen, X, Falush, D (2007). Documentation for structure software: Version 2.2.
Pujol, B, Wilson, AJ, Ross, RIC, Pannell, R (2008). Are QST-FST comparisons for natural populations meaningful? Molecular Ecology 17: 4782–4785.
R Development Core Team. (2015). R: A Language and Environment for Statistical Computing. R Foundation for Statistical Computing, Vienna, Austria. URL http://www.R-project.org.
Rabinowitz, D (1978) Dispersal properties of mangrove propagules. Biotropica 10: 47–57.
Rice WR (1989) Analysing tables of statistical tests. Evolution 43: 223–225.
Ricklefs, RE, Latham, RE (1993) Global patterns of diversity in mangrove floras. In: Species Diversity in Ecological Communities: Historical and Geographical Perspectives (Schluter, R., ed.), pp. 215–229. University of Chicago Press, Chicago, Illinois.
Robertson, AI, Duke, NC (1987). Mangroves as nursery sites: comparisons of the abundance and species composition of fish and crustaceans in mangroves and other nearshore habitats in tropical Australia. Marine Biology 96: 193-205.
Rohlf, D. J. (1994). Pacific salmon. There's something fishy going on here: a critique of the National Marine Fisheries Service's definition of species under the Endangered Species Act. Environmental Law 24:617–671.
Rossetto, M, Slade, RW, Baverstock, PR, Henry, RJ, Lee, LS (1999) Microsatellite variation and assessment of genetic structure in tea tree (*Melaleuca al*ternifolia - Myrtaceae). Molecular Ecology 8: 633–643.

Rousset, F (2007). GENEPOP'007: a complete reimplementation of the GENEPOP software for Windows and Linux. Molecular Ecology Notes 8: 103-106.
Saenger, P (1993). Management of Mangroves in the Kingdom of Saudi Arabia. Riyadh, Saline Water Conversion Corporation. Ministry for Agriculture and Water. Page 36.
Saenger, P (1998). Mangrove vegetation: an evolutionary perspective. Marine and Freshwater Research 49: 277–286.
Saenger, P (2002). Mangrove ecology, silviculture and conservation. Kluwer Academic Publishers, Dordrecht.
Saenger, P, & Brooks, LO (2008). Phenotypic leaf variation in Avicennia marina in tropical Australia: can discrete subpopulations be recognised in the field? Australian Journal of Botany 56(6) 487–492.
Safriel, UN, Volis, S, Kark, S (1994). Core and peripheral populations, and global climate change. Israel Journal of Plant Sciences 42: 331–345.
Saintilan, N, Wilson, N, Rogers, K, Rajkaran, A, Krauss, KW (2014). Mangrove expansion and salt marsh decline at mangrove poleward limits. Global Change Biology 20(1): 147–157.
Sasekumar, A, Chong, VC, Leh, MU, D'Cruz, R (1992). Mangroves as habitat for fish and prawns. Hydrobiologia 247: 195–207.
Schmitz, N, Anouk, V, Beekman, H, Gitundu, J, Koedam, N (2006). Influence of a salinity gradient on the vessel characters of the mangrove species *Rhizophora mucronata*. Annals of Botany 98: 1321–1330.
Schodde, R, Mason, IJ, Gill, HB (1982). The Avifauna of the Australian Mangroves. A brief review of composition, structure and origin, in Mangrove ecosystems in Australia. Structure, function and management. (Clough, BF, ed.) pp. 141-150, , Australian National University Press, Canberra.
Schoen DJ, Brown ADH (1993) Conservation of allelic richness in wild crop relative is aided by assessment of genetic markers. Proc. Nat. Acad. Sci. 90: 10623–10627.
Schwarzbach, A, Ricklefs, R (2001). The use of molecular data in mangrove plant research. Wetlands Ecol. Manage. 9: 195–201.
Shapcott, A (1995) The spatial genetic structure in natural populations of the Australian temperate rainforest tree *Atherosperma moschatum* (Labill.) (Monimiaceae). Heredity 74: 28–38.
Solomon, S, Qin, D, Manning, M, Chen, Z, Marquis, M, Averyt, KB, Tignor, M, Miller, HL. (eds.) (2007). Contribution of Working Group I to the Fourth Assessment Report of the Intergovernmental Panel on Climate Change. Cambridge University Press, Cambridge, United Kingdom and New York, NY, USA.
Souto, CP, Premoli, AC, Reich, PB. (2009). Leaf trait variation in Embothrium coccineum (Proteaceae) is shaped by complex Patagonian physiographic gradients. Revista Chilena de Historia Natural 82: 209–222.
Sugiyama, S. (2003). Geographical distribution and phenotypic differentiation in populations of *Dactylis glomerata* L. in Japan. Plant Ecology 169: 295–305.
Taiz L, Zeiger E (2006) Plant physiology. Redwood City, California Tomlinson PB (1986) The botany of mangrove. Cambridge University Press, New York
Tamaei, S (2013). Study of gray mangrove (*Avicennia marina*) afforestation for greening a desert coast: Gray mangrove afforestation on the banks of an aArtificial channel across a Sabkha and established biotic community. (Nawata, H, ed.) pp.22-27. Dryland Mangroves: Frontier Research and Conservation. Arab Subsistence Monograph Series, 2. Shoukadoh Book Sellers, Kamigyo-ku, Kyoto, Japan

Teas, H (Ed.), (1984). Biology and Ecology of Mangroves. (Vol. 8) W. Junk Publishers, The Hague, 188p.
Ter Braak, CJ, Smilauer, P (2002). CANOCO reference manual and CanoDraw for Windows user's guide: software for canonical community ordination (version 4.5). Ithaca (NY): Microcomputer Power. www. canoco. com.
Tomlinson, PB (1986) The Botany of Mangroves. Cambridge University Press, Cambridge, United Kingdom.
Triest, L (2008). Molecular ecology and biogeography of mangrove trees towards conceptual insights on gene flow and barriers: a review. Aquatic Botany 89(2): 138–154.
Valiela, I, Bowen, JL, York, JK (2001). Mangrove forests: One of the World's threatened major tropical environments. BioScience 51(10): 807–815.
Valladares, F, Gianoli, E, Gomez, JM (2007). Ecological limits to plant phenotypic plasticity. New Phytol. 176: 749–763.
Van Oosterhout, C, Hutchinson, WF, Wills, DP, Shipley, P (2004). MICRO-CHECKER: software for identifying and correcting genotyping errors in microsatellite data. Molecular Ecology Resources 4(3): 535–538.
Van Oosterhout, C, Weetman, D, Hutchinson, WF (2006). Estimation and adjustment of microsatellite null alleles in nonequilibrium populations. Molecular Ecology Resources 6(1): 255–256.
Vogler, A P, DeSalle, R (1994). Diagnosing units of conservation management. Conservation Biology 8: 354–363.
Volis, S, Mendlinger, S, Olsvig-Whittaker, L, Safriel, UN, Orlovsky, N (1998). Phenotypic variation and stress resistance in core and peripheral populations of *Hordeum spontaneum*. Biodivers. Conserv. 7: 799–813.
Vucetich, JA, Waite, TA (2000). Is one migrant per generation sufficient for the Walsh, GE (1974) Mangroves: a review. Ecology of halophytes (Reimhold, Rl, Queen, WH, eds.). pp. 51–174. Academic Press, New York.
Walsh, G E (1974). Mangroves: a review. In Ecology of halophytes (pp. 51–174).
Walther, G R, Post, E, Convey, P, Menzel, A, Parmesan, C, Beebee, TJC, Fromentin, JM, Hoegh-Guldberg, O, Bairlein, F (2002). Ecological responses to recent climate change. Nature 416: 389–395.
Waples, RS (2006). A bias correction for estimates of effective population size based on linkage disequilibrium at unlinked gene loci. Conservation Genetics 7(2): 167.
Waples, RS, Do, C (2010). Linkage disequilibrium estimates of contemporary Ne using highly variable genetic markers: a largely untapped resource for applied conservation and evolution. Evolutionary Applications 3(3): 244–262.
Waples, RS, Do, CHI (2008). LDNE: a program for estimating effective population size from data on linkage disequilibrium. Molecular Ecology Resources 8(4): 753–756.
Ward, RD, Friess, DA, Day, RH, MacKenzie, RA. (2016). Impacts of climate change on mangrove ecosystems: a region by region overview. Ecosystem Health and Sustainability 2(4): e01211.
Weber, JL (1990). Informativeness of human (dC-dA) n·(dG-dT) n polymorphisms. Genomics 7(4): 524–530.
Weir, BS (1996) Genetic Data Analysis II. Sinauer, Sunderland, MA.
Weir, BS, Cockerham, CC (1984). Estimating F-statistics for the analysis of population structure. Evolution 38: 1358–1370.

Wolff, M, Koch, V, Isaac, V (2000). A trophic flow model of the Caete mangrove estuary (North Brazil) with considerations for the sustainable use of its resources. Estuarine, Coastal and Shelf Science 50: 789–-803.

Woodworth, P, Foden, P, Pugh, J, Mathews, A, Aarup, T, Aman, A, Nkebi, E, Odametey, J, Facey, R, Esmail, MYA, Ashraf, M (2009). Insight into long term sea level change based on new tide gauge installations at Takoradi, Aden and Karachi. The International Hydrographic Review. May 2009.

Wright IJ, Reich PB, Cornelissen JHC, Falster DS, Groom PK (2005). Modulation of leaf economic traits and trait relationships by climate. Ecology and Biogeography 14:411–421.

Wright, S (1978) Evolution and the genetics populations, Vol. 4: Variability Within and Among Natural Populations. University of Chicago Press, Chicago.

Yap, HT (2000). The case for restoration of tropical coastal ecosystems. Ocean and Coastal Management 43: 841-851.

Yasseen, BT, Abu-Al-Basal, MA (2008). Ecophysiology of *Limonium axillare* and *Avicennia marina* from the coastline of Arabian Gulf-Qatar. J Coast Conserv. 12: 35–42.

Yoshimori, I, Seo, A, Nawata, H, Fouda, MM, Yoshikawa, K (2015). New microsatellite markers to analyze genetic structure of gray mangrove, *Avicennia marina* (Forsk.) Vierh. Journal of Arid Land Studies. 25(1): 11–16.

Young, A, Boshier, D, Boyle, T (Eds.) (2000). Forest Conservation Genetics: Principles and practice. CSIRO and CABI Publishing, Collingwood VIC, Australia.

Zolgharnein, H, Kamyab, M, Keyvanshokooh, S, Ghasemi, A, Nabavi, SMB. (2010). Genetic diversity of *Avicennia marina* (Forsk.) Vierh. populations in the Persian gulf by microsatellite markers. J. Fish Aquat. Sc. 5: 223–229.